Investigation of peripherally active and blood glucose-lowering dextromethorphan derivatives without central nervous side effects

Inaugural-Dissertation

zur Erlangung des Doktorgrades
der Mathematisch-Naturwissenschaftlichen Fakultät
der Heinrich-Heine-Universität Düsseldorf

vorgelegt von

Okka Scholz
aus Norden

Düsseldorf, Mai 2020

aus dem Institut für Vaskular- und Inselzellbiologie
des Deutschen Diabetes-Zentrums (DDZ)

und

dem Institut für Stoffwechselphysiologie
der Heinrich-Heine-Universität Düsseldorf

Gedruckt mit der Genehmigung der
Mathematisch-Naturwissenschaftlichen Fakultät der
Heinrich-Heine-Universität Düsseldorf

Berichterstatter:

1. Prof. Dr. Eckhard Lammert

2. Prof. Dr. Christine Rose

Tag der mündlichen Prüfung: 02. Juli 2020

Table of content

1. Abstract

Pancreatic islets represent the endocrine compartment of the pancreas and contain different hormone-releasing cell types, including insulin-secreting β-cells. These hormones are essential to maintain blood glucose concentrations within a narrow range (glucose homeostasis). The progressive dysfunction and demise of β-cells is associated with the onset and development of type 2 diabetes mellitus (T2DM), a not curable metabolic disorder that is accompanied by serious long-term complications. Several options for the treatment of diabetes are available, however, none of the currently available anti-diabetic drugs are able to stop disease progression. Thus, the development of β-cell protective agents that prevent or even reverse the onset of the disease is essential.

The over-the-counter (OTC) drug dextromethorphan (DXM) shows anti-diabetic and islet cell protective effects *in vitro* and *in vivo*, without inducing life-threatening hypoglycemia. Furthermore, DXM reveals positive effects on diabetic long-term complications, including cardiovascular endpoints. However, DXM is able to pass the blood-brain barrier (BBB), and potential central nervous side effects limit its use as an anti-diabetic medication. Within this project, we generated a series of novel derivatives of DXM to prevent compound distribution to the central nervous system while maintaining or improving the beneficial properties of the molecule on peripheral tissues.

We found that DXM derivatives with basic nitrogen-containing substituents showed a reduced BBB permeability and did not lead to neurological impairment in mice. Additionally, treatment with these derivatives resulted in increased glucose-stimulated insulin secretion from mouse and human pancreatic islets *in vitro* as well as elevated plasma insulin concentrations and improved glucose tolerance *in vivo*. Notably, the imidazole-containing DXM derivative Lam39 protected human islets against the β-cell toxin streptozotocin, whereas the existing anti-diabetic drug exendin-4 did not show a protective effect. Moreover, Lam39 was able to improve glucose tolerance in a mouse model of T2DM.

In summary, we were able to design and synthesize novel structural derivatives of the OTC drug DXM with a reduced BBB passage and without central nervous side effects while the insulinotropic, blood glucose-lowering and islet cell protective effects of the original drug were maintained or even improved. Therefore, our novel DXM derivatives have the potential to be developed into a new class of anti-diabetic drugs.

2. Zusammenfassung

Langerhans-Inseln stellen den endokrinen Teil des Pankreas dar und enthalten verschiedene hormonfreisetzende Zelltypen, einschließlich insulinsekretierende Betazellen. Diese Hormone sind erforderlich, um die Blutglukosekonzentration in einem engen Bereich zu halten (Glukosehomöostase). Die fortschreitende Dysfunktion und der Untergang von Betazellen wird mit dem Ausbruch und der Entwicklung von Typ 2 Diabetes mellitus (T2DM) assoziiert, einer nicht heilbaren Stoffwechselerkrankung, die mit schwerwiegenden Langzeitkomplikationen einhergeht. Es stehen verschiedene Optionen zur Behandlung von Diabetes zur Verfügung, jedoch kann keines der derzeit verfügbaren Antidiabetika das Fortschreiten der Krankheit stoppen. Daher ist die Entwicklung von betazellprotektiven Wirkstoffen, die den Ausbruch der Krankheit verhindern, oder sogar rückgängig machen, von wesentlicher Bedeutung.

Das frei verkäufliche Medikament Dextromethorphan (DXM) zeigt *in vitro* und *in vivo* antidiabetische und inselzellprotektive Effekte, ohne eine lebensbedrohliche Hypoglykämie hervorzurufen. Außerdem zeigt DXM positive Auswirkungen auf diabetische Langzeitkomplikationen, einschließlich kardiovaskulärer Endpunkte. Jedoch ist DXM in der Lage, die Blut-Hirn-Schranke (BHS) zu überwinden, wodurch potenzielle zentralnervöse Nebenwirkungen seine Verwendung als Antidiabetikum einschränken. Im Rahmen dieses Projekts haben wir eine Reihe neuer Derivate von DXM entwickelt, um die Ausbreitung der Substanz ins zentrale Nervensystem zu verhindern und gleichzeitig die vorteilhaften Eigenschaften des Moleküls auf das periphere Gewebe zu erhalten oder zu verbessern.

Wir haben herausgefunden, dass DXM Derivate mit basischen stickstoffhaltigen Substituenten eine verringerte BHS Permeabilität zeigten und nicht zu einer neurologischen Beeinträchtigung in der Maus führten. Außerdem führte die Behandlung mit diesen Derivaten *in vitro* zu einer gesteigerten Glukose-stimulierten Insulinsekretion muriner und menschlicher Inseln, sowie *in vivo* zu erhöhten Plasmainsulinkonzentrationen und einer verbesserten Glukosetoleranz. Insbesondere das Imidazol-haltige DXM Derivat Lam39 schützte menschliche Inseln gegen das Betazelltoxin Streptozotocin, wohingegen das verfügbare Antidiabetikum Exendin-4 keinen protektiven Effekt zeigte. Darüber hinaus konnte Lam39 die Glukosetoleranz in einem Mausmodell für T2DM verbessern.

Zusammenfassend konnten wir neue strukturelle Derivate des frei verkäuflichen Medikaments DXM mit reduzierter BHS Permeabilität und ohne zentralnervöse Nebenwirkungen entwickeln und synthetisieren, während die insulinotropen, blutglukosesenkenden und inselzellprotektiven Effekte des ursprünglichen Moleküls erhalten oder sogar verbessert wurden. Daher könnten unsere neuartigen DXM Derivate zu einer neuen Klasse von Antidiabetika entwickelt werden.

3. Introduction

3.1 The pancreatic islets

The pancreas is a lobular organ with an exocrine and an endocrine compartment, both having distinct physiological functions. It is located in the abdominal region and consists of a “head”, which is adjacent to the duodenum of the small intestine while the “tail” of the organ is attached to the spleen [1]. Following food intake, the exocrine pancreas (composed of acinar, centroacinar, and duct cells) releases digestive enzymes together with a bicarbonate-rich fluid across a branching network of ducts into the duodenum, facilitating the degradation and absorption of nutrients [2].

The endocrine part of the pancreas contains different hormone-secreting cell types that form small cell clusters. These so-called pancreatic islets or islets of Langerhans are complex “micro-organs” embedded within the surrounding exocrine part of the pancreas. A healthy human pancreas has around 3.2 million pancreatic islets, and the endocrine part makes up approximately 4.5% of the entire pancreatic tissue volume [3]. Each islet consists of 50-3,000 endocrine cells that are able to secrete various polypeptide hormones into the bloodstream [4]. Human pancreatic islets predominantly contain insulin-secreting β-cells (~57% of human pancreatic islets), glucagon-secreting α-cells (~33% of human pancreatic islets), and somatostatin-secreting δ-cells (~10% of human pancreatic islets) [3]. Particularly insulin and glucagon are essential hormones that are released into the circulatory system to maintain blood glucose concentrations around a specific set point, a process termed glucose homeostasis [5, 6].

Basically, the anatomy of pancreatic islets is comparable across different species: islets consist of clusters of endocrine cells and form highly vascularized and innervated micro-organs [7, 8]. However, differences between species exist, particularly between human and mouse islets [7, 9, 10]. Thus, it is important to understand these differences as well as the similarities between the species, since research findings are often extrapolated from mouse to human [7]. Mouse pancreatic islets consist of β-cells that form an inner core as well as α-cells and other endocrine cell types that are mainly located in the islet mantle [7]. In contrast, the organizational structure of human pancreatic islets is more complex and discussed controversially [11]. Studies indicate that the spatial distribution of different endocrine cell types throughout the islet is more random and apparently distinct from rodent islets [9, 12], allowing the different endocrine cell types to interact more closely [10]. There is a greater islet-to-islet variability in humans compared to rodents, since human islets show a higher range in composition of the different endocrine cell types within the islets, and further can show a compact or multilobular structure as well as different sizes [9-12].

The function and structure of pancreatic endocrine islet cells are influenced by multiple interactions with the immediate environment, facilitating, among others, the secretory output and the localization of cellular compartments [13, 14]. Endocrine cells are able to interact with other cells within the same islet either through paracrine extracellular interactions or via direct cell-cell contact [13]. Paracrine interaction includes, on the one hand, intra-islet hormone communication between the endocrine cells [5, 15], for example glucagon released from α-cells affects the insulin-secreting β-cells and might be necessary for the fine-tuning of glucose homeostasis [5]. On the other hand, there are also non-hormonal factors secreted by endocrine cells, such as glutamate, which are able to affect islet cell function [16, 17]. Moreover, the β-cell is directly in contact with other β-cells or other endocrine cell types that are immediately adjacent [9, 10], leading to an adequate insulin gene expression, islet insulin content, and glucose-stimulated insulin secretion (GSIS) [18, 19]. Several β-cell surface proteins play a role in the direct cell-cell contact, including gap junctions, tight junctions, adherens junctions, and Eph receptor-ephrin ligand interactions [20-23].

Pancreatic islets are vascularized structures in which fenestrated capillaries form a dense network, facilitating an efficient release of hormones into the bloodstream [8]. Most of the β-cells have at least one region of contact with vascular cells of this capillary network [21, 24]. Recent studies indicate that islet capillaries are dynamic structures, since contractile cells, such as smooth muscle cells and pericytes, are present in pancreatic islets and react to islet stimulation. Hereby, the capillary diameter can be regulated, and the local islet blood flow might be controlled during times of food intake and fasting, modulating hormonal outflow [25, 26].

Since pancreatic islets are richly innervated by the autonomic nervous system, the secretion of endocrine hormones is further regulated by neurotransmitters and hormones released by parasympathetic neurons (cholinergic; rest and digest mood) and sympathetic neurons (adrenergic; fight and flight mood) [1, 27, 28]. Food intake (hyperglycemic condition) induces the parasympathetic nervous system, facilitating insulin secretion by the release of acetylcholine and its binding to muscarinic receptors on β-cells. In response to hypoglycemia, the activity of the sympathetic nervous system inhibits the release of insulin and stimulates the release of glucagon via activation of adrenergic receptors on β-cells and α-cells by noradrenaline and adrenaline [27, 28].

In sum, pancreatic islets are micro-organs embedded within the pancreas that contain various hormone-releasing cell types, including insulin-secreting β-cells and glucagon-secreting α-cells, and are essential for glucose homeostasis by properly releasing these hormones into the circulatory system.

3.2 Regulation of insulin secretion and blood glucose homeostasis

Glucose is one of the main metabolic fuels and thus represents, next to lipids and proteins, an important energy source for the body [1]. Since serious complications can arise from increased blood glucose levels (hyperglycemia) as well as lower blood glucose levels (hypoglycemia), the appropriate regulation of insulin and glucagon secretion is essential to maintain blood glucose concentrations within a narrow range and thus ensure normal body function [5]. On the one hand, insulin is responsible for glucose uptake by tissues, particularly by skeletal muscle and adipose tissue, leading to a subsequent reduction of blood glucose levels. In contrast, glucagon counter-regulates insulin and is able to elevate the concentration of blood glucose by releasing glucose from hepatic stores [1]. Thus, the pancreas plays an essential role in glucose homeostasis. Additionally, there is a tight interaction of the pancreas with other organs, including the brain, intestine, liver as well as muscle and adipose tissue, via several hormones, neurotransmitters as well as cytokines. For example, acetylcholine, which represents the major neurotransmitter of the peripheral parasympathetic nervous system, stimulates insulin release from β-cells, and leptin, which is mainly produced by adipocytes, inhibits insulin release via activation of leptin receptors on β-cells [29-32].

Blood glucose concentrations increase due to food ingestion and endogenous glucose production. Particularly the increase of blood glucose levels subsequently leads to the secretion of insulin from pancreatic β-cells (GSIS) (**Fig. 1**). GSIS requires uptake of glucose into the β-cell and subsequent metabolic degradation of the molecule [1]. Glucose enters the cell via glucose transporters (GLUTs), precisely via GLUT1 and GLUT3 in human β-cells (**Fig. 1, step 1**) [33]. Following uptake into the cell, glucose is phosphorylated by glucokinase, and further metabolism, especially in the mitochondria, leads to the production of ATP and a concomitant fall in ADP concentration (**Fig. 1, step 2**). The increased cellular ATP/ADP ratio causes ATP-sensitive K^+ channels (K_{ATP} channels) to close (**Fig. 1, step 3**). The latter play a pivotal role in insulin release by linking cell metabolism to the membrane potential. At low blood glucose concentrations, K_{ATP} channels are open and the plasma membrane is hyperpolarized. The closure of these channels decreases the hyperpolarizing K^+ efflux, triggering plasma membrane depolarization (**Fig. 1, step 4**) followed by an opening of voltage-dependent Ca^{2+} channels (VDCCs) (**Fig. 1, step 5**) [6, 33]. Ca^{2+} influx via VDCCs leads to an increased intracellular Ca^{2+} concentration in the form of Ca^{2+} oscillations, which subsequently trigger an pulsatile secretion of insulin from the β-cell [34-36]. The latter is caused by exocytosis of secretory granules storing insulin (**Fig. 1, step 6**) [6, 33]. Ca^{2+} released from intracellular stores, such as the endoplasmic reticulum (ER), further enhances cytosolic Ca^{2+} levels and thus maintains insulin release [35, 37]. The

secreted and active form of insulin is due to proteolytic cleavage of proinsulin. Precisely, the C-peptide portion is removed, which allows the association of the A and B chains via disulfide bonds [1]. Insulin secretion from mouse and human pancreatic islets has a biphasic nature, meaning that the increase of glucose causes an initial rapid transient response that lasts less than ten minutes (first phase), subsequently followed by a slower and sustained release (second phase) [38].

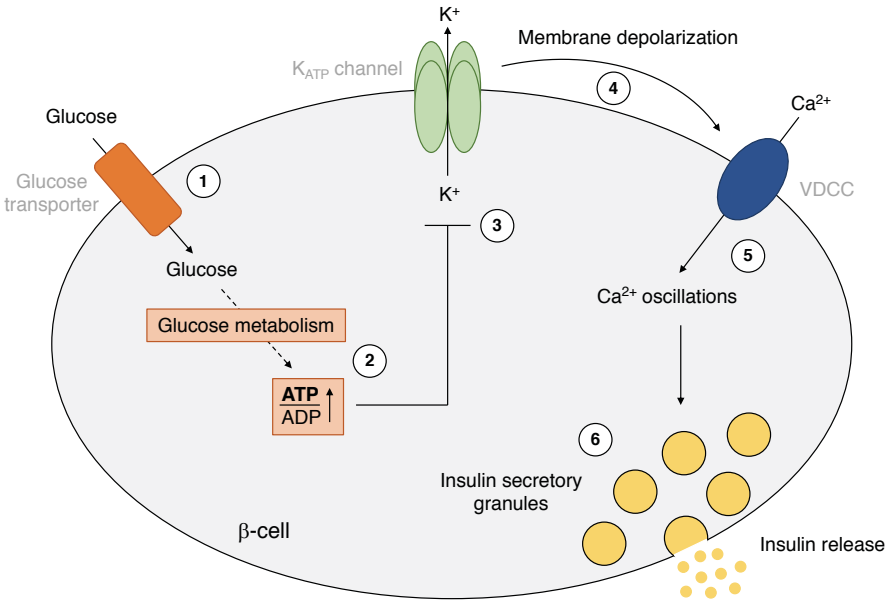

Figure 1: Model of glucose-stimulated insulin secretion (GSIS) from β-cells. Uptake of glucose into the β-cell (1) and subsequent glucose metabolism lead to an increased intracellular ATP/ADP ratio (2), causing ATP-sensitive K^+ channels (K_{ATP} channels) to close (3) and a subsequent depolarization of the plasma membrane (4). The change in membrane potential leads to an opening of voltage-dependent Ca^{2+} channels (VDCCs) (5), and the consequent increase of intracellular Ca^{2+} concentration in the form of Ca^{2+} oscillations triggers the fusion of insulin-containing secretory granules with the plasma membrane (6). The steps (1-6) are explained in the main text in more detail. Figure was illustrated by Okka Scholz, according to [1, 6, 33-35].

Other hormones and neurotransmitters are able to modulate the insulin secretion from β-cells [16, 17, 39, 40]. The gut-derived incretin hormones glucagon-like peptide-1 (GLP-1) and glucose-dependent insulinotropic polypeptide (GIP), which are released from enteroendocrine L-cells and K-cells, respectively, amplify glucose-dependent insulin secretion from β-cells in response to food ingestion [39, 40]. Furthermore, it is suggested that GLP-1 suppresses the glucagon secretion from α-cells [41]. The term “incretin effect” describes the observation that orally administered glucose increases the insulin release to a larger extent by inducing GLP-1 and GIP secretion, in contrast to intravenously administered glucose [29, 42]. Precisely, there is a two- to three-fold higher insulin secretion

in response to oral glucose challenge compared to intravenous glucose challenge [40]. GLP-1 and GIP bind to their respective receptors (GLP-1 receptor and GIP receptor) that are expressed in pancreatic β-cells [43, 44], leading to receptor activation and thus conversion of ATP into cyclic adenosine monophosphate (cAMP) via adenylyl cyclase. Increase of cAMP levels further activates protein kinase A (PKA) and exchange protein directly activated by cAMP 2 (Epac2), causing the potentiation of postprandial insulin release from β-cells by amplifying exocytosis as well as by enhancing closure of K_{ATP} channels, electrical activity of the cell, and the release of Ca^{2+} from intracellular stores [6, 29].

Furthermore, polypeptide hormones that are secreted from other pancreatic endocrine cell types are able to modulate insulin secretion from β-cells. For example, somatostatin released by δ-cells has an inhibitory effect on insulin release, resulting from activation of somatostatin receptors on β-cells and a subsequent repolarization of the plasma membrane. In addition to the effect on glucose-induced electrical activity of the β-cells, somatostatin is able to directly inhibit insulin release by affecting exocytosis of insulin secretory granules [33, 45, 46].

Additionally, multiple studies indicate that the excitatory neurotransmitter glutamate is able to affect insulin secretion [16, 47-50]. In the β-cell, glucose metabolism causes the production of glutamate by mitochondria. Subsequently, cytosolic glutamate has an amplifying effect on the action of Ca^{2+}, indicating that intracellular glutamate contributes to the secretory response to glucose stimulation [48, 51]. This potentiating effect of glutamate on insulin secretion might be due to targeting the insulin secretory granules. Several research groups have shown that glutamate uptake into the granules is crucial for insulin exocytosis [48, 52-54]. Interestingly, it is further suggested that cytosolic glutamate plays a key role in cAMP/PKA signaling and thus is essential for incretin-induced insulin secretion [50]. Next to glutamate, other neurotransmitters, including gamma-aminobutyric acid (GABA), are present in insulin secretory granules and play important regulatory roles regarding insulin secretion [55, 56].

To sum up, maintaining of blood glucose homeostasis is a complex process in which the pancreatic endocrine hormones insulin and its counter-regulator glucagon play a crucial role. Several external factors, including hormones and neurotransmitters, are able to affect β-cell signaling, resulting in an appropriate insulin release and blood glucose concentration.

3.3 Regulation of metabolism by insulin

Insulin release from pancreatic β-cells is particularly stimulated by elevated blood glucose levels. Secreted insulin in turn mediates its physiological effects by binding to insulin receptors (IRs) located on the plasma membrane of target cells and thus plays a central role in glucose metabolism and cell growth. The typical insulin-sensitive tissues are liver, skeletal muscle, and adipose tissue. However, IRs are also expressed in other tissues of the body [57, 58]. The IR is a heterotetrameric receptor tyrosine kinase. Binding of insulin to its receptor triggers intracellular tyrosine kinase domain autophosphorylation and subsequent phosphorylation and activation of intracellular proteins, such as members of the insulin receptor substrate (IRS) family. These proteins in turn interact with several downstream signaling molecules that are essential for the diversified insulin response [57-60]. For example, the protein kinase Akt is suggested to be substantial in transmission of insulin signaling and thus for maintenance of blood glucose concentrations, as it is involved in pathways that control glucose transport in muscle and adipose tissue, suppression of hepatic glucose production (gluconeogenesis) as well as activation of hepatic synthesis of fatty acids (lipogenesis) [57, 58, 60].

As an anabolic hormone, insulin causes the uptake of glucose, fatty acids, and amino acids from the bloodstream into the cells, and further promotes the synthesis and intracellular storage of carbohydrates, lipids, and proteins [1, 57]. Due to binding to its receptor, insulin increases glucose uptake into muscle and adipose tissue by stimulating the translocation of GLUT4-containing storage vesicles to the plasma membrane [57, 58]. Moreover, insulin action promotes glycogen synthesis (glycogenesis) as well as inhibits the breakdown of glycogen (glycogenolysis) in skeletal muscle and liver, and further rapidly reduces hepatic gluconeogenesis and subsequent glucose release into the circulatory system, leading to a potent regulation of blood glucose levels [1, 58, 60]. Additionally, lipogenesis and synthesis of proteins is increased due to insulin action while the degradation of lipids (lipolysis) and proteins is suppressed [1, 57].

Next to the typical insulin-sensitive tissues, such as liver, skeletal muscle as well as adipose tissue, insulin action on other tissues, including the central nervous system (CNS) and pancreatic β-cells, may also play a crucial role in the regulation of glucose homeostasis [57, 58]. IRs and insulin signaling proteins are widely distributed in the brain, and an important function of insulin in this tissue is the inhibition of appetite and thus the reduction of food intake and control of body weight. Next to the regulation of energy balance, insulin signaling in the brain is thought to play an essential role in the regulation of reproduction [29, 58, 61, 62]. Furthermore, β-cells contain IRs and insulin signaling proteins that may contribute to the regulation of β-cell secretory function and therefore to the regulation of

glucose homeostasis [63-65]. However, the role of insulin as a direct autocrine signal for β-cells that triggers the insulin response remains controversial [66].

In summary, insulin is an anabolic hormone with several physiological functions. It plays an important role in the regulation of glucose homeostasis and mediates its blood glucose-lowering effects due to multiple mechanisms, initiated mainly by binding to IRs expressed in target tissues.

3.4 Diabetes mellitus - a metabolic disorder

Diabetes mellitus is a multifactorial and heterogenous metabolic disorder, characterized by chronically elevated blood glucose levels (hyperglycemia), largely resulting from insufficient insulin secretion from pancreatic β-cells to maintain blood glucose concentrations in a physiological range [6, 67]. The incidence and prevalence of the disease are increasing globally. Approximately 463 million people were affected by diabetes in 2019 worldwide, meaning that 1 in 11 adults (20-79 years) suffered from the disease (9.3% of the global population). Globally, around 4.2 million people (20-79 years) died from diabetes-related causes in 2019. Diabetes is among the top ten causes of death and associated with a global healthcare expenditure of approximately US-$ 760 billion in that year. The disease represents one of the fastest growing global health problems, with a predicted number of around 578 million people (10.2% of the global population) that will be affected in 2030. Furthermore, there is a high percentage of people with undiagnosed diabetes, which is currently around 50% (232 million people) [67, 68].

On the one hand, classical symptoms like polyuria (frequent urination) and polydipsia (excessive thirst) that result from osmotic diuresis followed by glucosuria (excretion of glucose into the urine) can be used to diagnose diabetes. The latter occurs due to blood glucose concentrations exceeding the capacity of sodium-glucose linked transporters (SGLTs) located in the renal tubule system and responsible for the reabsorption of glucose from the primary urine [69, 70]. On the other hand, several diagnostic tests for diabetes are recommended, including the measurement of fasting plasma glucose or the two-hour measurement of plasma glucose after glucose challenge (75 g) during an oral glucose tolerance test (OGTT). Criteria of the World Health Organization (WHO) define diabetes as fasting plasma glucose values of $\geq$ 7.0 mmol/l (126 mg/dl) or two-hour post-load plasma glucose of $\geq$ 11.1 mmol/l (200 mg/dl) [67, 71]. Furthermore, people with a HbA1c value (glycated hemoglobin) $\geq$ 6.5% (48 mmol/mol) are considered to have diabetes [72].

The recently published report of the WHO on the classification of diabetes mellitus divides the disorder into various classes [73]. The two major classes are type 1 diabetes mellitus (T1DM), an autoimmune disease occurring frequently in childhood, and type 2 diabetes mellitus (T2DM) that represents the most common type of diabetes, occurring mainly in adults and accounting for approximately 90-95% of all diabetes worldwide. Furthermore, several intermediate forms of diabetes are described that have both, some characteristics of T1DM and T2DM [74]. Monogenic defects of β-cell function, including maturity-onset diabetes of the young (MODY) as well as neonatal diabetes mellitus, represent other specific types of diabetes [75, 76]. Compared to T1DM and T2DM, monogenic diabetes results from a single gene rather than from multiple genes and environmental factors, and is much less common, accounting for around 1.5-2% of all cases [77]. MODY is an inherited early-onset diabetes (generally before the age of 25 years) that results from β-cell dysfunction and is non-insulin-dependent [78]. If diabetes is diagnosed before the age of six month, it is more likely monogenic neonatal diabetes rather than T1DM [75]. Additional specific types of diabetes can also arise as a consequence of other conditions, including diseases of the exocrine pancreas (pancreatitis or pancreatic cancer) [79, 80], endocrine disorders (excess release of several hormones that antagonize insulin action, e.g. cortisol or growth hormones) [81], and several drugs [82] or viruses (e.g. congenital rubella) [83, 84]. Another class of diabetes is hyperglycemia in pregnancy (HIP), which is divided in gestational diabetes mellitus and diabetes mellitus in pregnancy [85, 86]. Gestational diabetes is diagnosed during pregnancy for the first time and is defined by lower glucose cut-off points compared to those for diabetes in the non-pregnant state [85], whereas diabetes in pregnancy is defined by the same criteria as in non-pregnant women and includes persons who have previously known diabetes [87]. However, the most cases of HIP are gestational diabetes mellitus, accounting for approximately 75-90% [86].

T1DM is an autoimmune disease caused by the immune-mediated destruction of the insulin-secreting β-cells, leading to an inability to produce enough insulin endogenously. Once β-cells are destroyed, patients lose blood glucose control due to insulin deficiency and require lifelong insulin replacement [88, 89]. The number of children and adolescents (up to 19 years) living with diabetes increases annually. In 2019, already over 1.1 million children and adolescents suffered from T1DM worldwide [67]. Shortly after diagnosis and upon first insulin doses, the requirements of exogenous insulin often decrease transiently, reflecting partial recovery of β-cell function. This partial remission (termed “honeymoon phase”) lasts a few weeks to months, before the decline in insulin production begins [90].

Manifestation of T1DM develops as a consequence of a combination of various immunologic, genetic as well as environmental events. Due to a breakdown in self-tolerance, autoreactive immune cells (T-lymphocytes, B-lymphocytes, macrophages, and

dendritic cells) surround or infiltrate pancreatic islets (termed peri-insulitis and insulitis), initiating an inflammatory process that results in the progressive destruction of β-cells [89]. The extent of cell destruction may vary, but it has been estimated that clinical onset with classic hyperglycemic symptoms occurs more frequently, when less than 30% of the β-cells remain [90, 91]. T1DM is a polygenic disorder, whereby the human leukocyte antigen (HLA) genotype confers approximately 50% of the genetic risk to develop the disease. Specific combinations of DR and DQ alleles at the HLA loci are associated with a decreased or increased risk [92-94]. Thus, genetics plays a strong role in T1DM risk. Individuals with an affected first-degree relative have an approximately 15-fold increased relative risk to develop the disease compared to the general population [95]. Furthermore, several environmental factors may trigger the pathogenesis of T1DM, including infection with congenital rubella virus [83] as well as enterovirus infections during pregnancy and childhood [96, 97]. Other putative risk factors are foreign antigens in the infant nutrition [98], and childhood vaccination (for example against hepatitis B), which all might lead to an introduction of several peptides to the developing immune system that contain amino acid sequences similar to islet autoantigens, probably initiating autoimmunity against pancreatic β-cells [99].

T2DM is characterized by peripheral and hepatic insulin resistance as well as relative insulin deficiency due to pancreatic β-cell dysfunction (**Fig. 2**). The epidemiology of the disease is mainly affected by environmental factors, whereas genetic factors are also involved [100]. The incidence of the disease increases with age, but a rising number of children and adolescents suffer from T2DM [101]. The organs involved in the onset of the disease are mainly the pancreas, skeletal muscle, and liver, but also include the adipose tissue, small intestine or brain [100]. Diabetes affects the metabolism of lipids and carbohydrates, which represent the two major cellular metabolic substrates, causing the disruption of metabolic pathways as well as the production of harmful metabolites [102].

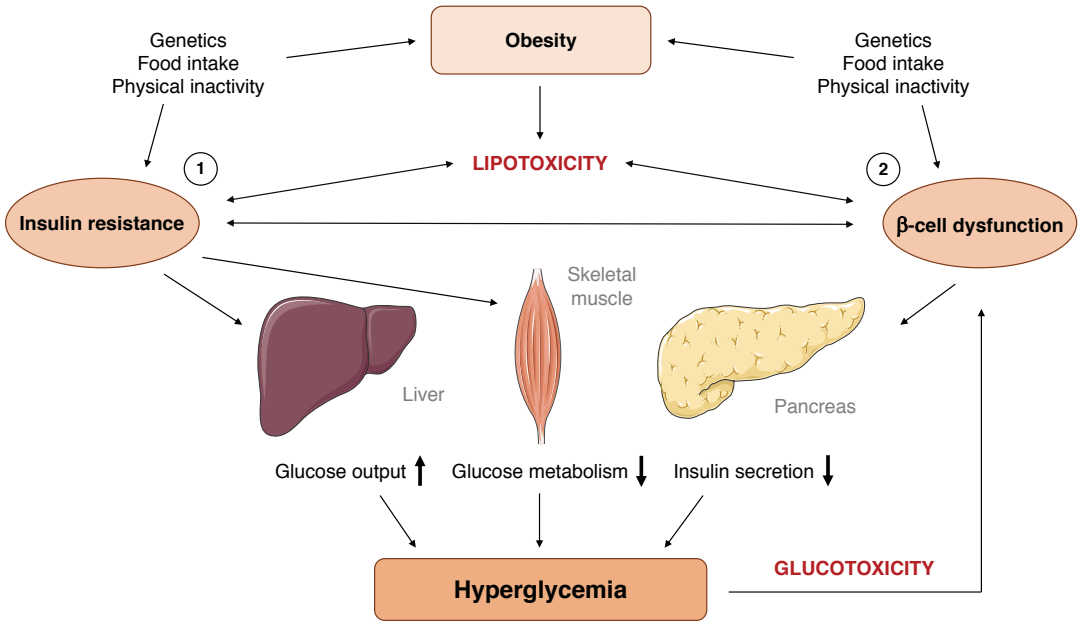

Figure 2: Pathogenesis of type 2 diabetes mellitus (T2DM). Insulin resistance (1) and β-cell dysfunction (2) represent two main pathophysiological factors contributing to hyperglycemia and the onset of T2DM. Pancreatic β-cells are initially able to compensate for insulin resistance by an increased insulin release, however, this compensatory effect decreases due to the continuous increase of blood glucose concentrations (glucotoxicity) and the inflammatory response of adipose tissue (lipotoxicity). Both, glucotoxicity and lipotoxicity contribute to β-cell dysfunction and death. The parts (1,2) are explained in the main text in more detail. Figure was illustrated by Okka Scholz, according to [69]. Images used in this figure were provided by Servier (Servier Medical Art, https://smart.servier.com). Servier Medical Art by Servier is licensed under a Creative Commons Attribution 3.0 Unported License.

A crucial step in the development of T2DM is the reduced response of the body to insulin, a process termed peripheral insulin resistance (**Fig. 2, part 1**). Insulin resistance causes the inability of insulin-dependent tissues, such as skeletal muscle and adipose tissue, to take up glucose into the cells and utilize it as a metabolic substrate. This is because the cells fail to properly respond to normal concentrations of circulatory insulin, as insulin plays a key role in glucose entry into the cells [103, 104]. Thus, insulin resistance in peripheral tissues can finally lead to an increase of plasma glucose levels. Furthermore, hepatic insulin resistance contributes to elevated plasma glucose concentrations due to the reduction of glycogen synthesis as well as the increase of gluconeogenesis [105, 106]. A number of mechanisms, including inflammation, oxidative and ER stress as well as mitochondrial dysfunction are suggested to contribute to the development of insulin resistance [104]. When insulin resistance occurs, as often happens in obese individuals, β-cells are initially able to compensate for the reduced action of insulin by increasing insulin secretion and expanding β-cell mass, leading to the maintenance of normal glucose homeostasis. Further

reduction in insulin sensitivity results in elevated blood glucose levels, since β-cells are no longer able to release enough insulin. Thus, when impaired glucose tolerance occurs, insulin resistance is already well established [102, 107, 108].

However, insulin resistance alone does not necessarily cause hyperglycemia and the development of T2DM. The demise of pancreatic β-cells (**Fig. 2, part 2**) leads to the inability to compensate for the increased demand of insulin and is associated with the onset and progression of the disease [44, 108-110]. The pathogenesis of T2DM develops over several years and eventually results in a reduction of functional β-cell mass to 40-60% compared to normal β-cell mass [111]. Various factors lead to the loss of functional β-cell mass, including β-cell exhaustion due to the prolonged elevated release of insulin as well as β-cell death through apoptosis [108, 112, 113]. Recent studies further proposed that loss of β-cell identity or β-cell dedifferentiation into other endocrine cell types play an essential role in the progressive loss of β-cell mass in T2DM [114-116], however, this is discussed controversially [117].

The basis for β-cell dysfunction and death in T2DM is multifactorial and includes glucotoxicity and lipotoxicity [118]. Chronic exposure to high blood glucose concentrations causes toxic effects on structure and function of organs, including pancreatic islets, a process termed glucotoxicity [119]. The subsequent overstimulation of β-cells and sustained glucose metabolism are associated with insulin secretory failure in T2DM [120]. For example, it is suggested that an excessive and prolonged production of reactive oxygen species (ROS) and chronic oxidative stress due to enhanced glucose metabolism in β-cells is a central mechanism for glucotoxicity [119, 120]. ROS includes free radicals, such as superoxide (O_2^-), hydroxyl radical (HO•), and non-radicals, including hydrogen peroxide (H_2O_2), and represents an unavoidable byproduct of mitochondrial respiration during glucose stimulation of β-cells, which might be even required for normal GSIS [121, 122]. Chronically increased extracellular glucose concentrations lead to an excessive glycolysis and mitochondrial oxidative phosphorylation, with the concomitant elevation of ROS release from the electron transport chain [120, 122, 123]. Next to the mitochondrial production, other non-mitochondrial sources of increased ROS generation exist, including NADPH oxidase (NOX) that oxidizes NADPH and directly produces ROS through the reduction of molecular oxygen [120, 124, 125]. Additionally, β-cells are especially vulnerable to oxidative stress, since the expression of enzymes involved in anti-oxidant defense is unusually low in these cells compared to other tissues. This imbalance may lead to the high susceptibility of β-cells for damage induced by oxidative stress [120, 126]. The potential deleterious consequences of excessive ROS production, including oxidative damage to other molecules (e.g. proteins) in the form of molecular alterations, may lead to β-cell dysfunction and death due to multiple mechanisms, such as changes in enzyme activity, ion channel transport or receptor signal

transduction [122, 127]. Targets for oxidative damage in the β-cell are, among others, the critical proteins pancreatic and duodenal homeobox-1 (PDX-1) and MafA, a member of the basic leucine zipper family of transcription factors, which bind and activate the insulin promoter. Consequently, the loss of these transcription factors leads to a defective insulin gene expression, a reduction of islet insulin content as well as an impaired insulin secretion from β-cells [119, 120, 128, 129].

Obesity and physical inactivity are strongly associated with insulin resistance and the development of T2DM. Approximately 60% of patients with T2DM are obese (body mass index (BMI) $\geq$ 30 kg/m^2) and display insulin resistance [130]. An excessive caloric intake results in an enlargement of adipocytes due to an increased storage of fatty acids in the form of triglycerides within these cells. Ongoing metabolic overload of the adipose tissue finally leads to adipocyte dysfunction, resulting in an increased secretion of adipokines (cytokines), including monocyte chemoattractant protein-1 (MCP-1) and tumor necrosis factor-α (TNF-α), and thus in an adipokine-mediated inflammatory response in adipose tissue [131, 132]. Chronic inflammation of adipose tissue is further mediated by the infiltration of immune cells, including monocytes and macrophages, which in turn secrete TNF-α and other inflammatory cytokines [69, 131]. This leads to a reduced triglyceride synthesis and storage in adipocytes as well as an enhanced lipolysis and thus to elevated concentrations of circulating free fatty acids (FFAs) that can reach toxic levels, and the formation of ectopic triglyceride storage in non-adipose tissues, including skeletal muscle, liver as well as pancreatic β-cells (lipotoxicity) [131, 133]. High levels of circulating FFAs and ectopic lipid accumulation in turn disrupt insulin signaling pathways and may trigger β-cell dysfunction [69, 131]. Thus, lipid accumulation within the pancreatic islets likely contributes to β-cell dysfunction, and finally leads to hyperglycemia and the subsequent development of T2DM [102, 134]. Furthermore, systemic inflammation is associated with β-cell dysfunction, and fatty acids may increase the production of inflammatory cytokines in islets [107, 135, 136].

Leptin represents another adipokine that is produced by adipocytes. It regulates several physiological processes, including satiety, appetite, and glycemia, by the activation of leptin receptors that are expressed by neurons in the hypothalamus [137, 138]. Circulatory leptin is directly proportional to the fat mass of the body [139]. Since individuals with T2DM are often obese and thus show hyperleptinemia, the development of central resistance or tolerance to the metabolic actions of leptin is suggested [137, 138]. Next to the regulation of feeding behavior, leptin also plays a role in the regulation of inflammatory responses. Precisely, it enhances the production of pro-inflammatory cytokines, such as TNF-α, while the production of anti-inflammatory cytokines, including interleukin-4 (IL-4), is suppressed [132].

Additionally, other factors play a role in the pathogenesis of T2DM. Several genes and mutations are important contributors of insulin resistance and β-cell dysfunction [69, 107]. By meta-analysis of genome-wide association studies more than 100 T2DM-associated loci were identified [140, 141]. For example, the transcription factor 7-like 2 gene (*TCF7L2*) confers risk of developing T2DM by decreasing the survival rate of pancreatic β-cells [142, 143].

Furthermore, all types of diabetes share common long-term complications, primarily due to the elevated blood glucose concentrations that especially affect the nervous and cardiovascular (CV) system. Chronically elevated blood glucose levels increase the risk of macrovascular complications, such as myocardial infarction and stroke as well as microvascular complications, including blindness (diabetic retinopathy) and renal failure (diabetic nephropathy), and further complications, such as peripheral nerve damage (diabetic neuropathy) [6, 67, 144]. CV diseases are the most prevalent causes of morbidity and mortality associated with T2DM [145, 146]. Therefore, an intensive control and management of blood glucose and lipid levels as well as blood pressure is essential to reduce the risk of complications [147]. Individuals with diabetes have a more than two times higher rate of various CV diseases, including myocardial infarction and ischemic stroke, compared to individuals without diabetes [148]. Moreover, T2DM is also associated with non-vascular diseases, such as mental and nervous system disorders, infections, liver disease as well as cancer [102, 149]. Studies indicate that diabetes is associated with an excess risk of several types of cancer, including liver, pancreas, and kidney cancer [150].

In sum, diabetes mellitus is a heterogenous and complex metabolic disorder, which is characterized by chronically elevated blood glucose concentrations as well as a progressive dysfunction of insulin-producing β-cells, and a combination of environmental factors and genetic predisposition leads to the onset of the disease. A huge problem regarding diabetes is that many patients still develop serious microvascular and macrovascular complications.

3.5 Current possibilities to treat diabetes

Since the pathophysiology of T1DM and T2DM is different, there are distinct options available to treat the disease. However, the common goal of all available treatment strategies is to maintain blood glucose levels within or near to the physiological range. Nowadays, neither T1DM nor T2DM can be cured, nevertheless, the optimal control of blood glucose levels is crucial to prevent acute complications as well as diabetic long-term complications [69, 151].

T1DM is characterized by the destruction of the insulin-producing β-cells, resulting in an absolute insulin deficiency, and consequently leading to the lifelong administration of exogenous insulin [88, 89]. The therapy of T1DM typically consists of continuous subcutaneous insulin infusions (CSII, insulin pump) or multiple daily injections of insulin. Several insulin analogues exist with differing pharmacokinetic profiles, ranging from ultrafast-acting insulins that are able to reduce blood glucose levels within minutes after administration to ultralong-acting insulin that mimics basal insulin secretion with slight peaks of action [74, 88]. Insulin therapy is further developing to decrease the risk of hypoglycemia on the one hand, and enhance the quality of life of patients on the other hand. One example is a closed-loop system, which acts as an artificial pancreas and integrates conventional CSII and continuous glucose monitoring systems with a computer algorithm, providing the possibility to adapt the delivery rate of insulin to the current interstitial glucose concentrations and thus optimizing blood glucose fluctuations [152, 153].

Since obesity and physical inactivity are associated with the development of T2DM, it is suggested that the onset of T2DM can be prevented by weight reduction and lifestyle interventions, including exercise and diet [154, 155]. However, in everyday life this is difficult to achieve for many patients, leading to a pharmacological treatment of the disease [156, 157]. For pharmacological therapy of T2DM, several blood glucose-lowering agents are available that differ in their drug target and thus in their modes of action. The different classes of anti-diabetic drugs address distinct problems and stages of the disease and may be prescribed in combination to maintain blood glucose homeostasis more effectively [29, 100, 158]. Metformin belongs to the class of biguanide and represents the most widely used first-line medication for the management of T2DM. Oral metformin treatment decreases hepatic glucose output, enhances glucose uptake into peripheral tissues (e.g. skeletal muscle), and further stimulates the secretion of GLP-1 [159, 160]. Due to the progressive character of T2DM, second-line agents are added to metformin if glycemic targets are no longer reached. Thus, monotherapy is often insufficient to maintain blood glucose levels, leading to a combination of anti-diabetic drugs [100]. Sulfonylureas often represent the first choice for dual therapy. This class of oral drugs stimulates endogenous insulin secretion from β-cells by binding to the sulfonylurea receptor 1 (SUR1) subunit of the K_{ATP} channel, leading to an inhibition of the latter [29, 161]. Furthermore, incretin-based therapies include subcutaneous injection of GLP-1 receptor agonists (GLP-1 analogues) as well as oral administration of dipeptidyl peptidase-4 (DPP-4) inhibitors. Since DPP-4 rapidly inactivates GLP-1, the inhibition of DPP-4 enhances the endogenous concentration of GLP-1. The activation of GLP-1 receptors by GLP-1 analogues increases insulin release and reduces glucagon release in a glucose-dependent manner, delays gastric emptying as well as improves satiety [162, 163]. The latest oral anti-diabetic drugs that were introduced to the

market are SGLT2 inhibitors. These drugs act on the kidney and increase urinary excretion of glucose due to the inhibition of SGLT2 in the renal proximal tubule and thus prevent the reabsorption of glucose from the urine, leading to a decline of blood glucose concentrations [107, 164]. Moreover, the resulting urinary calorie loss of up to 320 kcal per day leads to a significant reduction of weight [165]. Since the disease has a progressive nature, the additional administration of exogenous insulin can become necessary to maintain glycemic control. The main advantage of insulin therapy is the blood glucose-lowering effect in a dose-dependent manner over a wide range [158, 166].

Nonetheless, current diabetes therapy has multiple limitations. Firstly, some of the described drugs are able to induce adverse side effects that impede the treatment and might be even life-threatening [100]. For example, during the treatment with metformin gastrointestinal side effects are common, and further this drug should not be used in patients with severe chronic kidney disease because of concerns of lactic acidosis [158, 167]. Insulin and sulfonylureas can cause life-threatening hypoglycemic events due to the high circulating insulin concentrations, and because sulfonylureas increase insulin release in a glucose-independent manner [29, 168]. There is an up to six times increased hypoglycemic risk due to sulfonylurea treatment compared to metformin treatment [169]. Furthermore, sulfonylureas are associated with adverse CV outcomes [158, 170]. The main side effects of GLP-1 receptor agonists are gastrointestinal impairments, including nausea and vomiting [158]. Additionally, GLP-1 analogues are contraindicated in patients with a history of chronic pancreatitis, although this remains controversial [171, 172]. The glucose-lowering effect of SGLT2 inhibitors depends on renal function, and due to dose reduction, these drugs are less effective in patients showing moderate to severe renal impairment [158, 173]. Moreover, this class is associated with an increased risk of urinary tract or genital infections [174], and a higher risk of amputation, especially at the level of the metatarsal or toe [175].

Although the available anti-diabetic drugs transiently adjust blood glucose to normal concentrations, current drugs are not able to sustainably restore normal β-cell function and mass and thus cannot sufficiently maintain long-term glycemic control [176-180]. Therefore, the development of novel β-cell protective agents that are able to prevent or even reverse the onset of diabetes is essential. Animal experiments suggest that the incretin hormone GLP-1 induces β-cell proliferation as well as neogenesis, and further prevents β-cell apoptosis [181]. Moreover, it was shown that GLP-1 receptor agonists and DPP-4 inhibitors transiently improve β-cell function. However, no evidence for a clinically relevant enhancement of β-cell function and preservation of β-cell mass exists [177, 180]. Taken together, none of the available anti-diabetic drugs are able to substantially and durably protect against β-cell death [179]. Thus, pancreatic islets are important targets for the

development of new agents, since their decline is associated with the onset and progression of the disease [108-110].

Furthermore, current anti-diabetic drugs are not able to adequately prevent the development of diabetic long-term complications [182]. Since CV diseases represent the greatest causes of death associated with T2DM, and CV safety of anti-diabetic drugs has become an essential requirement for registration, the development of novel angio- and cardioprotective drugs that have positive effects on diabetic micro- and macrovascular complications is essential [100, 107].

To sum up, there is a wide range of options for the treatment of diabetes. Nevertheless, no anti-diabetic drugs are currently available that are able to stop disease progression or even show curative effects. There is an urgent need for novel medications with fewer adverse events, beneficial effects on diabetic long-term complications, and particularly durable β-cell protective properties. Such drug would be beneficial for T1DM and T2DM, since a decline in functional β-cell mass occurs in both types.

3.6 Dextromethorphan as a potential anti-diabetic drug

Dextromethorphan (DXM) is an ingredient of many commonly used over-the-counter (OTC) cough suppressants and has been in use for more than five decades due to its good safety profile, even in pediatric patients [16, 183]. It is a dextrorotatory morphinan that shows structural similarities to morphine and other opioids [184, 185]. Following its absorption from the gut, the pro-drug DXM is quickly metabolized in the liver to its main de-methylated metabolite dextrorphan (DXO), mediated by a cytochrome P450 (CYP) liver enzyme [185]. Next to the treatment of acute cough, DXM is already in use as a suppressant for diabetic neuropathic pain and pseudobulbar affect [186-189], for the treatment of nonketotic hyperglycinemia [190, 191] as well as other neuropsychiatric disorders [192]. DXM and DXO have a multi-faced pharmacology and exert their medical effects via several different mechanisms, including the inhibition of N-Methyl-D-Aspartate (NMDA) receptors, serotonin transporters, and vascular NOX as well as the activation of σ_1 receptors [185, 193-196].

Previously, further medical effects of DXM and its active metabolite DXO have been identified, including anti-diabetic effects, both *in vitro* and *in vivo* (**Fig. 3**) [197, 198]. These effects might be caused due to blocking of pancreatic membrane-bound ionotropic NMDA receptors by DXM/DXO.

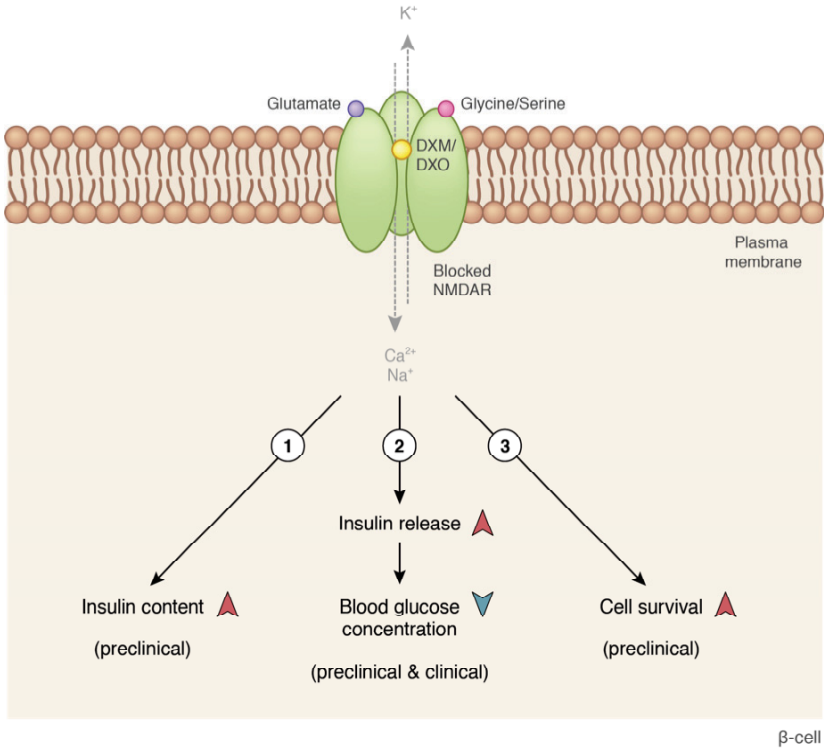

Figure 3: Proposed effects of DXM and DXO on β-cells. Treatment with DXM/DXO leads to an increased islet insulin content (1), an enhanced insulin secretion from β-cells and thus a decrease of blood glucose concentrations (2) as well as an increased islet cell survival under diabetogenic conditions (3). Described effects might be caused by inhibition of membrane-bound ionotropic N-Methyl-D-Aspartate (NMDA) receptors. The NMDA receptor is blocked by its antagonists DXM/DXO, leading to an interrupted ion flow through the receptor. In brackets: preclinical or clinical evidence of shown propositions. The parts (1-3) are explained in the main text in more detail. Figure was drafted by Okka Scholz, and illustrated by Yousun Koh [199]. Permission: Copyright Clearance Center RightsLink® Service, order number: 4810680538357.

Firstly, it was shown that the treatment with DXM increases the insulin content of isolated mouse pancreatic islets during long-term treatment of leptin receptor-deficient mice (*db/db* mice), an animal model of human T2DM (**Fig. 3, part 1**) [200]. Experiments with *db/db* mice furthermore displayed that the long-term treatment leads to a significantly higher α-cell and β-cell area as well as an increased total number of islets per pancreas compared to control mice, indicating that treatment with DXM is beneficial for islet physiology [197]. Secondly, DXM and DXO are able to increase GSIS from β-cells and thus reduce blood glucose concentrations (**Fig. 3, part 2**). Precisely, the treatment of isolated mouse and human pancreatic islets leads to an increased insulin release compared to untreated control islets. Notably, this insulinotropic effect can be observed only under stimulatory glucose concentrations while the basal insulin secretion remains largely unaffected. Furthermore, *in vivo* experiments reveal that DXM and DXO are able to improve glucose tolerance in mice. The treatment with DXO results in significantly increased plasma insulin levels and

thus reduces blood glucose concentrations during glucose tolerance tests with mice compared to untreated control mice. Again, DXO acts in a glucose-dependent manner, whereby hypoglycemic events are avoided. Moreover, the long-term treatment of *db/db* mice with DXM leads to significantly reduced fasting blood glucose concentrations and thus to an improved glucose tolerance compared to control animals, indicating that DXM has the potential to preserve β-cell function [197]. Additionally, when DXM is applied to *db/db* mice that are already at a diabetic level (around 400 mg/dl), one week of treatment reduces blood glucose levels by approximately 200 mg/dl. After six weeks of treatment, blood glucose concentrations of DXM-treated mice are still around 200 mg/dl, whereas the blood glucose concentrations of control mice further increase to around 500 mg/dl. Thus, DXM is able to reverse hyperglycemia in diabetic mice [144]. Thirdly, treatment of pancreatic islets with DXM and DXO increases islet cell survival under inflammatory and diabetogenic conditions (**Fig. 3, part 3**). Experiments with human pancreatic islets reveal that treatment with DXO leads to significantly lower rates of islet cell death induced by a mixture of cytokines (TNF-α, IL-1β, and IFN-γ) compared to untreated islets. Thus, DXO is able to protect pancreatic islets against cytokine-induced cell death. Additionally, the long-term application of DXM reduces islet cell death in *db/db* mice *in vivo* [197]. Further studies show that treatment of diabetic mice, induced by high-fat diet and the β-cell toxin streptozotocin (STZ), with the NMDA receptor antagonist memantine also increases pancreatic islet cell survival [201].

Notably, DXM is able to improve insulin secretion and glucose tolerance even in type 2 diabetic patients (**Fig. 3, part 2**) [197, 198]. The first of two clinical trials (registered phase 2a, double-blinded, placebo-controlled, randomized, multiple crossover, single-dose proof-of-concepts studies) with 20 patients each reveal that a single oral administration of DXM (270 mg) significantly increases maximum serum insulin concentrations as well as improves glucose tolerance during an OGTT compared to placebo treatment. Notably, DXM does not affect fasting blood glucose or fasting serum insulin concentrations und thus does not induce hypoglycemia [197]. The second clinical trial shows that a single-dose of DXM (60 mg) enhances the blood glucose-lowering effect of sitagliptin, a DPP-4 inhibitor. Compared to sitagliptin alone, the combination of sitagliptin with DXM significantly reduces maximum blood glucose concentrations, improves glucose tolerance as well as increases the baseline-adjusted area under the curve (AUC) for serum insulin concentrations during the first 30 minutes of an OGTT. Thus, the combination of the two agents seems to preferentially restore the early phase of insulin secretion in patients with T2DM [198].

Besides its anti-diabetic effects, further effects of DXM have been shown that could be beneficial for diabetic patients. In preclinical studies, DXM reduces oxidative stress and inhibits atherosclerotic plaque as well as neointima formation in the vascular system of mice [196]. Moreover, it is suggested that DXM as well as NMDA receptor inhibition reduce

hypertension in rats and that DXM is even able to improve clinical hypertension, leading to the attenuated development of CV diseases [195, 202, 203]. Consistent with these beneficial effects, DXM is further able to increase endothelial function in two clinical trials, as determined by an increase in FMD (flow-mediated dilation), both after single-dose and long-term application [144, 204]. Precisely, single-dose and oral administration of 30 mg DXM increases the FMD by approximately 1.5% in individuals, including an obese, a smoker, and a diabetic one [144]. Furthermore, oral treatment of habitual smokers with 120 mg/day DXM for six month significantly enhances the FMD by around 2% as well as attenuates vascular oxidative stress and serum concentrations of inflammatory markers (e.g. IL-6) [204]. Thus, preclinical and clinical data suggest that DXM has anti-oxidative and anti-inflammatory properties and therefore can improve endothelial function, indicating that this drug has the potential to reduce diabetic CV complications. DXM or NMDA receptor antagonists have also been suggested for the treatment of further long-term complications associated with diabetes, such as diabetic retinopathy, nephropathy, and neuropathies [144, 205-207] as well as for adjunct treatment of cancer [208-210].

Taken together, DXM and DXO are able to increase GSIS from mouse and human pancreatic islets as well as improve glucose tolerance in mice and even in individuals with T2DM. Notably, the administration does not introduce hypoglycemia even in the fasted state in mice and humans [144, 197, 198]. Additionally, DXM and DXO display beneficial effects on islet physiology and promote islet cell survival under diabetogenic conditions [197]. Since the demise of pancreatic islets (caused by islet dysfunction, dedifferentiation, and death) is associated with the onset and progression of diabetes mellitus, islets represent a key target for identification of novel anti-diabetic drugs [44, 108, 109, 112, 114]. Moreover, DXM also reveals positive effects on the long-term complications of diabetes, including CV endpoints, indicating that DXM/DXO might be a novel strategy for the treatment of T2DM.

3.7 Aims of the study

Since DXM and DXO are able to pass the blood-brain barrier (BBB), they can induce central nervous side effects in higher concentrations, such as nausea, dizziness or fatigue [197, 198]. This would be an exclusion criterion for a medication that patients need to take on a daily basis. Thus, the application of DXM for treatment of T2DM and its long-term complications is limited due to these side effects as well as due to the potential misuse of DXM as a recreational drug [211, 212]. For that reason, the development of peripherally active derivatives of the molecule would be useful to avoid the distribution of the molecule to the CNS.

Here, novel derivatives of DXM were generated to exclude the central nervous side effects while maintaining or improving the insulinotropic, blood glucose-lowering as well as islet cell protective properties of the molecule (**Fig. 4**). To this end, several derivatives were chemically synthesized (**Fig. 4, step 1**) and first analyzed for their ability to increase GSIS from primary mouse pancreatic islets *in vitro* (**Fig. 4, step 2**). All derivatives that enhanced GSIS were tested for their ability to increase plasma insulin concentrations and improve glucose tolerance *in vivo* during glucose tolerance tests (**Fig. 4, step 3**). Liquid chromatography-tandem mass spectrometry (LC-MS/MS) was further used to determine the *in vivo* concentration of the derivatives in cerebrospinal fluid (CSF) *versus* plasma (**Fig. 4, step 4**). The derivatives that revealed a reduced BBB permeability were subsequently analyzed in different behavioral tests in mice to evaluate whether the derivatives no longer induce behavioral changes characteristic of their original drug (**Fig. 4, step 5**). The DXM derivative with the strongest effects was further analyzed, including its insulinotropic effect on isolated human pancreatic islets as well as its ability to protect mouse and human pancreatic islets from cell death (**Fig. 4, step 6**). To investigate the islet cell protective effect, laser scanning microscopy (LSM)-based live cell imaging was conducted on isolated mouse and human pancreatic islets treated with the lead compound.

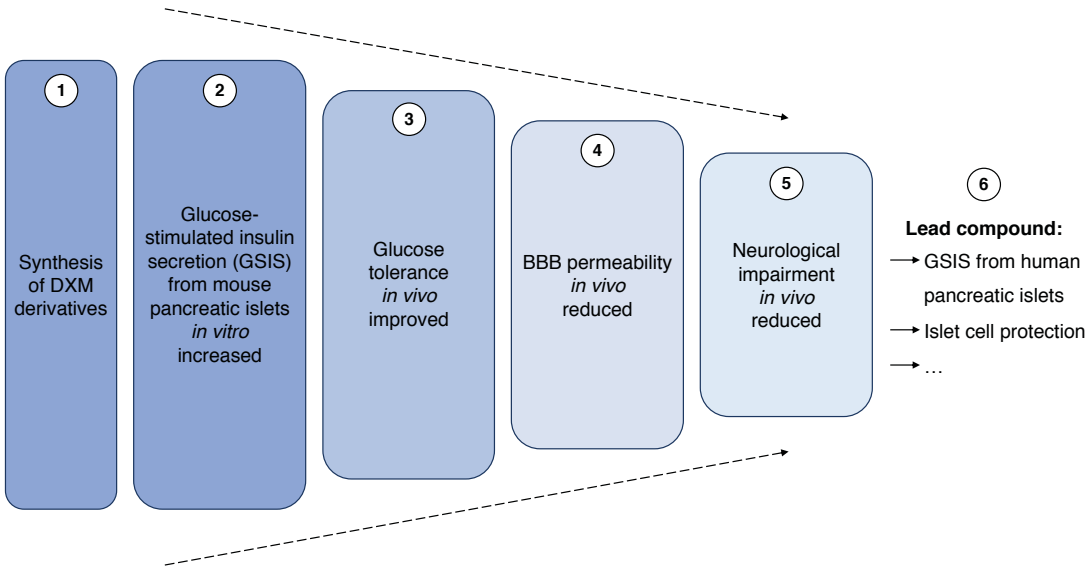

Figure 4: Gradual optimization of DXM derivatives. Several novel DXM derivatives were generated by medicinal chemistry (1). With the help of different tests (2-6) (both, *in vitro* and *in vivo*) the derivatives with the best anti-diabetic effects and lowest blood-brain barrier (BBB) permeability were selected successively. The steps (1-6) are explained in the main text in more detail. Figure was illustrated by Okka Scholz.

With this study, novel chemical derivatives of the OTC drug DXM were designed and characterized in several biological and functional tests, especially *in vivo* tests. Hereby, the derivatives with the best anti-diabetic effects, lowest BBB permeability and thus no CNS-related side effects were selected gradually. From a medical point of view, these molecules have the potential to be further developed into a new class of anti-diabetic drugs and might be useful to delay or even prevent diabetes progression. This is of particular interest, since around 460 million people suffer from diabetes worldwide, associated with around 4 million deaths in 2019 [68].

4. Experimental procedures

The description of the following methods will be used in part for the publication of the presented data in a scientific journal (see section 8).

Chemicals were obtained from Gibco®, Life Technologies™ unless otherwise specified.

4.1 Mouse models

For *in vitro* experiments and determination of BBB permeability, male C57BL/6J mice were purchased from Janvier. For GTTs, neurological tests (rotarod test and hanging-wire test) as well as investigation of pharmacokinetic profiles, male C57BL/6N mice were purchased from Charles River. Male BKS.Cg-*Dock7*^{m} +/+ *Lepr*^{db}/J mice (*db/db* mice) were purchased from Jackson Laboratory and used for GTTs. The age of C57BL/6 mice was above 9 weeks for *in vitro* experiments and determination of BBB permeability, and above 7 weeks for GTTs, neurological tests as well as analysis of pharmacokinetic profiles. The age of *db/db* mice was above 6 weeks. The room in which all mice were kept was controlled for temperature (22 °C), humidity (55%), and lighting (from 6 a.m. to 6 p.m.). All mice were fed with standard laboratory chow and water *ad libitum*. All animal experiments were approved by the local Animal Ethics Committee of the Landesamt für Natur, Umwelt und Verbraucherschutz Nordrhein-Westfalen (LANUV North Rhine-Westphalia, Germany), and conducted according to the German Animal Protection Laws.

4.2 *In vitro* methods

4.2.1 Cell culture

INS1E cells were cultured in a humidified atmosphere at 37 °C and 5% CO_2 in RPMI 1640 GlutaMAX™ medium containing:

10% (v/v) heat-inactivated FBS
100 U/ml penicillin
100 µg/ml streptomycin
11.2 mM HEPES
1 mM sodium pyruvate

175 µM 2-mercaptoethanol
2 mM L-glutamine
11.1 mM glucose (Sigma-Aldrich)

Cells were split after reaching a confluency of 90% and were screened negative for the presence of mycoplasma during a qPCR-based mycoplasmacheck (Eurofins Genomics).

4.2.2 Isolation of mouse pancreatic islets

Mouse pancreatic islets were isolated according to a protocol previously described [213], with minor changes using Liberase TL Research Grade (Roche). Enzymatic digestion at 37 °C was stopped after 17.5 min by adding DMEM GlutaMAX™ medium (1 g/l glucose) supplemented with 15% FBS. After wash and filter steps, islets were separated from pancreatic exocrine tissue by gradient centrifugation (1,200 rpm, 25 min), and collected from the interface between Histopaque-1077 (Sigma-Aldrich) and DMEM GlutaMAX™ medium (1 g/l glucose). After isolation, islets were washed twice using CMRL 1066 medium (islet medium) containing:

15% (v/v) heat-inactivated FBS
100 U/ml penicillin
100 µg/ml streptomycin
0.15% $NaHCO_3$
0.05 mM 2-mercaptoethanol
11.5 mM or 10 mM glucose (Sigma-Aldrich)

Functional experiments were performed after culturing one night in a humidified atmosphere at 37 °C and 5% CO_2.

4.2.3 Human pancreatic islets

Human pancreatic islets were provided by the NIDDK-funded Integrated Islet Distribution Program (IIDP) at City of Hope in Duarte, California, United States (NIH Grant # 2UC4DK098085), and from San Raffaele Scientific Institute, Milan, Italy. Studies and protocols were approved by the respective ethics committees (ethics committee of the Medical Faculty, Heinrich Heine University Düsseldorf, study number 3921; ethics

committee of the Instituto Scientifico Ospedale San Raffaele; ethics committee of the IIDP centers).

Human islets were isolated from pancreata of organ donors using collagenase digestion followed by density gradient purification. After isolation, the islet suspension had a viability of 90-95% and a purity of > 75%. Upon arrival, the human islets were washed up to three times with islet medium (containing the ingredients as described above). Functional experiments were performed after culturing one night in a humidified atmosphere at 37 °C and 5% CO_2.

4.2.4 Insulin secretion from pancreatic islets and INS1E cells

Isolated pancreatic islets or INS1E cells were first starved for 1 h in KRH buffer containing:

15 mM HEPES
5 mM KCl (Chemsolute, Th. Geyer)
120 mM NaCl (Carl Roth)
24 mM $NaHCO_3$
2 mM $CaCl_2$ (Sigma-Aldrich)
0.01 mM glycine (Sigma-Aldrich)
1 mg/ml bovine serum albumin (Sigma-Aldrich)

For starvation KRH buffer was supplemented with 2 mM glucose (Sigma-Aldrich) and the respective DXM derivative. To determine the insulin secretion from isolated pancreatic islets, the islets were first incubated in fresh KRH buffer ± DXM derivative containing 2 mM glucose (low glucose) to measure the basal insulin secretion. Subsequently, islets were incubated in KRH buffer ± DXM derivative containing 20 mM glucose (high glucose) to measure GSIS. For both conditions (low glucose and high glucose) the same islets were used and incubated for 1 h in the respective buffer. To measure the secreted insulin from INS1E cells, the KRH buffer used for starvation was replaced by KRH buffer ± DXM derivative containing either 2 mM glucose (low glucose) or 16.7 mM glucose (high glucose), and cells were incubated for 1 h in the respective buffer. All incubation steps during insulin secretion assays were performed at 37 °C and 5% CO_2. All compounds used were solved in water. Supernatant was collected after each incubation step to determine the secreted amount of insulin. To measure the insulin content, islets were lysed using RIPA buffer containing:

50 mM Tris-HCl (pH 7.4) (Sigma-Aldrich)
150 mM NaCl (Carl Roth)
1% IGEPAL (Sigma-Aldrich)
0.25% Na-deoxycholate (AppliChem)
1 mM EDTA (Ambion)

Subsequently, insulin concentrations of supernatants as well as islet lysates were measured using an ultra-sensitive rat insulin ELISA (Crystal Chem) in combination with an Infinite M200 NanoQuant reader (Tecan). Secreted insulin was normalized to insulin content when using islets and shown as percentage of basal control insulin secretion. For insulin secretion assays performed with INS1E cells, secreted insulin was normalized to total protein content measured with Pierce BCA Protein Assay Kit (Thermo Scientific).

4.2.5 Measurement of cell viability in pancreatic islets

Cell viability of isolated mouse or human pancreatic islets was determined using the LIVE-DEAD Viability-Cytotoxicity Kit (Thermo Fisher Scientific). Islets were cultured in islet medium containing the ingredients as described above (except for glucose concentration of 10 mM) and treated with the DXM derivative either alone or in combination with STZ (Sigma-Aldrich). Mouse islets were pre-incubated with or without DXM derivative for 24 h before starting the incubation for 24 h with 2 mM STZ with or without 1 µM of the derivative. Human islets were pre-incubated with or without DXM derivative for 24 h and subsequently incubated for 24 h with 40 mM or 50 mM STZ with or without 10 µM of the derivative. All incubation steps were performed at 37 °C and 5% CO_2. All compounds used were solved in water. To visualize viable and dead cells, whole islets were co-stained with 2 µM calcein AM, 4 µM ethidium homodimer-1 and Hoechst (1:1,000) in KRH buffer (prepared as described above) containing 10 mM glucose (Sigma-Aldrich) and incubated for 1 h at 37 °C and 5% CO_2.

4.3 *In vivo* methods

4.3.1 Glucose tolerance test

For GTTs, mice were fasted overnight for 16 h. Glucose (Sigma-Aldrich) (1.5 mg/g BW) alone or glucose together with a DXM derivative was administered via i.p. injection. Blood

glucose concentrations were measured before and 15, 30, 60, 90, and 120 min after i.p. injection by collecting blood from the tail tip. At all times, blood glucose concentrations were determined twice using a Monometer Futura glucometer (MedNet GmbH). Plasma insulin concentrations were measured before and 30 min after i.p. injection. For this, blood was collected from the tail tip during GTT using EDTA tubes (Sarstedt). Plasma was collected following centrifugation (2,000 rcf, 5 min), and insulin concentrations were subsequently determined using an ultra-sensitive rat insulin ELISA (Crystal Chem) in combination with an Infinite M200 NanoQuant reader (Tecan).

4.3.2 Determination of blood-brain barrier permeability

To determine the BBB permeability, DXO or the derivatives together with glucose (Sigma-Aldrich) (1.5 mg/g BW) were administered via i.p. injection. 30 min after i.p. injection, CSF was collected from the *cisterna magna*, and blood was collected from the heart using EDTA tubes (Sarstedt). For this, mice were anesthetized using Ketamin (Ketanest, Pfizer) (100 mg/kg BW) and Xylazin (Rompun, Bayer) (10 mg/kg BW). Plasma was collected following centrifugation (2,000 rcf, 5 min). Subsequently, the concentration of DXO and the derivatives in CSF and plasma was measured by LC-MS/MS.

4.3.3 Measurement of neurological impairment - rotarod test

To measure the motor coordination and balance of mice, DXO or the derivatives (solved in PBS) or PBS alone were administered via i.p. injection. 30 min after i.p. injection, mice were put on a rotating and accelerating rod, and the time mice could hold on the rod was determined. One day before performing the first experiment, mice got used to the experimental setup. For this, mice had to run on the rotating rod for 5 min in total.

4.3.4 Measurement of neurological impairment - hanging-wire test

To measure the muscle strength and condition of mice, DXO or the derivatives (solved in PBS) or PBS alone were administered via i.p. injection. 30 min after i.p. injection, mice were put on a grid that was subsequently turned 180 degrees, and the time mice could hold on the grid was determined. One day before performing the first experiment, mice got used to the experimental setup. For this, mice had to hold on the turned grid for 5 min in total.

4.3.5 Pharmacokinetics

To analyze the pharmacokinetic profile of the molecules, DXO or the derivative (solved in PBS) were administered via i.p. injection. Blood samples were collected before and 15, 30, 60, 120, and 300 min after i.p. injection from the tail tip of mice using EDTA tubes (Sarstedt). Plasma was collected following centrifugation (2,000 rcf, 5 min), and the plasma concentration of DXO and the derivative was subsequently determined using LC-MS/MS.

4.4 Biochemical and analytical methods

4.4.1 ELISA

Insulin concentrations in collected supernatants and lysates of mouse or human pancreatic islets, INS1E cells as well as plasma samples of mice were measured using an ultra-sensitive rat insulin ELISA (Crystal Chem). The results were determined by using an Infinite M200 NanoQuant reader (Tecan). ELISAs were performed according to the manufacturer's protocol.

For quantification of insulin secretion from mouse or human pancreatic islets, released insulin was normalized to insulin content and shown as percentage of basal control insulin secretion. For insulin secretion measurements with INS1E cells, released insulin was normalized to total protein content measured with Pierce BCA Protein Assay Kit (Thermo Scientific).

4.4.2 Liquid chromatography-tandem mass spectrometry

CSF or plasma samples, including the stable labelled deuterated internal standards d3-DXM and d3-DXO, were analysed by ultra-pressure liquid chromatography coupled to tandem mass spectrometry (UPLC-MS/MS). The UPLC-I Class and the tandem mass spectrometer Xevo-TQS (Waters) were used for the analysis. DXM and DXO were separated on an Aquity UPLC BEH C18 column (1.7 µm, 100 mm × 2.1 mm, Waters). The column oven temperature was 40 °C, the flow rate 0.4 ml/min, and the injection volume was 2 µL. The first mobile phase A consisted of 5 mM ammonium acetate, including 0.05% formic acid while the second mobile phase B consisted of acetonitrile. An isocratic elution mode (A:B, 65:35) was applied.

Tandem mass spectrometric analysis was performed in positive electrospray ionization mode. Multiple reaction monitoring (MRM) mode with following mass transitions were applied *m/z*: 272 > 171 (DXM), 275 > 171 (d3-DXM), 258 > 157 (DXO), 261 > 157 (d3-DXO), 338 > 265 (Lam39) and 338 > 279 (Lam39). Collision-induced dissociation (CID) energy of 40 V was used for fragmentation of DXM/d3-DXM and 30 V for DXO/d3-DXO and Lam39. Mass transitions for Lam28 were: 315.2 > 227.1 *m/z* (CID 35 V) and 315.2 > 258.1 *m/z* (CID 25 V). For Lam38 the mass transitions were: 342.2 > 254.1 *m/z* (CID 35 V) and 342.2 > 285.1 *m/z* (CID 30 V). All three DXM derivatives were separated as mentioned above by a C18 UPLC column. The software MassLynx V4.1 (Waters) was used for the acquisition and processing of data. Quantification was performed by the software TargetLynx (Waters).

4.4.3 Imaging and image analysis

To obtain single islet images, LSM images were acquired as maximum intensity projections of z-stacks using a Zeiss LSM 710 coupled to an Axio Observer.Z1 microscope (Carl Zeiss MicroImaging GmbH) equipped with a Plan-Apochromat 20x/0.8 objective. Images were analyzed using Fiji (ImageJ) image analysis software [214]. To determine the area of dead cells, ethidium homodimer-1 positive area was normalized to the total nuclei area, calculated as the merge of Hoechst and ethidium homodimer-1 positive area. The area of dead cells as well as total nuclei area was determined by global Otsu thresholding.

4.5 Statistics

Statistical significance was determined using Prism Version 7 (GraphPad Software, Inc.). For comparisons of two groups, unpaired two-sided Student's *t*-test was performed. For multiple comparisons, one-way or two-way ANOVA followed by Tukey's, Sidak's or Dunnett's multiple comparison test was used. *P* values were determined as indicated in the figure legends. All quantified data are presented as mean ± standard error of the mean (SEM), except for GTTs and pharmacokinetics in which all values are mean ± standard deviation (SD). Assays for measurement of cell viability were blinded. No outliers were excluded. Excel (Microsoft Corporation) and Prism Version 7 were used for analyses.

4.6 Personal contributions

Okka Scholz was supervised by Prof. Dr. Eckhard Lammert, funded by the German Center for Diabetes Research (DZD e.V.).

The following experiments were performed by Okka Scholz (stated within each figure legend): insulin secretion assays with isolated mouse and human pancreatic islets *in vitro*, determination of plasma insulin concentrations *in vivo*, glucose tolerance tests *in vivo*, determination of blood-brain barrier permeability *in vivo*, neurological tests (rotarod test and hanging-wire test) *in vivo*, analysis of pharmacokinetic profiles *in vivo*.

Okka Scholz further supervised Ara Aboolian during his internship of three months (July-September 2019), who works on related topics to this thesis.

Dr. Silke Otter supported Okka Scholz during most of the *in vivo* experiments, and contributed to some *in vitro* results (stated within each figure legend).

Dr. Dr. Alena Welters (Department of General Pediatrics, Neonatology and Pediatric Cardiology, University Children's Hospital, Düsseldorf) started the project, performed experiments with the initially developed DXM derivatives, and was involved in the establishment of *in vivo* methods.

Laura Wörmeyer performed the islet cell viability measurements (stated within each figure legend).

Dr. Diran Herebian (Department of General Pediatrics, Neonatology and Pediatric Cardiology, University Children's Hospital, Düsseldorf) performed LC-MS/MS measurements.

Dr. Miguel Sanz and Dr. Alexander Piechot (Taros Chemicals GmbH & Co. KG, Dortmund) were responsible for the synthesis of new DXM derivatives.

5. Results

5.1 Synthesis and characterization of derivatives of dextromethorphan

To develop derivatives of dextromethorphan (DXM) that display a reduced blood-brain barrier (BBB) penetration and thus induce no neurological impairment, the structure of the molecule was modified using medicinal chemistry (**Fig. 5a**). To this end, different polar residues were added at position two of the molecule to increase its polarity, and a gradual optimization of the molecular structure was performed. After synthesis (**Fig. 5a, step 1**) as well as purification and quality control (**Fig. 5a, step 2**) of the proposed derivatives, the novel molecules (**Fig. 5a, step 3**) were tested in different biological and functional tests (**Fig. 5a, step 4**) to evaluate their medical effects *in vitro* and *in vivo* (**Fig. 5a, step 5**). Based on these results, new molecular structures were proposed (**Fig. 5a, step 6**) in order to find a DXM derivative that has anti-diabetic and islet cell protective properties, but without inducing central nervous side effects. The novel molecules were used for biological and functional tests if they showed a purity > 95% as determined by ^{1}H nuclear magnetic resonance (NMR) spectroscopy as well as ultra-high performance liquid chromatography (UHPLC).

Some of the first polar residues that were added to DXM were carboxylic acid-containing groups. Although these derivatives displayed a statistically significant reduction in BBB permeability compared to dextrorphan (DXO), they completely lost peripheral effects, including their ability to increase glucose-stimulated insulin secretion (GSIS) from pancreatic islets. While synthesizing and testing further molecules, we found that DXM derivatives with basic nitrogen-containing residues (that is, dimethylamine, pyrrolidine, and imidazole), introduced at position two of the molecule, still exerted the beneficial peripheral effects of DXM, but without inducing the central nervous side effects of the original drug (**Fig. 5b-d**).

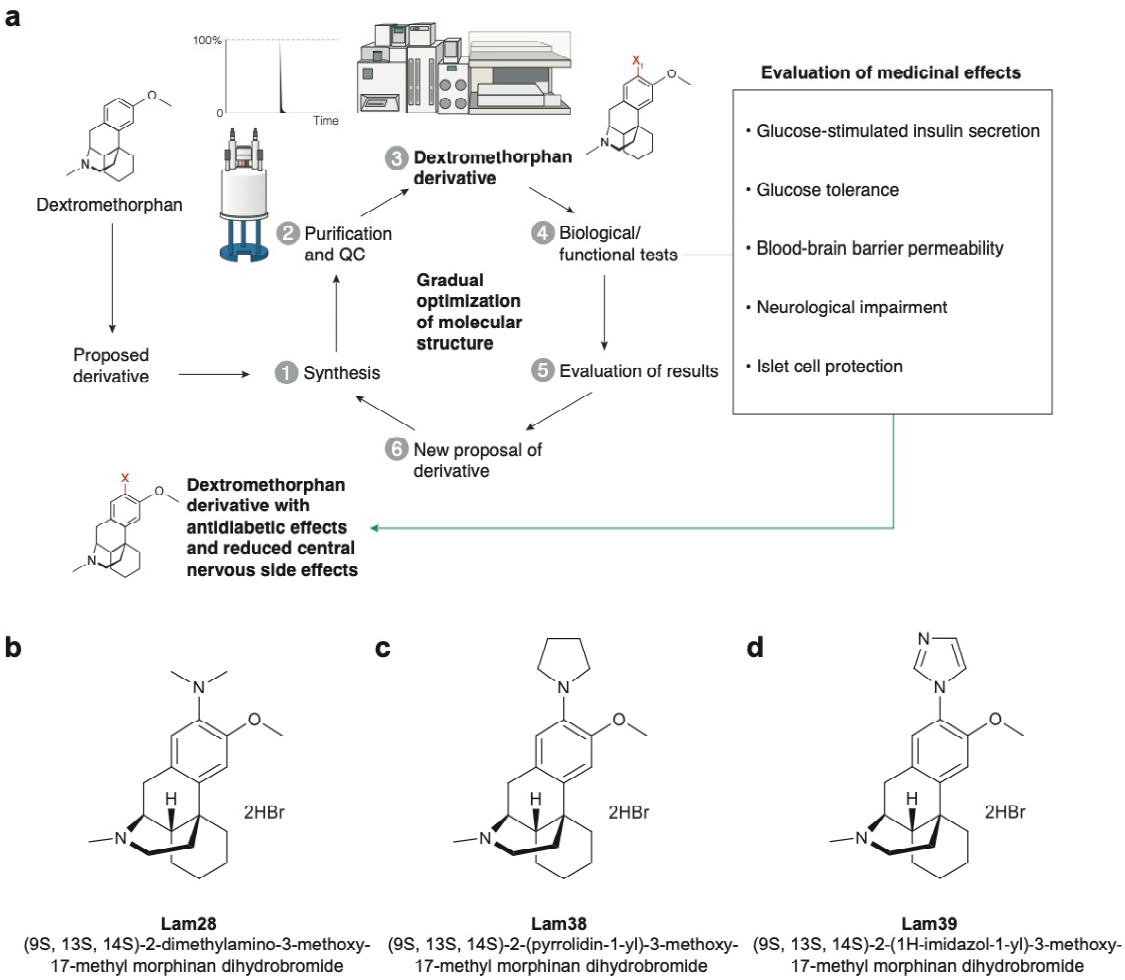

Figure 5: Synthesis and initial characterization of DXM derivatives. (**a**) Workflow of design and testing of novel DXM derivatives. Quality Control (QC) by ultra-high performance liquid chromatography (UHPLC) and nuclear magnetic resonance (NMR) analysis. After synthesis (1) and QC (2) of the proposed molecules, the novel derivatives (3) were tested in several biological and functional tests (4, and box to the right). Based on these results (5), new molecules were proposed (6). The steps (1-6) were repeated in order to find a derivative that has anti-diabetic properties as well as reduced central nervous side effects. Figure was drafted by Okka Scholz, and illustrated by Yousun Koh. (**b-d**) Structures of DXM derivatives Lam28, Lam38, and Lam39.

To investigate whether the anti-diabetic properties of the molecules were maintained, the synthesized derivatives were first tested on their ability to selectively enhance the GSIS from isolated mouse pancreatic islets. All derivatives that displayed an insulinotropic effect *in vitro* were further tested for their anti-diabetic effects *in vivo* by determining their ability to increase plasma insulin levels as well as lower blood glucose concentrations during glucose tolerance tests. Moreover, it was important that the newly synthesized derivatives do not pass the BBB, thus the *in vivo* concentrations of the derivatives in the cerebrospinal fluid (CSF) were determined and compared to the respective plasma concentrations by liquid chromatography-tandem mass spectrometry (LC-MS/MS). To further study whether the

novel derivatives still induce behavioral changes characteristic of their original drug, different neurological tests were performed *in vivo*.

Since the effects of the imidazole-containing DXM derivative (termed Lam39) were the strongest, further studies were conducted to characterize this molecule in more detail. For this, Lam39 was tested on its ability to enhance GSIS from mouse pancreatic islets and INS1E rat insulinoma cells in a dose-dependent manner as well as its ability to selectively increase GSIS from human pancreatic islets. Additionally, the dose-dependent effect of Lam39 on glucose tolerance *in vivo* as well as the effect of the derivative on glucose tolerance in a type 2 diabetes mouse model (*db/db* mice) were analyzed. Finally, the ability of Lam39 to protect isolated mouse and human pancreatic islets from cell death induced by the β-cell toxin streptozotocin (STZ) was tested, and the *in vivo* pharmacokinetic profile of the derivative was investigated.

In the following part, the results of the three best working derivatives (termed Lam28, Lam38, and Lam39) as well as the results of further analysis of Lam39 are shown.

5.2 Effect of dextromethorphan derivatives on insulin secretion *in vitro*

Firstly, the synthesized derivatives were tested for their ability to increase the GSIS from isolated mouse pancreatic islets, but without affecting the basal insulin secretion. The derivative with the strongest effects (Lam39) was then further tested for its ability to selectively enhance the GSIS from human pancreatic islets as well as from INS1E rat insulinoma cells in a dose-dependent manner. For these tests, pancreatic islets or INS1E cells were incubated with the derivatives, both under low glucose and high glucose concentrations. Afterwards, the amount of secreted insulin was measured.

5.2.1 Higher insulin secretion from mouse pancreatic islets induced by the derivatives

As a first step, the synthesized derivatives were investigated regarding their stimulatory effects on GSIS from isolated mouse pancreatic islets (**Fig. 6a-c**). The derivative Lam39 was further tested for its ability to enhance the insulin secretion from mouse islets in a dose-dependent manner (**Fig. 6d**) as well as under different non-stimulatory and stimulatory glucose concentrations (**Fig. 6e**). Furthermore, the effect of Lam39 on GSIS compared to DXO was investigated (**Fig. 6f**).

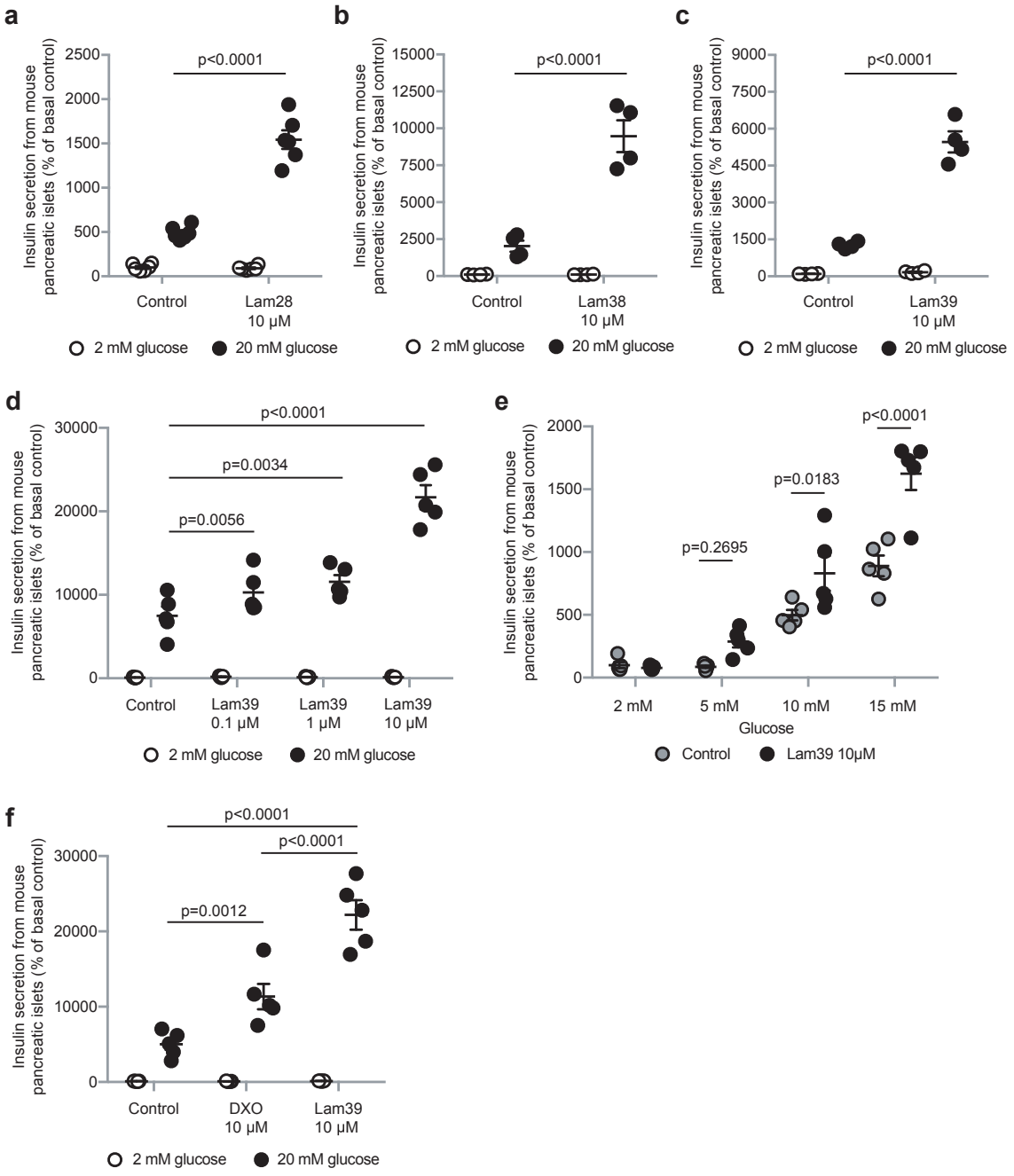

Figure 6: DXM derivatives increase glucose-stimulated insulin secretion from mouse pancreatic islets. (**a**-**c**) Insulin secretion from isolated mouse pancreatic islets in the absence or presence of a derivative. n = 4-6 islet batches each. (**d**) Insulin secretion from isolated mouse pancreatic islets due to the treatment with different concentrations of Lam39, and (**e**) due to the treatment with Lam39 under different glucose concentrations. n = 5 islet batches each. (**f**) Insulin secretion from isolated mouse pancreatic islets in the absence or presence of Lam39 compared to DXO. n = 5 islet batches each. Statistical testing: (a-c,f) two-way ANOVA followed by Tukey's multiple comparison test. (d,e) two-way ANOVA followed by Sidak's multiple comparison test. All values are mean ± SEM. Presented experiments for panel (a-e) were performed by Okka Scholz. Presented experiment for panel (f) was performed by Silke Otter.

The derivatives Lam28, Lam38 and Lam39 enhanced GSIS from isolated mouse pancreatic islets at a concentration of 10 µM (**Fig. 6a-c**). The stimulatory effects of all three derivatives on insulin secretion were statistically significant ($p < 0.0001$), whereas the basal insulin secretion was not affected. Additionally, the derivative Lam39 enhanced GSIS also at lower concentrations (1 µM and 0.1 µM), but in a dose-dependent manner (**Fig. 6d**). Moreover, a dose of 10 µM did not increase insulin secretion at low glucose concentration of 2 mM, but enhanced insulin release at higher and stimulatory glucose concentrations of 10 mM as well as 15 mM in a statistically significant manner ($p = 0.0183$ and $p < 0.0001$, respectively) (**Fig. 6e**). Compared to DXO, the derivative Lam39 significantly stronger enhanced GSIS from mouse pancreatic islets ($p < 0.0001$) (**Fig. 6f**).

5.2.2 Higher insulin secretion from human pancreatic islets induced by the derivative Lam39

The derivative Lam39 was further tested for its ability to enhance the insulin secretion from pancreatic islet preparations isolated from six different human donors (**Fig. 7a-f**), including one donor with type 2 diabetes mellitus (T2DM) (**Fig. 7f**).

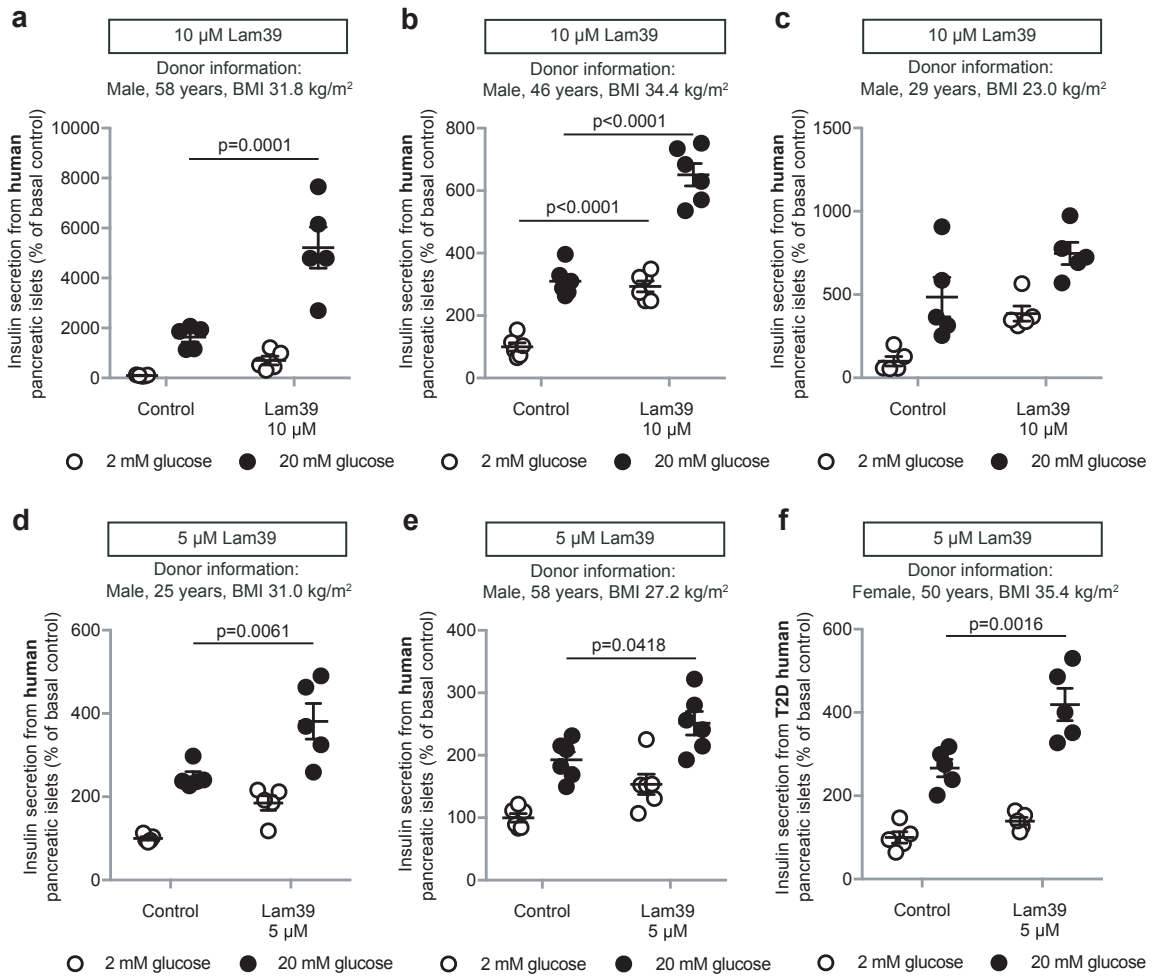

Figure 7: DXM derivative Lam39 increases glucose-stimulated insulin secretion from human pancreatic islets. (**a**-**e**) Insulin secretion from isolated human pancreatic islets in the absence or presence of Lam39. n = 5-6 islet batches each. (**f**) Insulin secretion from type 2 diabetic (T2D) human pancreatic islets in the absence or presence of Lam39. n = 5 islet batches each. Donor information is stated in the respective figure panel. Statistical testing: (a-f) two-way ANOVA followed by Tukey's multiple comparison test. All values are mean ± SEM. Presented experiments for panel (a,c-f) were performed by Okka Scholz. Presented experiment for panel (b) was performed by Silke Otter.

At a concentration of 10 µM, the derivative Lam39 significantly enhanced GSIS in two of three human islet preparations (**Fig. 7a-c**). However, the basal insulin secretion was also significantly increased ($p < 0.0001$) in one of three tests (**Fig. 7b**). At a lower concentration of 5 µM, the stimulatory effect of Lam39 on GSIS was maintained, but without significantly affecting the basal insulin release (**Fig. 7d-f**). Furthermore, Lam39 selectively increased GSIS from a human islet preparation received from a donor with T2DM in a statistically significant manner ($p = 0.0016$) (**Fig. 7f**).

5.2.3 Dose-dependent effect of the derivative Lam39 on insulin secretion from INS1E cells

To further investigate the insulin secretory capacity of Lam39, the derivative was tested for its ability to increase the insulin secretion from INS1E rat insulinoma cells at different concentrations in a range between 0.1 µM and 100 µM (**Fig. 8**).

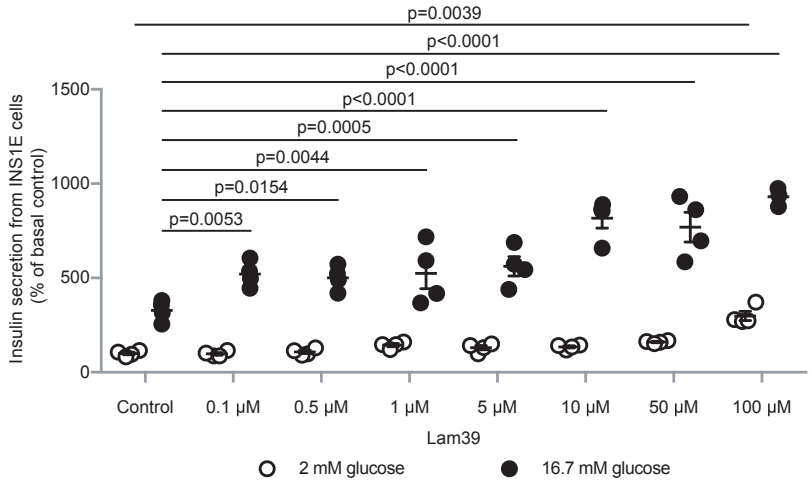

Figure 8: Dose-dependent effect of DXM derivative Lam39 on glucose-stimulated insulin secretion from INS1E cells. Insulin secretion from INS1E cells due to the treatment with different concentrations of Lam39. n = 3-4 samples each. Statistical testing: two-way ANOVA followed by Sidak's multiple comparison test. All values are mean ± SEM. Presented experiment was performed by Silke Otter.

The derivative Lam39 significantly increased GSIS from INS1E cells in a dose-dependent manner (**Fig. 8**). Even at a low concentration of 0.1 µM, a significant effect on insulin secretion was observed (p = 0.0053). Notably, the basal insulin secretion was not affected due to the treatment with Lam39, unless used at a high concentration (100 µM).

5.3 Effect of dextromethorphan derivatives on plasma insulin levels and glucose tolerance

Many derivatives that enhanced GSIS from mouse pancreatic islets *in vitro* failed to lower blood glucose concentrations in glucose tolerance tests *in vivo* (data not shown). Therefore, it was essential to investigate the anti-diabetic effects of the three derivatives Lam28, Lam38 and Lam39 *in vivo*. For this, plasma insulin levels and blood glucose concentrations

were measured during intraperitoneal (i.p.) glucose tolerance tests in C57BL/6 mice as well as in a type 2 diabetes mouse model (*db/db* mice).

5.3.1 Higher plasma insulin concentrations upon treatment with the derivatives

Firstly, the three derivatives were investigated regarding their effect on plasma insulin levels in C57BL/6 mice (**Fig. 9a-c**). For this, blood was taken before and 30 minutes after i.p. administration of glucose together with Lam28, Lam38 or Lam39, and plasma insulin concentrations were determined.

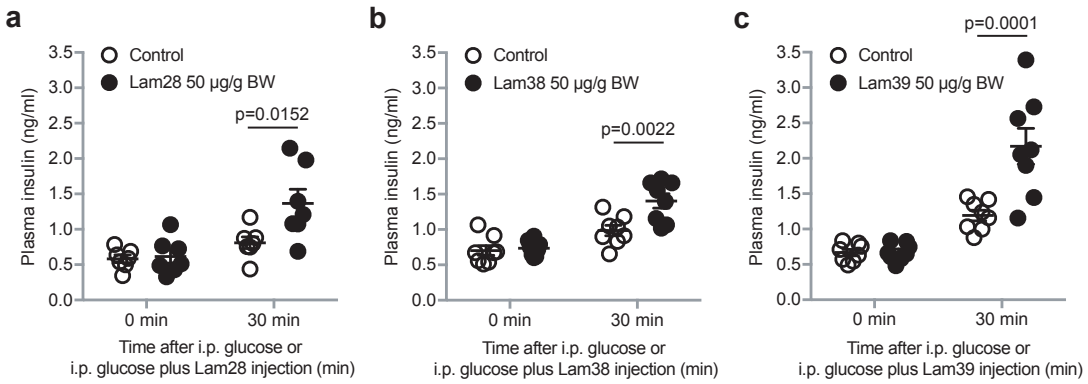

Figure 9: DXM derivatives increase plasma insulin concentrations *in vivo*. (**a-c**) *In vivo* plasma insulin levels before and 30 min after i.p. administration of the derivatives together with glucose (1.5 mg/g BW). (a) n = 7 mice each, (b,c) n = 8 mice each. Statistical testing: (a-c) two-way ANOVA followed by Tukey's multiple comparison test. All values are mean ± SEM. Presented experiments were performed by Okka Scholz.

When the derivatives Lam28, Lam38 and Lam39 were tested in mice, all of them significantly increased plasma insulin levels 30 minutes after i.p. glucose and derivative administration compared to glucose administration alone (**Fig. 9a-c**). Here, the strongest effect on plasma insulin concentrations was observed due to the treatment with the derivative Lam39 (p = 0.0001) (**Fig. 9c**).

5.3.2 Lower blood glucose concentrations upon treatment with the derivatives

The effect of the derivatives on blood glucose levels was measured during i.p. glucose tolerance tests with C57BL/6 mice (**Fig. 10a-c**). Furthermore, the respective areas under the curve (AUC) within the first two hours ($AUC_{0\text{-}120min}$) were calculated (**Fig. 10d-f**).

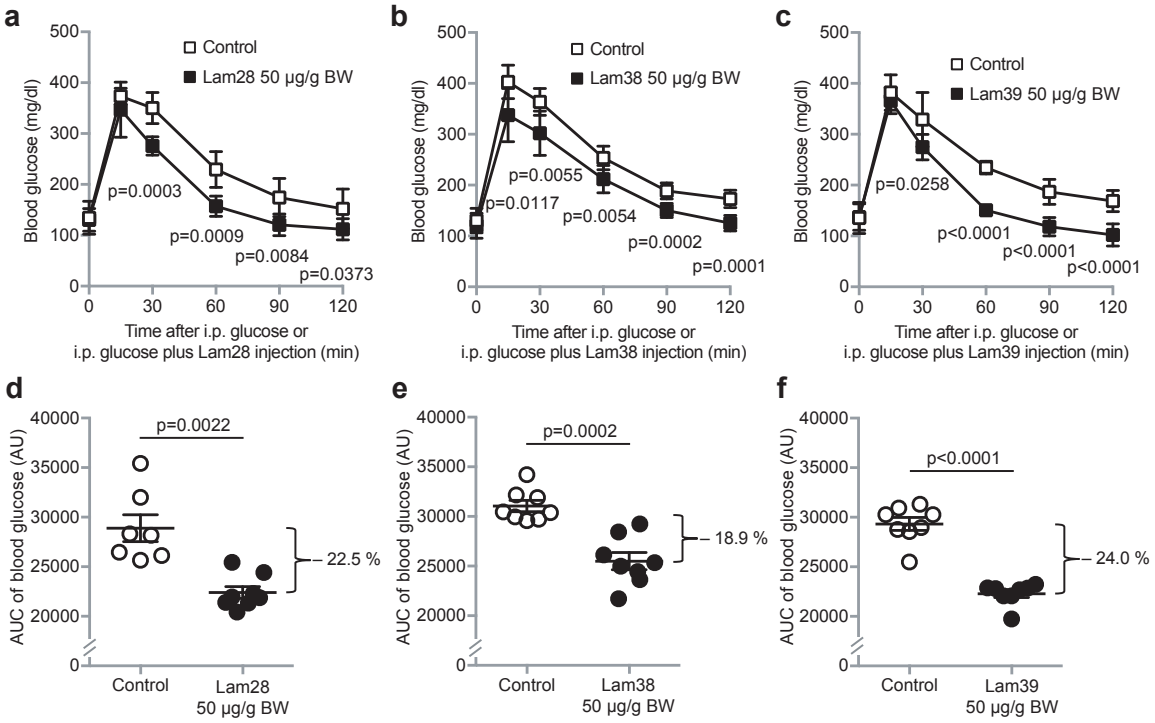

Figure 10: DXM derivatives increase glucose tolerance *in vivo*. (**a**-**c**) Blood glucose concentrations of mice during glucose tolerance (1.5 mg/g BW) tests with or without i.p. administration of the derivatives. n = 8 mice each, except n = 7 mice for control group in (a). (**d**-**f**) AUC calculations of blood glucose levels of (a-c). Statistical testing: (a-c) unpaired two-sided Student's *t*-test with Holm-Bonferroni correction. (d-f) unpaired two-sided Student's *t*-test. For glucose tolerance tests (a-c) all values are mean ± SD, for AUC calculations (d-f) all values are mean ± SEM. Presented experiments were performed by Okka Scholz, assisted by Silke Otter.

The derivatives lowered blood glucose concentrations *in vivo* during glucose tolerance tests, but without inducing hypoglycemic events (**Fig. 10a-c**). The $AUC_{0\text{-}120min}$ showed statistically significant reductions in mice treated with the derivatives Lam28, Lam38 and Lam39 compared to the respective control mice ($p = 0.0022$, $p = 0.0002$, and $p < 0.0001$, respectively) (**Fig. 10d-f**). Here, the strongest effect on glucose tolerance was observed due to the treatment with the derivative Lam39 (**Fig. 10c,f**).

5.3.3 Dose-dependent effect of the derivative Lam39 on blood glucose concentrations

To further investigate the effect of the derivative Lam39 on blood glucose concentrations of C57BL/6 mice, additional glucose tolerance tests with different concentrations were performed (**Fig. 11a-c**). Furthermore, the respective $AUC_{0\text{-}120min}$ were calculated (**Fig. 11d-g**). To find out which plasma concentration is needed to lower the blood glucose

levels in mice, the plasma concentrations of Lam39 during glucose tolerance tests were determined by LC-MS/MS (**Fig. 11h**).

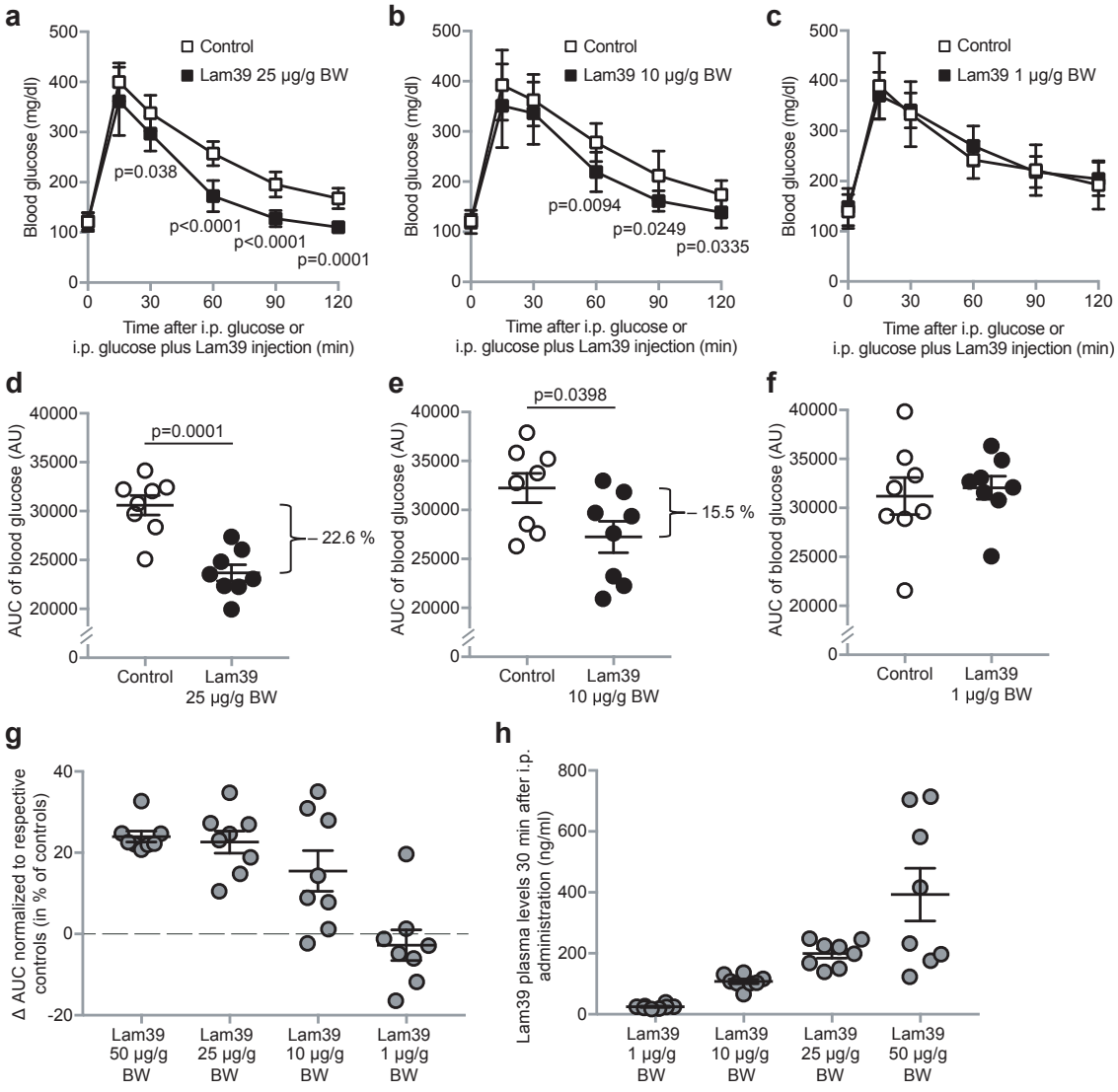

Figure 11: Dose-dependent effect of DXM derivative Lam39 on glucose tolerance *in vivo*. (**a-c**) Blood glucose concentrations of mice during glucose tolerance (1.5 mg/g BW) tests with or without i.p. administration of different concentrations of Lam39. Concentration used is stated in the respective figure panel. n = 8 mice each. (**d-f**) AUC calculations of blood glucose levels of (a-c). (**g**) Δ AUC of blood glucose levels in % of respective controls of (d-f) and (Fig. 10f). (**h**) Plasma concentrations of Lam39 30 min after i.p. administration of different concentrations of Lam39. Statistical testing: (a-c) unpaired two-sided Student's *t*-test with Holm-Bonferroni correction. (d-f) unpaired two-sided Student's *t*-test. All values are mean ± SEM, except for glucose tolerance tests (a-c) in which all values are mean ± SD. Presented experiments were performed by Okka Scholz, assisted by Silke Otter.

At a concentration of 25 µg/g body weight (BW) a blood glucose-lowering effect was observed upon treatment with the derivative Lam39 (**Fig. 11a**), whereas at 10 µg/g BW

there was still a slight effect on glucose tolerance in mice (**Fig. 11b**). At a concentration of 1 µg/g BW no blood glucose-lowering effect was observed (**Fig 11c**). The $AUC_{0\text{-}120min}$ showed statistically significant reductions in the mice treated with 25 µg/g BW and 10 µg/g BW compared to the respective control mice ($p = 0.0001$ and $p = 0.0398$, respectively) (**Fig. 11d,e**). Thus, the derivative Lam39 decreased blood glucose levels and thus the $AUC_{0\text{-}120min}$ in glucose tolerance tests in a dose-dependent manner (**Fig. 11a-g**), correlating with the plasma concentrations 30 minutes after i.p. administration of Lam39 (**Fig. 11h**).

5.3.4 Lower blood glucose concentrations in a diabetic mouse model upon treatment with the derivative Lam39

The derivative Lam39 was further tested for its ability to improve glucose tolerance in a type 2 diabetes mouse model (*db/db* mice). For this, the effect of Lam39 on blood glucose concentrations was measured during i.p. glucose tolerance tests with *db/db* mice (**Fig. 12a**), and furthermore, the respective $AUC_{0\text{-}120min}$ was calculated (**Fig. 12b**).

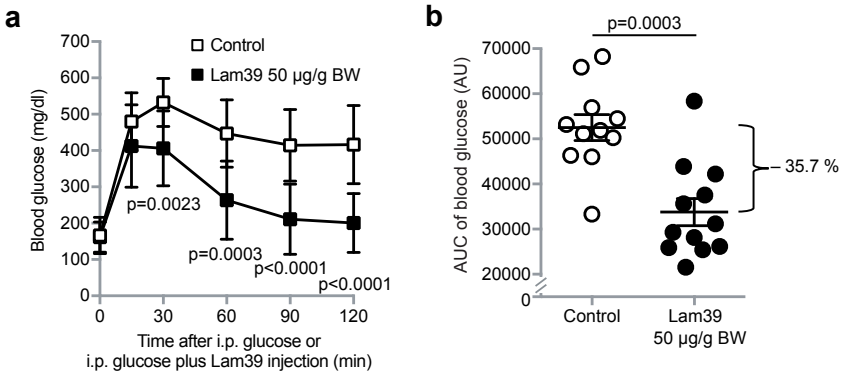

Figure 12: DXM derivative Lam39 improves glucose tolerance in a diabetic mouse model (*db/db* mice). (**a**) Blood glucose concentrations of *db/db* mice during glucose tolerance (1 mg/g BW) test with or without i.p. administration of Lam39. n = 11 mice for control group, n = 12 mice for Lam39 group. (**b**) AUC calculation of blood glucose levels of (a). Statistical testing: (a) unpaired two-sided Student's *t*-test with Holm-Bonferroni correction. (b) unpaired two-sided Student's *t*-test. For glucose tolerance test (a) all values are mean ± SD, for AUC calculation (b) all values are mean ± SEM. Presented experiments were performed by Okka Scholz, assisted by Silke Otter.

The derivative Lam39 lowered blood glucose concentrations in *db/db* mice during a glucose tolerance test, but without inducing hypoglycemic events (**Fig. 12a**). The $AUC_{0\text{-}120min}$ showed a statistically significant reduction in mice treated with Lam39 compared to control mice ($p = 0.0003$) (**Fig. 12b**).

5.4 Blood-brain barrier permeability of dextromethorphan derivatives and effect on behavior of mice

Since DXM and DXO are able to pass the BBB and can induce central nervous side effects in higher concentrations, the distribution of the derivatives to the central nervous system (CNS) of C57BL/6 mice was measured. Additionally, two neurological tests (rotarod test and hanging-wire test) were performed to investigate the neurological impairment of C57BL/6 mice after i.p. administration of Lam28, Lam38, and Lam39.

5.4.1 The derivatives reveal a reduced blood-brain barrier penetration

Firstly, the BBB permeability of the three derivatives was measured. For this, 30 minutes after i.p. administration of the derivatives, the CSF was collected from the *cisterna magna* of C57BL/6 mice while blood was taken from their left cardiac ventricle (**Fig. 13a**). To determine the respective concentrations, the collected CSF and plasma samples were analyzed by LC-MS/MS. Subsequently, the ratios between CSF concentrations and plasma concentrations were determined (**Fig. 13b,c**) and compared to the original drug.

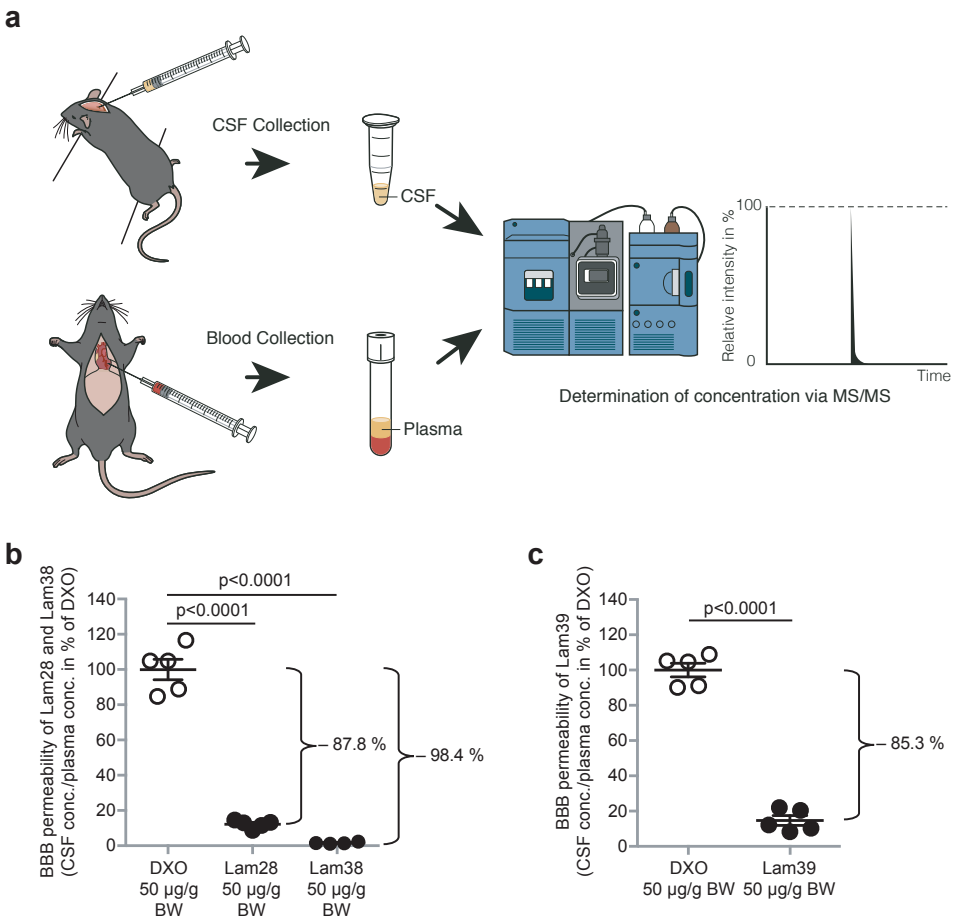

Figure 13: DXM derivatives display reduced blood-brain barrier (BBB) permeability. (**a**) Workflow of determination of BBB permeability of the derivatives. Cerebrospinal fluid (CSF) was taken from the *cisterna magna* while blood was taken from the heart in order to determine the concentrations of DXO, Lam28, Lam38 and Lam39 by liquid chromatography-tandem mass spectrometry (LC-MS/MS). CSF and blood samples were taken 30 min after i.p. administration of the derivatives. Figure was drafted by Okka Scholz, and illustrated by Yousun Koh. (**b**,**c**) BBB permeability of Lam28, Lam38 and Lam39 compared to DXO. n = 5 mice for DXO, Lam28 and Lam39, n = 4 mice for Lam38. Statistical testing: (b) one-way ANOVA followed by Dunnett's multiple comparison test. (c) unpaired two-sided Student's *t*-test. All values are mean ± SEM. Presented experiments were performed by Okka Scholz.

The derivatives Lam28, Lam38 and Lam39 displayed significant reduced ratios between CSF and plasma concentrations compared to DXO ($p < 0.0001$ each) (**Fig. 13b,c**). Thus, the distribution of the derivatives to the CNS was reduced compared to the original drug.

5.4.2 The derivatives do not induce behavioral changes characteristic of the original drug

To further investigate the influence of the derivatives on the behavior of C57BL/6 mice, two different neurological tests were performed. During a rotarod test, the motor coordination and balance of mice was measured. For this, 30 minutes after i.p. administration of the derivatives, treated mice were put on a rotating and accelerating rod, and the time was measured that the mice run on the rod without falling down (**Fig. 14a**).

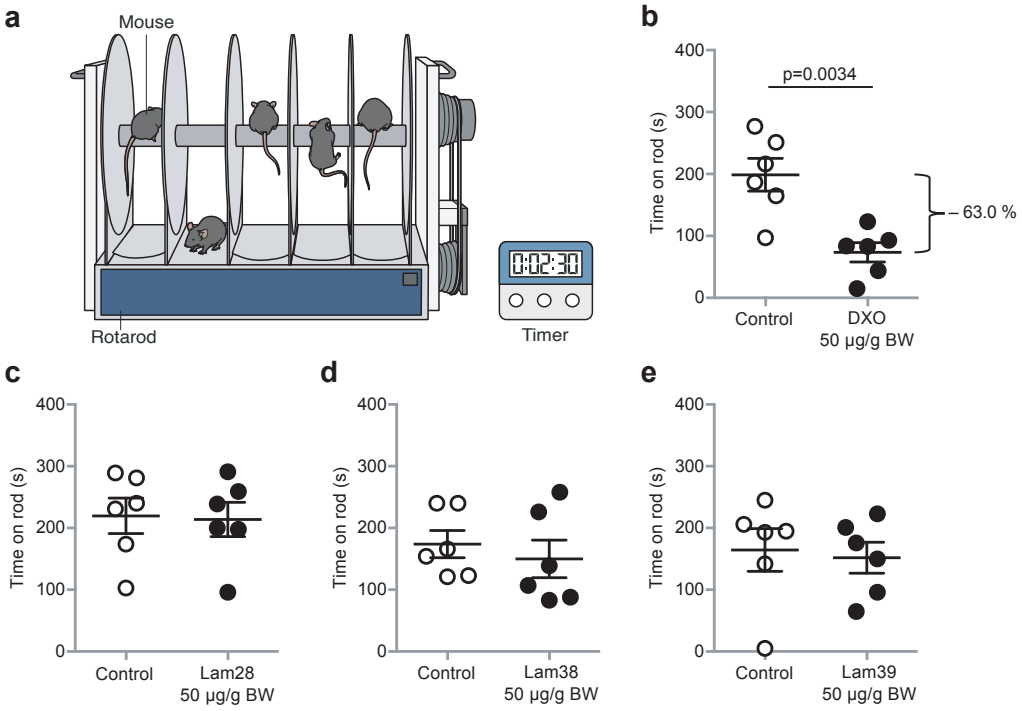

Figure 14: DXM derivatives do not impair motor coordination and balance of mice. (**a**) Illustration of a rotarod device. Figure was drafted by Okka Scholz, and illustrated by Yousun Koh. (**b-e**) 30 min after i.p. administration of (b) DXO, (c) Lam28, (d) Lam38, and (e) Lam39, mice were put on a rotating and accelerating rotarod device, and the time mice could stay on the rod was measured. n = 6 mice each. Statistical testing: (b-e) unpaired two-sided Student's *t*-test. All values are mean ± SEM. Presented experiments were performed by Okka Scholz, assisted by Silke Otter.

DXO significantly reduced the time that mice were able to run on the rotating rod ($p = 0.0034$) compared to the control mice (**Fig. 14b**). In contrast to DXO, the three derivatives did not display any differences compared to the respective control mice, thus the time on rod was not reduced (**Fig. 14c-e**).

Secondly, a hanging-wire test was performed to measure the muscle strength and condition of mice. For this, 30 minutes after i.p. administration of the derivatives, treated mice were put on a grid that was subsequently turned upside-down, and the time was measured that the mice hold on the grid without falling down (**Fig. 15a**).

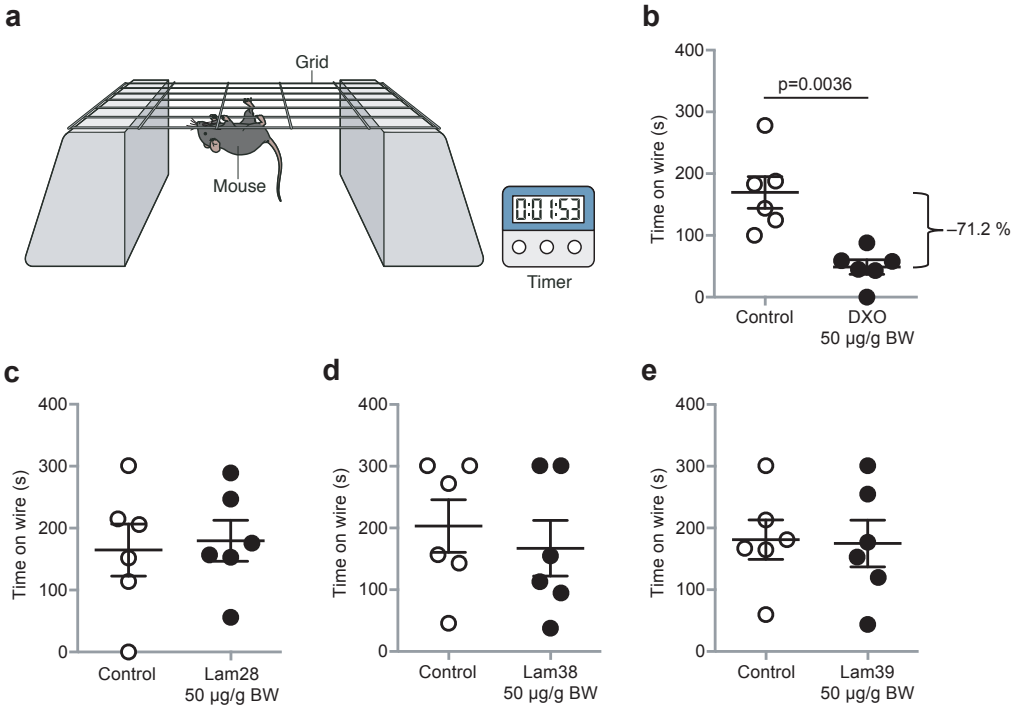

Figure 15: DXM derivatives do not impair muscle strength and condition of mice. (**a**) Illustration of experimental setup of a hanging-wire test. Figure was drafted by Okka Scholz, and illustrated by Yousun Koh. (**b-e**) 30 min after i.p. administration of (b) DXO, (c) Lam28, (d) Lam38, and (e) Lam39, mice were put on a grid, which was turned 180 degrees, and the time mice could hang on the grid was measured. n = 6 mice each. Statistical testing: (b-e) unpaired two-sided Student's *t*-test. All values are mean ± SEM. Presented experiments were performed by Okka Scholz, assisted by Silke Otter.

DXO significantly reduced the time that mice were able to hold on the grid (p = 0.0036) compared to the control mice (**Fig. 15b**). Differences between the three derivatives and the respective control mice could not be detected, thus the time on wire was not reduced (**Fig. 15c-e**). Hence, in both tests, the behavioral changes observed in mice treated with DXO were absent in mice treated with the three derivatives.

5.5 Effect of dextromethorphan derivative Lam39 on pancreatic islet cell survival

T2DM is characterized by a decline of pancreatic islets, leading to diabetes progression and eventually, diabetes manifestation. Next to insulin secretory defects, this process involves islet cell dedifferentiation as well as islet cell death [17, 44, 108, 109, 114]. Therefore, it was important to investigate the effects of the lead compound Lam39 on pancreatic islet cell viability. For this, isolated mouse and human pancreatic islets were incubated with Lam39, and islet cell death was measured by laser scanning microscopy (LSM)-based live cell imaging of live and dead cells.

5.5.1 The derivative Lam39 protects mouse pancreatic islets from cell death

Firstly, the long-term effect of Lam39 on pancreatic islet cell viability under standard cultivation conditions was studied. For this, isolated mouse islets were incubated with or without Lam39 for 66 hours (**Fig. 16a,b**). To analyze whether the derivative even affects STZ-induced islet cell death, isolated mouse islets were incubated with the β-cell toxin STZ either alone or in combination with Lam39 (**Fig. 16c,d**).

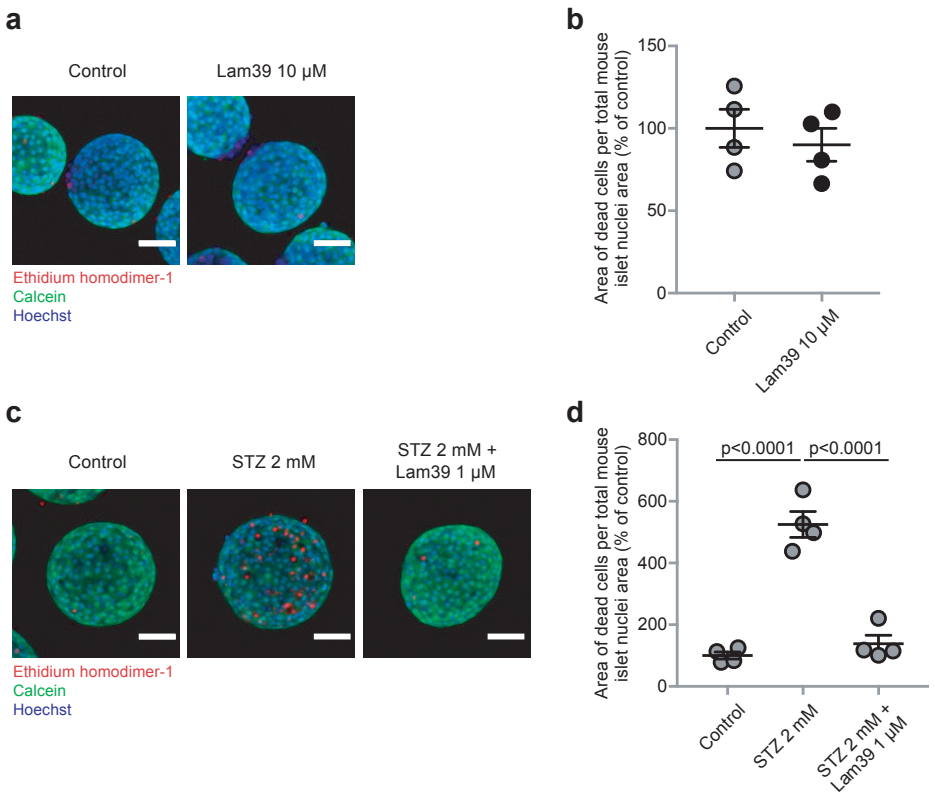

Figure 16: DXM derivative Lam39 exerts protective effects in mouse pancreatic islets. (**a**) Representative laser scanning microscopy (LSM) images (maximum intensity projections) of mouse pancreatic islets (n ≥ 63 islets each) incubated with or without 10 µM Lam39 for 66 h. Blue (Hoechst), nuclei; red (ethidium homodimer-1), dead cells; green (calcein), viable cells. (**b**) Area of dead cells in mouse pancreatic islets treated as described in (a). n = 4 islet batches each with 15-17 islets per batch for each group. (**c**) Representative LSM images (maximum intensity projections) of mouse pancreatic islets (n ≥ 48 islets each) incubated with or without 2 mM STZ either alone or in combination with 1 µM Lam39 for 24 h. Same staining as in (a). (**d**) Area of dead cells in mouse pancreatic islets treated as described in (c). n = 4 islet batches each with 10-15 islets per batch for each group. Statistical testing: (b) unpaired two-sided Student's *t*-test. (d) one-way ANOVA followed by Tukey's multiple comparison test. All values are mean ± SEM. (a,c) Scale bars, 50 µm. Presented experiment for panel (a,b) was performed by Silke Otter. Presented experiment for panel (c,d) was performed by Laura Wörmeyer.

Under standard cultivation conditions for 66 hours, the derivative Lam39 did not decrease islet cell survival (**Fig. 16a,b**). When mouse islets were treated with STZ, the derivative was able to significantly reduce islet cell death ($p < 0.0001$) (**Fig. 16c,d**). Thus, the derivative Lam39 could prevent STZ-induced pancreatic islet cell death.

5.5.2 The derivative Lam39 protects human pancreatic islets from cell death

To study whether there is also a protective effect of the derivative Lam39 on human islets, pancreatic islet preparations isolated from a human donor with T2DM (**Fig. 17a,b**) as well as from a healthy human donor (**Fig. 17c,d**) were incubated with STZ either alone or in combination with Lam39. Additionally, the effect of Lam39 on islet cell survival was compared to the existing anti-diabetic drug exendin-4 (**Fig. 17c,d**).

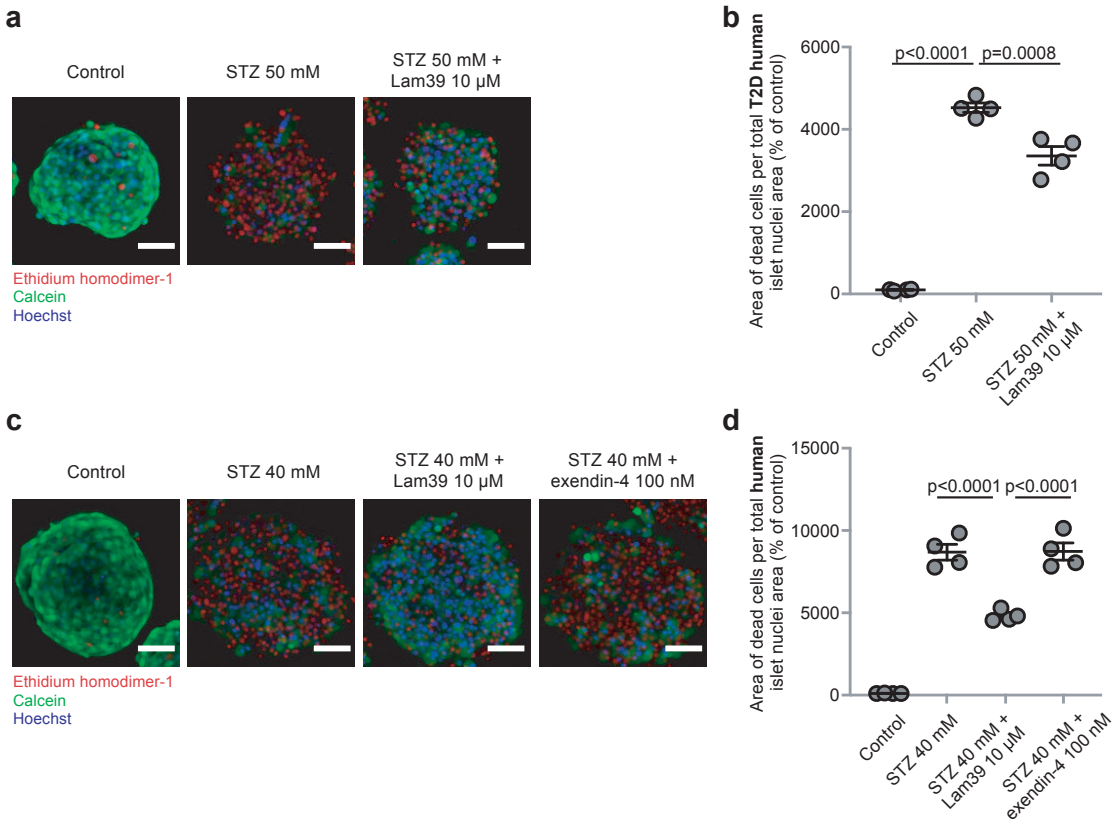

Figure 17: DXM derivative Lam39 exerts protective effects in human pancreatic islets. (**a**) Representative laser scanning microscopy (LSM) images (maximum intensity projections) of type 2 diabetic (T2D) human pancreatic islets (n ≥ 52 islets each) incubated with or without 50 mM STZ either alone or in combination with 10 µM Lam39 for 24 h. Blue (Hoechst), nuclei; red (ethidium homodimer-1), dead cells; green (calcein), viable cells. (**b**) Area of dead cells in T2D human pancreatic islets treated as described in (a). n = 4 islet batches each with 10-22 islets per batch for each group. (**c**) Representative LSM images (maximum intensity projections) of human pancreatic islets (n ≥ 55 islets each) incubated with or without 40 mM STZ either alone or in combination with 10 µM Lam39 or 100 nM exendin-4 for 24 h. Same staining as in (a). (**d**) Area of dead cells in human pancreatic islets treated as described in (c). n = 4 islet batches each with 12-18 islets per batch for each group. Islet donors: (a,b) 42-year-old female with type 2 diabetes mellitus (T2DM), BMI 40.3 kg/m^2. (c,d) 49-year-old male, BMI 34,8 kg/m^2. Statistical testing: (b,d) one-way ANOVA followed by Tukey's multiple comparison test. All values are mean ± SEM. (a,c) Scale bars, 50 µm. Presented experiments were performed by Laura Wörmeyer.

The derivative Lam39 was able to significantly reduce the degree of STZ-induced cell death in human islets isolated from an individual with T2DM ($p = 0.0008$) (**Fig. 17a,b**). Moreover, Lam39 displayed a significantly increased islet cell protective effect compared to exendin-4 ($p < 0.0001$) (**Fig. 17c,d**). Thus, the derivative Lam39 was able to protect human pancreatic islets against cell death induced by STZ treatment, whereas an existing and commonly used anti-diabetic drug did not show a protective effect.

5.6 Pharmacokinetic profile of the dextromethorphan derivative Lam39

To investigate the *in vivo* pharmacokinetic profile of Lam39, plasma concentrations were measured in C57BL/6 mice over a period of five hours, and compared to the original drug (**Fig. 18a,b**). For this, the derivative was administered i.p. and subsequently blood was collected. To determine the respective concentrations, the collected plasma samples were analyzed by LC-MS/MS.

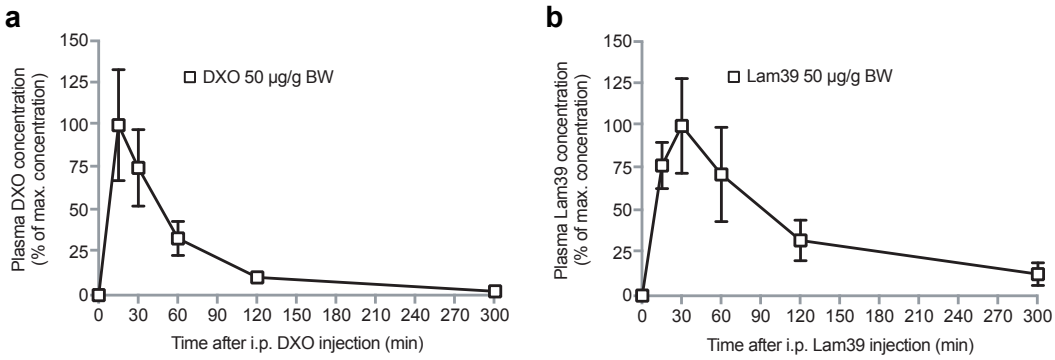

Figure 18: DXM derivative Lam39 displays a higher elimination half-life compared to DXO. (**a,b**) Plasma concentrations of DXO and Lam39 (in % of maximum concentration) 15, 30, 60, 120, and 300 min after i.p. administration. Concentration used is stated in the respective figure panel. n = 5 mice each. All values are mean ± SD. Presented experiments were performed by Okka Scholz.

With DXO, the highest plasma concentrations were detected 15 minutes after i.p. administration, the elimination half-life was around 45 minutes, and after five hours, almost the entire amount of the molecule was eliminated from the blood (**Fig. 18a**). The highest plasma levels of Lam39 were measured 30 minutes after i.p. injection. One hour after administration, around 70% of the maximum concentration was still detectable in the blood, and the elimination half-life was approximately one and a half hours. Five hours after injection, around 15% of the maximum concentration remained in the plasma (**Fig. 18b**).

6. Discussion

6.1 Dextromethorphan and its novel derivatives as a potential drug for diabetes treatment

The aim of this study was to develop novel derivatives of the over-the-counter (OTC) drug dextromethorphan (DXM) and thus make the original drug impermeable to the blood-brain barrier (BBB) to avoid central nervous side effects, but without losing the positive effects of the molecule on diseased peripheral tissues. Since the BBB permeability of DXM and the associated neurological impairment [197, 198] represent an exclusion criterion for an anti-diabetic drug that needs to be taken on a daily basis, the structure of the original drug was modified using medicinal chemistry (**Fig. 5**). The novel derivatives were subsequently characterized in several biological and functional tests, especially *in vivo* tests, and thus a gradual optimization of the molecular structure was performed. The goal was achieved by adding polar basic nitrogen-containing residues at position two of the molecule, leading to a substantially reduced distribution to the central nervous system (CNS) and thus reduced CNS-related side effects. Furthermore, the new derivatives maintained the properties of DXM that were previously shown to be useful for the treatment of diabetes mellitus [144, 197, 198]. This includes the ability to selectively increase glucose-stimulated insulin secretion (GSIS), reduce blood glucose excursions without inducing life-threatening hypoglycemia as well as protect pancreatic islets from cell death. Thus, by modifying the structure of the original drug and excluding the central nervous side effects the application of novel DXM derivatives for the treatment of diabetes was facilitated.

DXM and its derivatives are based on the structure of morphinans, which are mainly in use for the treatment of pain and inflammatory diseases [215-217]. The developed molecules are structurally different compared to anti-diabetic drugs that are currently available on the market. DXM, the starting substance of the novel derivatives, is a commonly used medication for the treatment of several diseases, including acute cough, diabetic neuropathic pain as well as neurological and neuropsychiatric disorders, and is already in clinical use for more than five decades. Besides its proven medical effects, DXM has a good safety profile, even in pediatric patients [16, 183, 186, 187, 192]. Furthermore, DXM was recently shown to selectively enhance GSIS and lower blood glucose concentrations in patients with type 2 diabetes mellitus (T2DM) [197, 198]. Thus, DXM has already been tested in the human disease setting, indicating that the developed DXM derivatives have a higher chance to work in patients compared to totally new molecules with chemical structures that have never been tested in humans.

Regarding the pharmacokinetic profile of the developed DXM derivatives, the molecules were rather quickly metabolized and eliminated from the blood plasma after intraperitoneal (i.p.) administration in mice (**Fig. 18b**). The highest plasma concentration of the lead compound Lam39 was measured approximately 30 minutes after i.p. injection, and the elimination half-life, that is the time required for the amount of agent in the body to decrease by half, was around one and a half hours. Five hours after administration, approximately 15% of the maximum concentration was still present in the plasma. Since an anti-diabetic drug needs to be taken over a longer period of time as well as on a regular basis, it would be beneficial to extend the elimination half-life of the agent and thus reduce the frequency of drug intake. For DXM, a possibility to increase the bioavailability of the molecule is already established. DXM is usually quickly metabolized to its major O-demethylated metabolite dextrorphan (DXO), catalyzed by the liver enzyme cytochrome P450 2D6 (CYP2D6). Due to this rapid hepatic first-pass metabolism and subsequent elimination from the blood, the bioavailability of DXM is rather limited [185]. In order to increase plasma concentration and thus systemically available DXM, the coadministration with low dose of quinidine is suggested, an agent that is able to suppress the O-demethylation of DXM by inhibiting CYP2D6. Consequently, there is an elevation and prolongation of DXM plasma levels due to the reduction of its metabolization and thus an extended elimination half-life of approximately 13 hours. This allows to maintain more consistent DXM plasma concentrations and bioavailability, leading to an increased ability to reach target sites and a less frequent intake of the drug [185, 218]. The combination of DXM hydrobromide and quinidine sulfate was approved by the US Food and Drug Administration in 2010 as well as by the European Medicines Agency in 2013 for the treatment of pseudobulbar affect. Fixed-dose DXM/quinidine capsules (Neudextra®) enable quinidine to suppress the metabolization of DXM, leading to higher plasma levels of DXM without using a larger dose of the drug [185, 188, 189]. In clinical trials, the combination of DXM and quinidine further demonstrates therapeutic effects on diabetic peripheral neuropathic pain as well as agitation in patients with Alzheimer disease [187, 219].

Another possibility to increase the duration of effective plasma concentrations of the developed DXM derivatives and thus extend the period of therapeutic effect of the molecules could be the development of an extended-release capsule product. This type of treatment is already established for the therapy of other diseases, including Parkinson disease [220-223]. The benefit of such formulation is the inclusion of both, immediate-release and extended-release beads to provide an initial rapid onset of the effect as well as a subsequent continuous release of the drug to maintain more constant therapeutic plasma concentrations for a prolonged duration. Furthermore, the frequency of oral intake is reduced due to the extended release of the drug.

Since the novel DXM derivatives were able to protect human islets against cell death, these agents are not exclusively interesting for the treatment of T2DM that is characterized by the progressive demise of insulin-producing β-cells [44, 108-110], but also for patients who suffer from type 1 diabetes mellitus (T1DM). The latter is characterized by the immune-mediated destruction of pancreatic β-cells, resulting in the requirement of lifelong replacement of endogenous insulin [88, 89]. The risk to develop T1DM has become increasingly predictable, as it is known that the disease usually has a preclinical and presymptomatic phase that can be identified by circulating islet autoantibodies, which are detectable in the blood before disease onset [224-227]. An early diagnosis of T1DM offers the possibility for an early therapeutic intervention and β-cell protection, and may preserve β-cell function and mass. Thus, since a decline in functional β-cell mass occurs in both types, such a β-cell protective agent would be relevant for the treatment of T1DM as well as T2DM, and would have the potential to delay or even stop diabetes progression by inhibiting β-cell death.

Two randomized clinical trials have shown that the original drug DXM is able to improve insulin secretion and glucose tolerance even in patients with T2DM [197, 198]. Firstly, individuals treated with a single high dose of DXM (270 mg) show improved glucose tolerance and enhanced maximum serum insulin concentrations during an oral glucose tolerance test (OGTT) compared to placebo treatment [197]. Furthermore, a single low dose of DXM (60 mg) is sufficient to enhance the blood glucose-lowering effect of sitagliptin, a dipeptidyl peptidase-4 (DPP-4) inhibitor, when compared to sitagliptin alone. The combination of the two agents improves glucose tolerance as well as increases the serum insulin concentrations within the first phase of an OGTT stronger than the sole administration of sitagliptin. Thus, DXM and sitagliptin in combination might restore the early phase of insulin secretion in patients with T2DM [198]. These findings suggest an additive action of DXM and sitagliptin, indicating that DXM and its developed derivatives could serve as a valuable adjunct therapy for currently available treatment options for diabetes, including DDP-4 inhibitors. Therefore, it is important to investigate the potential additive effect of the novel derivatives and other existing anti-diabetic drugs.

To sum up, the DXM derivatives might represent potential new drugs for the treatment or adjunct treatment of diabetes, since the structure of the original drug was modified as to exclude CNS-related side effects while maintaining or even improving the beneficial effects of the molecule on peripheral tissues, especially the pancreas. The developed derivatives are structurally new agents, but based on an existing and commonly used drug with a good safety profile, and furthermore, the possibility to increase the bioavailability of DXM might be transferable on the novel derivatives. The latter are

interesting not solely for the treatment of T2DM, but also for other types that are accompanied by a decline of pancreatic β-cells.

6.2 Advantages of dextromethorphan and its novel derivatives over existing anti-diabetic drugs

The currently available anti-diabetic drugs have several limitations. Some medications can lead to adverse side effects, especially life-threatening hypoglycemia due to an elevation of insulin secretion in a glucose-independent manner [29, 168, 169]. Furthermore, existing anti-diabetic drugs are not able to sustainably restore β-cell function and thus cannot durably maintain glycemic control [176-180]. Even with glucagon-like peptide-1 (GLP-1) receptor agonists as well as DPP-4 inhibitors there is no clinically relevant improvement of β-cell function and maintenance of β-cell mass [177, 180]. Therefore, no anti-diabetic medications are currently available that are able to stop the progression of diabetes. Additionally, current diabetes therapy does not adequately prevent the development of long-term complications that are associated with the disease [182].

Our developed DXM derivatives might have the potential to fill this gap. Firstly, the blood glucose-lowering effect of DXM/DXO and its novel derivatives occurs in a glucose-dependent manner, whereby life-threatening hypoglycemic events are avoided. DXM/DXO administration does not induce hypoglycemia even in the fasted state in mice and humans [144, 197, 198]. Notably, the insulinotropic effect of the developed DXM derivatives could also be observed only under stimulatory glucose concentrations, whereas the basal insulin secretion was largely unaffected (**Fig. 6-8**), and furthermore, the treatment of fasted mice did not induce hypoglycemia (**Fig. 10-12**).

Additionally, the treatment of pancreatic islets with DXM/DXO increases islet cell survival under inflammatory and diabetogenic conditions. Precisely, DXO is able to protect isolated human pancreatic islets against cytokine-induced cell death, and moreover, the long-term treatment with DXM lowers the rate of islet cell death in diabetic mice (*db/db* mice) [197]. Other studies indicated that treatment of diabetic mice, induced by high-fat diet as well as the β-cell toxin streptozotocin (STZ), with the N-Methyl-D-Aspartate (NMDA) receptor antagonist memantine also leads to an increased pancreatic islet cell survival [201]. Thus, DXM/DXO as well as NMDA receptor inhibition increase survival of mouse and human pancreatic islets, providing a possible mechanism by which DXM attenuates the progression of diabetes in diabetic mice [144, 197, 201]. Furthermore, the novel DXM derivative Lam39 was able to protect isolated mouse and human pancreatic islets from cell death induced by the β-cell destructive toxin STZ (**Fig. 16,17**), an agent that causes β-cell

death *in vitro* and thus induces a crucial clinical feature of diabetes [228, 229]. Although a higher concentration of STZ was required to induce cell death in human islets compared to mouse islets, Lam39 was still able to significantly increase human islet cell survival (**Fig. 17**). There was even a protective effect on pancreatic islets isolated from an individual with T2DM (**Fig. 17a,b**), and notably, the derivative was able to protect human islets from cell death, whereas the existing anti-diabetic drug exendin-4, a GLP-1 receptor agonist, did not show a protective effect (**Fig. 17c,d**).

Another important point is that the original drug DXM also shows beneficial effects on the long-term complications of diabetes, including macrovascular and microvascular complications. Preclinical as well as clinical studies indicated that DXM has anti-oxidative and anti-inflammatory features [144, 196, 204]. Notably, this drug is able to increase the endothelial function in two clinical trials [144, 204], and further reduces hypertension even in humans [195, 202], suggesting that DXM has the potential to attenuate the development of diabetic cardiovascular (CV) complications. This is of particular interest, since CV diseases represent the most prevalent causes of morbidity and mortality that are associated with T2DM [145, 146]. Additionally, DXM and NMDA receptor antagonists have been suggested for the treatment of other complications that can be caused by chronically elevated blood glucose levels, including diabetic retinopathy, nephropathy as well as painful neuropathies [144, 205-207]. Notably, studies suggested that these compounds might also be useful for adjunct cancer treatment [208-210]. This could be an advantageous characteristic, as diabetes is associated with an increased risk of several cancer types [150]. Therefore, these findings suggest that DXM and possibly its novel derivatives reveal multiple effects that could be beneficial for patients with diabetes.

Diabetes is currently classified into two main forms: T1DM and T2DM, but particularly T2DM is a complex and heterogenous disease, and patients who suffer from this disease have a variety of phenotypes as well as susceptibilities to diabetes-associated complications. Recent studies proposed to assign patients to different subgroups of T2DM with distinct clinical characteristics, particularly to improve clinical management and develop subgroup-specific treatment strategies [230]. Furthermore, recent data-driven cluster analysis proposed five replicable clusters of patients with diabetes that reveal distinct disease progression as well as risk of diabetes-associated complications. Notably, two of five clusters are characterized by insulin deficiency or low insulin secretion as well as relatively low body mass index (BMI) and thus without predominant obesity compared to other clusters. Additionally, individuals within these two clusters show poor blood glucose control, and furthermore, ketoacidosis at diagnosis is most frequent within these patients [231, 232]. Therefore, the currently available treatment options for T2DM, which aim at substantially reducing the BMI or reducing blood glucose levels due to ketoacidosis-prone

glucose excretion, especially inhibitors of the sodium-glucose linked transporter 2 (SGLT2), are not the most optimal therapies for patients within these clusters [233, 234]. Moreover, recent analysis based on simple clinical features suggested that the progression of diabetes (probably due to the decline of pancreatic β-cells) proceeds faster when T2DM is diagnosed at a younger age [235]. Therefore, the developed DXM derivatives might have the potential to fill a gap in the currently available treatment options, and might lead to an attenuation of diabetes progression that is caused by the demise of pancreatic β-cells.

All in all, when taken as a glucose-lowering medication, DXM and its developed derivatives may slow down or even prevent diabetes progression due to its islet cell protective effects, and furthermore, these molecules may reduce diabetic long-term complications, including CV diseases. Pancreatic islets represent a main target for the development of new anti-diabetic drugs, as their demise probably leads to the onset as well as the progression of the disease [108-110]. Moreover, CV safety represents an essential requirement for the registration of a novel anti-diabetic medication. Thus, the development of cardioprotective agents that exert positive effects on diabetic macro- as well as microvascular complications is crucial [100, 107]. There is a pressing clinical need for novel anti-diabetic drugs that reveal fewer adverse side effects, beneficial effects on diabetic long-term complications as well as β-cell protective properties. Therefore, DXM and particularly its developed derivatives might be a novel strategy for the treatment of patients that suffer from diabetes.

6.3 Potential transfer of modification strategy on peripherally active morphinans in general

DXM is a dextrorotatory morphinan that shows structural similarities to morphine and other opioids, but does not have relevant activity at opioid receptors [184, 185]. Opioids represent powerful drugs for the treatment of severe pain and certain inflammatory diseases. However, the clinical effectiveness of these molecules is limited due to adverse side effects, including sedation, analgesic tolerance, addiction as well as opioid-induced hyperalgesia [215-217]. Thus, the indiscriminate activation of opioid receptors leads to pain relief, but also triggers severe adverse side effects. Since more than 30% of Americans suffer from acute or chronic pain, it is not surprising that opioid analgesics currently represent the most commonly prescribed class of drugs in the US. The broad and chronic use of opioids for pain management has recently resulted in a strongly increased incidence of overdoses, addiction as well as mortality, a phenomenon termed opioid crisis [236, 237]. Therefore, the challenge is to selectively reduce or prevent opioid-induced adverse side effects in order to

improve patient safety, but without altering their pain-relieving properties. The first efforts to achieve this goal have been recently described in different studies [215-217, 238-240]. Particularly the structural modification of existing opioids to develop peripherally restricted molecules may prevent central nervous side effects that mainly result from passage of the BBB and following activation of central opioid receptors. For example, it was shown that the opioid morphine can be covalently attached to hyperbranched polyglycerol, leading to a higher molecular weight and hydrophilicity of the molecule and thus to a reduced BBB penetration. In contrast to conventional morphine, this conjugate is able to selectively activate opioid receptors in inflamed peripheral tissue, but not central opioid receptors, and thus diminish pain without inducing central nervous side effects [215].

In addition to the modification of opioids, a cannabinoid-1 receptor (CB_1R) inverse agonist has been successfully designed as to not penetrate the BBB and thus not lead to central nervous side effects. Different studies suggested that peripherally restricted blockade of CB_1Rs reduces ethanol intake as well as appetite and body weight, and improves glycemic control, indicating that these molecules could have therapeutic potential in the treatment of alcoholism, obesity, and T2DM [241-243].

During this study, novel peripherally restricted derivatives of the morphinan DXM were designed in order to exclude its central nervous side effects while maintaining or even improving its anti-diabetic and islet cell protective properties. DXM derivatives with polar basic nitrogen-containing residues were still able to exert the peripheral effects of the original drug, but without substantial distribution to the CNS. Therefore, these substituents could be of potential interest for the design of peripherally active molecules, such as morphinans, in general.

6.4 Future directions

Recent studies indicated that DXM and DXO enhance GSIS and glucose tolerance via the blockade of pancreatic NMDA receptors. Data from mice lacking pancreatic NMDA receptors (specific deletion of the *Grin1* gene encoding the obligatory GluN1 subunit of NMDA receptors) provided evidence that DXO requires these receptors for acting as an insulin secretagogue as well as blood glucose-lowering drug [197]. The developed imidazole-containing DXM derivative Lam39 also inhibited receptor currents of heterologous expressed NMDA receptors (GluN1/GluN2D) in *Xenopus laevis* oocytes in a dose-dependent manner, but to a lesser extent compared to DXM and DXO (IC_{50} values of dose-response curves: DXO 0.21 ± 0.07 µM, DXM 4.17 ± 0.61 µM, Lam39 337 ± 29.12 µM). Thus, the NMDA receptor represents probably not the only target that mediates the

insulinotropic, blood glucose-lowering as well as islet cell protective effects of Lam39, leading to the conclusion that another drug target must be involved.

Conducted radioligand binding studies indicated that the lead compound Lam39 acts as an antagonist at the α_{2A}-adrenergic receptor (α_{2A}-AR) in a dose-dependent manner (IC_{50} value: 1,67 µM), which represents a member of the G protein-coupled receptor (GPCR) superfamily [244, 245]. Pancreatic islets are highly innervated by adrenergic nerve branches, and furthermore, α_{2A}-ARs are expressed in both, mouse and human β-cells [28, 246]. Several members of the GPCR superfamily are known to modulate the secretion of insulin from pancreatic β-cells [247]. Studies reported that pancreatic α_{2A}-ARs play a crucial role in inhibition of insulin secretion following treatment with agonists of the receptor or stimulation of sympathetic pancreatic nerves, leading to an impaired glucose tolerance [248-251]. Additionally, overexpression of α_{2A}-ARs has been associated with an impaired GSIS, elevated fasting blood glucose levels as well as an increased risk to develop T2DM [252, 253]. It was suggested that the activation of α_{2A}-ARs expressed on the surface of pancreatic β-cells inhibits insulin secretion by modulating cyclic adenosine monophosphate (cAMP) levels. The activated receptor couples to inhibitory G proteins (G_i), leading to an inhibition of adenylyl cyclase and thus to reduced conversion of ATP to cAMP, and eventually decreased protein kinase A (PKA)-mediated exocytosis of insulin secretory granules [247, 253, 254]. Moreover, activation of the protein phosphatase calcineurin, which interferes with insulin granule recruitment, has also been proposed to contribute to the described effect [253, 255]. On the other hand, α_{2A}-AR knockout mice show enhanced insulin secretion, reduced blood glucose levels as well as improved glucose tolerance [256, 257], and pharmacological receptor antagonism lowers blood glucose concentrations while increasing insulin levels by inhibiting active α_{2A}-ARs on β-cells, providing a potential new pathway for therapeutic intervention [253, 258-261]. Hence, the α_{2A}-AR has been identified as a regulator of insulin and blood glucose homeostasis. For long-term clinical use, a receptor antagonist targeting more specifically β-cell α_{2A}-ARs and therefore inducing no central nervous side effects would be preferred. Thus, one possibility could be that Lam39 may exert its insulinotropic and blood glucose-lowering effect due to blockade of pancreatic α_{2A}-ARs, and further might represent a peripherally restricted antagonist of this receptor.

Another issue that has to be addressed is the potential molecular mechanism leading to the protection of pancreatic islets against STZ-induced cell death due to the treatment with Lam39. The β-cell destructive toxin STZ is widely used to induce diabetes in different animal species and thus produce models to study diabetes pathogenesis as well as potential therapies, since the treatment with STZ leads to clinical features in animals that are similar to those associated with diabetes in human individuals [262-265]. Precisely, it selectively destroys pancreatic β-cells due to targeted uptake of STZ into the cell by the

glucose transporter GLUT2 [229, 266, 267]. Various studies indicated that the β-cell toxicity of STZ is mediated by diverse mechanisms, including oxidative stress due to the increased production of reactive oxygen species (ROS), resulting in cellular damage [266, 268-271]. Thus, an anti-oxidant agent would be beneficial to reduce oxidative stress and therefore slow down or even prevent the progressive β-cell dysfunction and death, leading to the onset and further progression of diabetes. Previous preclinical as well as clinical studies reported that DXM is able to reduce oxidative stress, probably due to the inhibition of NADPH oxidase (NOX) activity and the consequent decrease of superoxide production [196, 202, 204, 272, 273], suggesting that DXM and its novel derivatives could serve as protective anti-oxidative agents. Thus, Lam39 may inhibit STZ-induced oxidative stress and cell damage by reducing ROS levels, which leads to an increased β-cell viability, providing a possible mechanism by which Lam39 might attenuate the progression of diabetes.

Since there is evidence that the original drug DXM inhibits atherosclerotic plaque formation in the vascular system of mice [196] as well as increases flow-mediated dilation (FMD) in two clinical trials and thus improves endothelial function [144, 204], it is of particular interest to investigate whether the developed DXM derivatives also exert CV protective effects. To analyze the potential of the derivatives to reduce diabetic CV complications, different experimental approaches and mouse models could be used. Firstly, animal models of human T2DM (*db/db* mice) [200] or T1DM (multiple injections of STZ) [265] could be treated with the derivatives to analyze whether the diabetes-induced CV injury can be reduced or even prevented. To assess the potential CV protection of the derivatives, different parameters could be analyzed, including blood pressure, endothelial function via FMD measurement [274, 275], and various blood parameters, such as pro-inflammatory factors or cholesterol levels. Secondly, the effect of the derivatives on the progression of atherosclerosis could be investigated by using an animal model of this disease. ApoE (apolipoprotein E) knockout mice, which carry an inactive gene that prevents the expression of the protein apoE, develop increased blood levels of cholesterol, and ultimately form atherosclerotic plaques in the aorta [276]. To investigate whether the derivatives are able to slow down or even stop the development of atherosclerosis in apoE knockout mice under obese/prediabetic (high fat diet) as well as diabetic conditions (multiple injections of STZ), the respective mice could be treated with the derivatives and subsequently analyzed via FMD measurement as well as regarding atherosclerotic plaque formation. Thirdly, it could be studied whether the potential CV protective effects of the derivatives depend on endothelial nitric oxide synthase (eNOS), an enzyme that produces the messenger molecule nitric oxide (NO), which is involved in maintaining a functional and intact endothelium as well as counteracts the development of vascular diseases. For this, eNOS-deficient mice, which are characterized by an elevated blood pressure and a reduced

heart rate, could be treated with the derivatives to investigate whether these molecules still exert their potential CV protective effects [277].

To further optimize the novel DXM derivatives in terms of drug safety, *in vitro* pharmacological profiling is currently performed (SafetyScreen44™, provided by Eurofins Pharma Discovery Services). To this end, the interaction of the developed DXM derivative Lam39 with 44 selected off-targets that are recommended by four major pharmaceutical companies is investigated, including GPCRs, ion channels, transporters, enzymes as well as nuclear receptors [278]. This quickly provides human data at an early stage of the drug discovery process and an early identification of undesirable off-target interactions, which may lead to adverse clinical side effects in humans and thus could hinder the development of a potential drug or even lead to market withdrawal if these effects are discovered after its approval. Thus, the goal of this approach is to reduce or eliminate off-target activity while maintaining or even increasing the desired therapeutic effect. This is an important point, since safety-related drug failures remain a major challenge for the pharmaceutical industry. Furthermore, potential drugs that enter the development with lower off-target interactions require less investigative *in vivo* safety studies, leading to fewer delays in development, fewer animals used as well es lower costs [278, 279].

Since there is evidence that the lead compound Lam39 binds to the human potassium voltage-gated channel subfamily H member 2 (*KCNH2*), also known as hERG, and blockade of hERG can elicit cardiac arrhythmias following a prolongation of the QT interval of the electrocardiogram (ECG) [280-282], this molecule is currently further structurally optimized. Thus, a number of novel structural derivatives of Lam39 are synthesized to further reduce the interaction with this off-target, and consequently decrease potential adverse side effects. The latest experiments revealed that it is possible to reduce the binding to hERG by slightly modifying the molecular structure of the existing derivative Lam39 while the ability to selectively increase GSIS *in vitro* is maintained. These derivatives of Lam39 now need to be further tested for their anti-diabetic effects *in vivo*, and additionally, it is important that the newly synthesized derivatives still do not penetrate the BBB and thus do not induce neurological impairment characteristic of the original drug DXM.

6.5 Conclusion

Taken together, it was possible to design and synthesize novel chemical derivatives of DXM that do not penetrate the BBB and thus do not induce CNS-related side effects characteristic of their original drug while the insulinotropic, blood glucose-lowering as well as islet cell protective effects of DXM were maintained or even improved. This goal was achieved by

screening a number of novel chemical entities with the help of different biological and functional tests (especially *in vivo* tests), leading to the gradually optimization of the molecular structure.

There is an urgent need for novel anti-diabetic drugs that have β-cell protective properties, and furthermore, reveal beneficial effects on diabetic long-term complications while inducing fewer adverse side effects. The developed peripherally restricted DXM derivatives might be able to fill this gap, as they *in vitro* and *in vivo* predominantly increased GSIS rather than basal insulin secretion and thus did not cause any life-threatening hypoglycemic events, and moreover, enhanced pancreatic islet cell survival even in human islets. The derivatives could be particularly valuable for subgroups or clusters of patients with diabetes who are characterized by islet cell death as well as insulin secretory defects. Additionally, based on previous reports, which indicated that DXM reveals positive effects on long-term complications associated with diabetes, such as CV endpoints as well as diabetic neuropathy and retinopathy, it is of interest to investigate whether the developed derivatives are also able to target diabetic micro- and macrovascular complications independent of their blood glucose-lowering effects. Notably, the basic nitrogen-containing substituents that were introduced at position two of the original molecule to reduce BBB permeability could further be of potential interest for the development of peripherally active molecules, such as morphinans, in general.

The structural optimization of the lead compound Lam39 is currently in progress to further exclude potential adverse side effects that could impede drug development. With these optimized derivatives additional studies need to be conducted, including the long-term effect on glucose homeostasis and islet cell viability in diabetic mice as well as larger animal models (e.g. pigs) with T2DM, the investigation of effects on CV endpoints and other diabetic long-term complications, and certainly, studies concerning the potential mechanism of action that leads to the beneficial therapeutic effects of the DXM derivatives. To sum up, after further development and optimization of the molecular structure, the derivatives could serve as novel medications for the therapy or adjunct therapy of diabetes, the most common metabolic disease in humans.

7. Supplementary information

7.1 Synthetic procedures of dextromethorphan derivatives

All chemicals were purchased from Sigma-Aldrich unless otherwise noted. Compound identity and purity were determined by NMR spectroscopy, using a Bruker 300 MHz. UHPLC was measured on an Agilent System with the following conditions: ACQUITY UHPLC BEH C18 (1.7 µm) 2.1 mm x 50 mm, temperature: 40 °C, detection: DAD + 6120 Quadrupole, inject-volume: 1 µl, flow: 1.2 ml/min. Solvents: A: water + 0.1% HCOOH; B: ACN + 0.1% HCOOH, gradient: 0 min. 2% B; 0.2 min. 2% B; 2.0 min. 98% B; 2.2 min. 98% B; 2.21 min. 2% B; 2.5 min. 2% B. Purification was carried out on mPLC Büchi Reveleris X2 System: UV-detector (200-500 nM), ELSD-detector (Laser 0.3 mW), reverse phase: Macherey-Nagel Chromabond C18 Flash cartridges (please see experimental part for detailed conditions). The synthesis of Lam28, Lam38 and Lam39 was carried out following the procedures mentioned in patent WO 2017/093519 A1 [283].

7.1.1 Lam28

(1S,9S,10S)-4-methoxy-N,N,17-trimethyl-17-azatetracyclo[7.5.3.$0^{1,10}$.$0^{2,7}$]heptadeca-2,4,6-trien-5-amine hydrobromide

(1*S*,9*S*)-5-iodo-4-methoxy-17-methyl-17-azatetracyclo[7.5.3.$0^{1,10}$.$0^{2,7}$]heptadeca-2,4,6-triene (47.8 g, 120.0 mmol), K_2CO_3 (33.3 g, 240.0 mmol), CuI (6.9 g, 36.0 mmol), L-Proline (84 g, 72.6 mmol) were suspended in DMSO (455.0 ml) and treated with dimethylamine (241.0 ml, 2 M soln. in THF). The resulting mixture was heated at 90 °C in a Parr reactor under nitrogen atmosphere. The reaction progress was monitored by UHPLC and after completion, the reaction mixture was treated with water (1000 ml) and extracted with ethyl acetate (5 x 200 ml) while maintaining the pH > 9. The organic phase was washed with 300 ml 5% NH_4OH, dried over $MgSO_4$ and concentrated under reduced pressure, affording 32.7 g crude product with 50% purity by UHPLC and ^{1}H-NMR. The crude compound was purified by flash column chromatography on reverse phase silica gel using H_2O (+ 0.1 HCOOH)/acetonitrile as eluents. After purification, 34.7 g product were obtained as formate salt with purity > 95% by ^{1}H NMR and UHPLC. 24.6 g of the pure product was further dissolved in 200 ml $CHCl_3$ and neutralized with 30 ml 0.5 M NaOH (pH = 9), yielding 21.3 g product as a free amine with purity > 95% by ^{1}H NMR. In order to obtain the corresponding hydrobromic salt, 21.3 g of the obtained product were suspended in water (40 ml) and

treated with 11.44 g of 48% aq. HBr. After final lyophilization, 25.22 g of the desired product were obtained with purity > 95% by ^{1}H NMR and UHPLC.

^{1}H NMR (300 MHz, MeOD-*d4*): δ 7.13 (s, 1H), 6.98 (s, 1H), 3.93 (s, 3H), 3.69–3.68 (m, 1H), 3.22–3.17 (m, 3H), 2.97 (s, 3H), 2.94 (s, 6H), 2.83–2.70 (m, 1H), 2.57 (d, *J* = 13.8 Hz, 1H), 2.11 (d, *J* = 11.5 Hz, 1H), 1.98 (t, *J* = 12.6 Hz, 1H), 1.76–1.42 (m, 6H), 1.32 (tt, *J* = 2.9, 9.6 Hz, 1H), 1.16 (dq, *J* = 3.8, 12.6 Hz, 1H); ^{13}C NMR (75 MHz, MeOD-*d4*): δ 153.0, 138.4, 136.0, 127.7, 120.1, 110.1, 61.8, 56.5, 44.7, 41.3, 37.1, 36.3, 26.9, 26.9, 22.9; MS (*m/z*): $[M+H]^{+}$ calcd. for $C_{20}H_{31}N_2O$, 315.2; found, 315.2.

7.1.2 Lam38

(1S,9S,10S)-4-methoxy-17-methyl-5-(pyrrolidin-1-yl)-17-azatetracyclo[7.5.3.0^{1,10}.0^{2,7}]heptadeca-2,4,6-triene dihydrobromide

(1*S*,9*S*)-5-iodo-4-methoxy-17-methyl-17-azatetracyclo[7.5.3.0^{1,10}.0^{2,7}]heptadeca-2,4,6-triene (11.0 g, 27.6 mmol), K_2CO_3 (7.7 g, 55.0 mmol), CuI (1.6 g, 8.4 mmol), L-Proline (1.9 g, 16.8 mmol) were suspended in DMSO (110.0 ml) and treated with pyrrolidine (7.9 g, 110.0 mmol). The resulting mixture was heated at 100 °C in a Parr reactor under nitrogen atmosphere. The reaction progress was monitored by UHPLC and after completion, the reaction mixture was treated with water (600 ml) and extracted with ethyl acetate (5 x 200 ml) while maintaining the pH > 9. The organic phase was washed with 300 ml 5% NH_4OH, dried over $MgSO_4$ and concentrated under reduced pressure, affording 10.1 g crude product with 65% purity by UHPLC. The crude compound was purified by flash column chromatography on reverse phase silica gel using H_2O (+ 0.1 HCl)/acetonitrile as eluents. After purification, 6.55 g product were obtained as hydrochloric salt with purity > 95% by ^{1}H NMR and UHPLC. The product was further dissolved in 200 ml $CHCl_3$ and neutralized with 30 ml 0.5 M NaOH (pH = 10), yielding 5.95 g product as a free amine with purity > 95% by ^{1}H NMR. In order to obtain the corresponding hydrobromic salt, 3 g of the obtained product were suspended in a mixture of water/acetonitrile 1:1 (10 ml) and treated with 1.6 ml 48% aq. HBr. After final lyophilization, 3.75 g of the desired product were obtained with purity > 95% by ^{1}H NMR and UHPLC.

^{1}H NMR (300 MHz, MeOD-*d4*): δ 7.51 (s, 1H), 7.09 (s, 1H), 3.93 (s, 3H), 3.75–3.57 (m, 5H), 3.31–3.24 (m, 1H), 3.16–3.02 (m, 2H), 2.87 (s, 3H), 2.66–2.51 (m, 2H), 2.37–2.13 (m, 4H), 2.04 (dt, *J* = 2.6, 12.4 Hz, 1H), 1.90 (dt, *J* = 4.7, 14.0 Hz, 1H), 1.64–1.31 (m, 6H), 1.18 (tt, *J* = 2.9, 12.6 Hz, 1H), 1.01 (dq, *J* = 3.7, 12.6 Hz, 1H); ^{13}C NMR (75 MHz, MeOD-*d4*): δ 152.6, 142.7, 128.8, 128.3, 123.3, 111.3, 61.4, 58.6, 57.3, 43.9, 41.5, 40.2, 37.5, 36.2, 26.9, 26.8, 25.2, 24.4, 22.9; MS (*m/z*): $[M+H]^+$ calcd. for $C_{22}H_{33}N_2O$, 341.2; found, 341.2.

7.1.3 Lam39

(1S,9S,10S)-5-(1H-imidazol-1-yl)-4-methoxy-17-methyl-17-azatetracyclo[7.5.3.0^{1,10}.0^{2,7}]heptadeca-2,4,6-triene dihydrobromide

(1*S*,9*S*)-5-iodo-4-methoxy-17-methyl-17-azatetracyclo[7.5.3.0^{1,10}.0^{2,7}]heptadeca-2,4,6-triene (11.0 g, 27.7 mmol), K_2CO_3 (7.7 g, 55.0 mmol), CuI (1.6 g, 8.4 mmol), L-Proline (1.9 g, 16.8 mmol) were suspended in DMSO (110.0 ml) and treated with imidazole (7.5 g, 110.0 mmol). The resulting mixture was heated at 100 °C in a Parr reactor under nitrogen atmosphere. The reaction progress was monitored by UHPLC and after completion, the reaction mixture was treated with water (600 ml) and extracted with ethyl acetate (5 x 200 ml) while maintaining the pH > 9. The organic phase was washed with 300 ml 5% NH_4OH, dried over $MgSO_4$ and concentrated under reduced pressure, affording 7.5 g product with 50% purity by UHPLC. The crude compound was purified by flash column chromatography on reverse phase silica gel using H_2O (+ 0.1 HCOOH)/acetonitrile as eluents. After purification, 3.52 g product as formate salt with purity > 95% by ^{1}H NMR and UHPLC were obtained. The isolated product was dissolved in 100 ml $CHCl_3$ and neutralized with 50 ml 1 M NaOH (pH = 10), yielding 3.25 g product as a free amine with purity > 95% by ^{1}H NMR. In order to obtain the corresponding hydrobromic salt, the obtained product was suspended in a mixture of water/acetonitrile 1:1 (10 ml) and treated with 1.6 ml 48% aq. HBr. After final lyophilization, 4.3 g of the desired product were obtained with purity > 95% by ^{1}H NMR and UHPLC.

^{1}H NMR (300 MHz, MeOD-*d4*): δ 9.23 (s, 1H), 7.83 (s, 1H), 7.66 (s, 1H), 7.44 (s, 1H), 7.14 (s, 1H), 3.84 (s, 3H), 3.65–3.59 (m, 1H), 3.32–3.25 (m, 1H), 3.17–2.97 (m, 2H), 2.88 (s, 3H), 2.72–2.50 (m, 2H), 2.08 (d, *J* = 12.4 Hz, 1H), 1.94 (dt, *J* = 4.4, 14.0 Hz, 1H), 1.68–1.34 (m, 6H), 1.23 (tt, *J* = 2.9, 12.6 Hz, 1H), 1.07 (dq, *J* = 3.1, 12.6 Hz, 1H); ^{13}C NMR (75 MHz, MeOD-*d4*): δ 153.3, 143.1, 137.6, 128.5, 127.2, 124.8, 123.8, 120.7, 111.1, 61.4, 57.1, 44.0, 41.6, 40.2, 37.6, 36.3, 27.0, 26.9, 26.8, 24.2, 22.9; MS (*m/z*): $[M+H]^+$ calcd. for $C_{21}H_{28}N_3O$, 338.2; found, 338.2.

7.2 Fiji/ImageJ macro scripts

The following Fiji/ImageJ macro scripts were used for quantification of cell viability (see section 4.2.5 and 4.4.3).

Syntax highlighting was performed with: http://www.planetb.ca/syntax-highlight-word.

Set ROI:

```
#@ String (visibility=MESSAGE, value="Choose the images to be processed:") topMsg
#@ File (label = "Input directory", style = "directory") input
#@ File (label = "Output directory", style = "directory") output
#@ String (label = "File suffix", value = ".czi") suffix
#@ Boolean(label = "Continue from manual breakpoint", value = false) continueBP
#@ Boolean(label = "Show all channels for validation", value = false) allWindows
#@ String (visibility=MESSAGE, value="Color allocation per channel for RGB output:") colMsg
#@ String(label = "C1", choices={"blue", "red", "green", "gray", "cyan", "magenta", "yellow"}, style="listBox") setChan1
#@ String(label = "C2", choices={"green", "red", "blue", "gray", "cyan", "magenta", "yellow"}, style="listBox") setChan2
#@ String(label = "C3", choices={"red", "green", "blue", "gray", "cyan", "magenta", "yellow"}, style="listBox") setChan3
#@ String(label = "(optional) C4", choices={"gray", "red", "green", "blue", "cyan", "magenta", "yellow"}, style="listBox") setChan4
#@ String (visibility=MESSAGE, value="Settings for ROI detection:") scriptMsg
#@ String (label = "Allowed Circularity", value = "0.05-1.00") set_circularity
#@ String(label = "Detect ROI based on:", choices={"merged channels", "single channel"}, style="radioButtonHorizontal") roiDetect
#@ String(label = "If single channel detection, use:", choices={"C1", "C2", "C3", "C4"}, style="listBox") setRoiChan
#@ Boolean(label = "Histogram mode scaling", value = false) set_histoscale
#@ Boolean(label = "Gaussian Blur Filter", value = false) set_gausslanFilter
#@ Double (label = "Gaussian Sigma", value = "2.0") set_gaussianSigma

/*  Last update:    24th July 2019
 *  Script author:  Anna Hamacher, HHU
 *
 *  Macro to process multiple images in a folder to
 *  - automatically segment the image (detect the pancreatic islets)
 *  - in case of faulty segmentation, allow a manual correction
 *  - re-run this macro to save ROIs after manual correction
 *  So far, apotome images can cause problems, if the bio-format importer of Fiji fails to stitch the tiles.
 *  After completion of the ROI setting, the ASPIQ_Measure Macro needs to be run.
 */

// General settings
separator = file.separator;
myChan = newArray(setChan1, setChan2, setChan3, setChan4);

// Main function
processFolder(input);

function processFolder(input) {
    list = getFileList(input);
    Array.sort(list);
    for (i = 0; i < list.length; i++) {
        // ignore subfolders for processing
        if(endsWith(list[i], suffix) && !(File.isDirectory(input + separator + list[i])))
            if (i == 0 && continueBP) {
                saveROI(input, output, list[i]);
            } else {
                processFile(input, output, list[i]);
            }
    }
}

function processFile(input, output, file) {
    print("Processing: " + input + separator + file);
```

```
    run("Bio-Formats Importer", "open=[" + input + separator + file + "] autoscale color_mode=Composite rois_import=[ROI manager] view=Hyperstack stack_order=XYCZT stitch_tiles series_1");
    run("Z Project...", "projection=[Max Intensity]");
    imageTitle = getTitle(); // needed for more than 1 til (string incl. "#1")
    imageId = getImageID();
    totalSlices = nSlices();

    // Decision of ROI detection on merged channels or a single channel
    if (roiDetect == "single channel") {
        run("Duplicate...", "duplicate channels=" + substring(setRoiChan, 1) + " title=[Working Copy "+ setRoiChan + "]");
    }
    // Clear ROIs
    roiManager("reset");
    selectWindow(imageTitle);
    // Keep original image open for cross-reference
    run("Duplicate...", "duplicate");
    selectWindow(imageTitle);
    // Change format to 8-bit
    run("8-bit");
    run("Split Channels");
    for (i=1; i <= totalSlices ; i++)  {
        selectWindow("C" + i + "-" + imageTitle);
        run("8-bit");
        // Improve contrast based on histogram mode in merged RGB image
        // Useful in case of stainings with much background noise (e.g. CD45)
        if (set_histoscale) {
            List.setMeasurements;
            // Get value "mode" and "max" from histogram function
            histogramMode = List.getValue("Mode");
            histogramMax = List.getValue("Max");
            setMinAndMax(histogramMode, histogramMax);
        }
    }
    // System colours: C1=red, C2=green, C3=blue, C4=gray, C5=cyan, C6=magenta, C7=yellow
    // Color assignment for RGB output image
    sysChan = newArray(myChan.length);
    for (c = 0; c < myChan.length; c++ ){
        if (myChan[c] == "red") { sysChan[c] = "c1"; }
        else if (myChan[c] == "green") { sysChan[c] = "c2"; }
        else if (myChan[c] == "blue") { sysChan[c] = "c3"; }
        else if (myChan[c] == "gray") { sysChan[c] = "c4"; }
        else if (myChan[c] == "cyan") { sysChan[c] = "c5"; }
        else if (myChan[c] == "magenta") { sysChan[c] = "c6"; }
        else if (myChan[c] == "yellow") { sysChan[c] = "c7";}
    }
    // Merging channels to RGB image for ROI detection
    if (totalSlices == 3) { // Merge only channel 1-3
        run("Merge Channels...", sysChan[0] + "=[C1-" + imageTitle + "] " + sysChan[1] + "=[C2-" + imageTitle + "] " + sysChan[2] + "=[C3-" + imageTitle + "] keep");
    } else { //merge channel 1-4
        run("Merge Channels...", sysChan[0] + "=[C1-" + imageTitle + "] " + sysChan[1] + "=[C2-" + imageTitle + "] " + sysChan[2] + "=[C3-" + imageTitle + "] " + sysChan[3] + "=[C4-" + imageTitle + "] keep");
    }
    if (roiDetect == "single channel") {
        selectWindow("Working Copy "+ setRoiChan);
    } else {
```

```
        selectWindow("RGB");
        run("Duplicate...", "title=[Working Copy of RGB]");
        selectWindow("Working Copy of RGB");
    }
    // Thresholding with filtering and noise reduction
    run("8-bit");
    run("Enhance Contrast...", "saturated=0.3");
    if (set_gaussianFilter) {
        run("Gaussian Blur...", "sigma=" + set_gaussianSigma + " scaled");
    }
    setOption("BlackBackground", true);
    setAutoThreshold("Otsu dark");
    run("Convert to Mask");
    run("Remove Outliers...", "radius=5 threshold=50 which=Bright");
    run("Fill Holes");
    run("Analyze Particles...", "size=900-Inifity circularity=" + set_circularity + " exclude include add");

    nROIs = roiManager("count");
    // Run watershed if no ROI detected (e.g. touching edges, lower circularity)
    if (nROIs == 0) {
        print ("Invalid operation, no ROI defined, trying Watershed!"); // Debug
        run("Watershed");
        run("Analyze Particles...", "size=900-Inifity circularity=" + set_circularity + " exclude include add");
        // Re-check the number of ROIs after watershed
        nROIs = roiManager("count");
    }

    // Use function Windows > Tile for the user to see all images at the same time for confirmation of ROIs
    if (allWindows) {
        run("Tile");
    }
    // End the automated islet detection, present result to the user for approval
    selectWindow("RGB");
    roiManager("Deselect");
    roiManager("Show All");

    // Ask user if ROIs are ok or need manual correction
    if (getBoolean("Are the suggested ROIs ok?")) {
        showMessage("Saving ROIs and overlay tiff...");
        saveROI(input, output, file);
        }
    else {
        showMessage("Please adjust the ROIs manually and re-run the script with <continue from manual breakpoint = yes>");
        exit(); // End macro for manual correction
    }
}

function saveROI(input, output, file) {

    setBatchMode(true);
    resultDir = output + separator + file + "_results";
    // Create the image specific result directory, if it doesn't exist yet
    if (!File.isDirectory(resultDir)) {
        File.makeDirectory(resultDir);
    }
```

```
    // Save RGB-Overlay for easier scroll through
    // roiManager("Update") needs to be done while editing ROIs manually!
    selectWindow("RGB");
    // Make sure only the updated existing ROI(s) gets flattened
    roiManager("Deselect");
    roiManager("Show All");
    roiManager("Show None");
    roiManager("Show All");
    run("From ROI Manager");
    run("Flatten");
    selectWindow("RGB-1");
    saveAs("Tiff", resultDir + separator + file + "_RGB-Overlay.tif");

    // Save all ROIs to zip for later reference
    roiManager("Deselect");
    roiManager("Save", resultDir + separator + file + "_RoiSet.zip");

    // Move the original image to the result subfolder, proceed with the list of images in the main directory
    File.rename(input + separator + file, resultDir + separator + file);

    setBatchMode(false);
    run("Close All");
}
```

Measure:

```
#@ String (visibility=MESSAGE, value="Choose the images to be processed:") topMsg
#@ File (label = "Main directory", style = "directory") workingDir
#@ String (label = "File suffix", value = ".czi") suffix
#@ String (visibility=MESSAGE, value="Choose threshold per channel:") thrMsg
#@ String(label = "C1", choices={"Otsu", "Triangle", "Default", "Li", "Moments", "Minimum", "Huang", "RenyiEntropy", "Yen", "IsoData", "Intermodes", "MaxEntropy"}, style="listBox") setThr1
#@ String(label = "C2", choices={"Otsu", "Triangle", "Default", "Li", "Moments", "Minimum", "Huang", "RenyiEntropy", "Yen", "IsoData", "Intermodes", "MaxEntropy"}, style="listBox") setThr2
#@ String(label = "C3", choices={"Otsu", "Triangle", "Default", "Li", "Moments", "Minimum", "Huang", "RenyiEntropy", "Yen", "IsoData", "Intermodes", "MaxEntropy"}, style="listBox") setThr3
#@ String(label = "(optional) C4", choices={"Otsu", "Triangle", "Default", "Li", "Moments", "Minimum", "Huang", "RenyiEntropy", "Yen", "IsoData", "Intermodes", "MaxEntropy"}, style="listBox") setThr4
#@ String(label = "Thresholding mode:", choices={"global", "local"}, style="radioButtonHorizontal") setThrMode
#@ String (visibility=MESSAGE, value="Note: global = on whole image; local = only on ROI area") thr2Msg
#@ String(label = "Thresholding on:", choices={"each channel", "single channel"}, style="radioButtonHorizontal") channelSelect
#@ String(label = "If single channel, use:", choices={"C1", "C2", "C3", "C4"}, style="listBox") setThrChan

/*  Last update:    19th November 2019
 *  Script author:  Anna Hamacher, HHU
 *  modified:       Laura Wömeyer
 *
 *  Macro to process multiple images in a folder to
 *  - measure specific thresholds inside this area for each channel
 *  - save the results in a directory for evaluation of the automation and reproducibility.
 *  So far, apotome images can cause problems, if the bio-format importer of Fiji fails to stitch the tiles.
 */

scriptStart = round(getTime()/1000);

// General settings
separator = File.separator;
myThr = newArray(setThr1, setThr2, setThr3, setThr4);

// Main function
run("Clear Results");
processFolder(workingDir);

function processFolder(workingDir) {
    list = getFileList(workingDir);
    Array.sort(list);
    for (i = 0; i < list.length; i++) {
        if(File.isDirectory(workingDir + separator + list[i])){
            processFolder("" + workingDir + separator + list[i]);
        }
        else if(endsWith(list[i], suffix)){
            processFile(workingDir, list[i]);
        }
    }
}

function processFile(workingDir, file) {
    print("Processing: " + workingDir + separator + file);

    setBatchMode(true);
    run("Bio-Formats Importer", "open=[" + workingDir + separator + file + "] autoscale color_mode=Composite rois_import=[ROI manager] view=Hyperstack stack_order=XYCZT stitch_tiles series_1");
    origTitle = getTitle();
    run("Z Project...", "projection=[Max Intensity]");
    imageTitle = getTitle(); // needed for more than 1 til (string incl. "#1")
    imageId = getImageID();
```

```
    // Decision of measurement on each or only a single channel
    if (channelSelect == "each channel") {
        iGlobal = 1;
        totalSlices = nSlices()-1;
    } else {
        iGlobal = substring(setThrChan, 1);
        totalSlices = iGlobal;
    }
    // Change image to 8-bit
    run("8-bit");
    run("Split Channels");
    for (i=iGlobal; i <= totalSlices ; i++)  {
        selectWindow("C" + i + "-" + imageTitle);
        run("8-bit");
    }
    // Clear ROIs
    roiManager("reset");
    // Import predefined ROIs
    roiManager("Open", workingDir + file + "_RoiSet.zip");
    nROIs = roiManager("count");
    if (nROIs < 0) {
        print (file + ": Invalid operation, no ROI defined!"); // Debug
        exit();
    }
    // Set measurement paramaters, don't limit to threshold
    run("Set Measurements...", "area area_fraction display redirect=None decimal=4");
    // First measure total area of each ROI
    for (j=0; j < nROIs; j++) {
        roiManager("Deselect");
        selectWindow("C" + iGlobal + "-" + imageTitle);
        roiManager("Select", j);
        run("Measure");
        roiManager("Deselect");
        }
    // Measurement of white aree, limit to threshold now
    run("Set Measurements...", "area area_fraction limit display redirect=None decimal=4");
    // Measure the area of each ROI on each specific channel threshold
    if (setThrMode == "local") {
        // Perform local thresholding by selecting the ROIs before thresholding
        for (j=0; j < nROIs; j++) {
            for (i=iGlobal; i <= totalSlices ; i++)  {
                selectWindow("C" + i + "-" + imageTitle);
                run("Select All");
                // Convert image for thresholding and measure the relevant area
                // This needs to be done per channel and per ROI
                thrWindow = "C" + i + " with Threshold " + myThr[i-1] + "_roi" + j;
                run("Duplicate...", "title=[" + thrWindow + "]");
                selectWindow(thrWindow);
                roiManager("Select", j);
                roiName = Roi.getName();
                setAutoThreshold(myThr[i-1] + " dark");
                setOption("BlackBackground", true);
                run("Convert to Mask");
                roiManager("Deselect");
                selectWindow(thrWindow);

                roiManager("Select", j);
                run("Measure");
                // Save each mask with ROI
                run("Flatten");
                saveAs("Tiff", workingDir + file + "_C" + i + "_Threshold_" + myThr[i-1] + "_roi_" + roiName + ".tif");
            }
        }
    }
    else {
        // Perform global thresholding on whole image
        for (i=iGlobal; i <= totalSlices ; i++)  {
            selectWindow("C" + i + "-" + imageTitle);
            run("Select All");
            // Convert image for thresholding and measure the relevant area
            // This needs to be done per channel and per ROI
            thrWindow = "C" + i + " with Threshold " + myThr[i-1];
            run("Duplicate...", "title=[" + thrWindow + "]");
            selectWindow(thrWindow);
            setAutoThreshold(myThr[i-1] + " dark");
            setOption("BlackBackground", true);
            run("Convert to Mask");
            for (j=0; j < nROIs; j++) {
                roiManager("Deselect");
                selectWindow(thrWindow);
                roiManager("Select", j);
                run("Measure");
            }
            // Save each mask
            roiManager("Deselect");
            saveAs("Tiff", workingDir + file + "_C" + i + "_Threshold_" + myThr[i-1] + ".tif");

                }
    }
//normalisation to pancreatic nuclei area
    imageCalculator("Add create", origTitle + "_C1_Threshold_Otsu" + ".tif", origTitle + "_C2_Threshold_Otsu" + ".tif");
    run("Convert to Mask");
    for (j=0; j < nROIs; j++) {
        roiManager("Deselect");
        selectWindow("Result of " + origTitle + "_C1_Threshold_Otsu" + ".tif");
        roiManager("Select", j);
        run("Measure");
        }
    roiManager("Deselect");
    saveAs("Tiff", workingDir + file + "_C" + i + "_results" + ".tif");

        }

    run("Close All");
    setBatchMode(false);


// Save the results to an overall file
timestamp = round(getTime()/1000);
selectWindow("Results");
saveAs("Results", workingDir + separator + "Overall_Quantification_Results_" + timestamp + ".csv");


// Get the total runtime of the script in seconds and display to user
scriptEnd = round(getTime()/1000);
totalRuntime = scriptEnd - scriptStart;
showMessage("ASPIQ Measure Script ended, runtime: " + totalRuntime + "s");
```

8. Publications

The main part of this study is in preparation for submission (publication date unknown):

Scholz O*, Otter S*, Welters A*, Wörmeyer L, Mrugala J, Hamacher A, Koch A, Sanz M, Hoffmann T, Herebian D, Klöcker N, Piechot A, Mayatepek E, Meissner T, Lammert E. (* equally contributed)

Synthesis and investigation of peripherally active, blood glucose-lowering dextromethorphan derivatives without central side effects.

Other publications:

2017: Scholz O, Welters A, Lammert E.

Role of NMDA receptors in pancreatic islets.

In: Hashimoto K. (eds) The NMDA Receptors. The Receptors, vol 30. Humana Press, Cham. p. 121-134.

Book Section.

9. References

1. Folias, A.E. and M. Hebrok, *Part VI Pancreas, Overview*, in *Metabolism of Human Diseases*, E. Lammert and M. Zeeb, Editor. 2014, Springer-Verlag Wien. p. 157-162.
2. Murtaugh, L.C. and M.D. Keefe, *Regeneration and repair of the exocrine pancreas.* Annu Rev Physiol, 2015. **77**: p. 229-49.
3. Ionescu-Tirgoviste, C., et al., *A 3D map of the islet routes throughout the healthy human pancreas.* Sci Rep, 2015. **5**: p. 14634.
4. Rutter, G.A., et al., *Pancreatic beta-cell identity, glucose sensing and the control of insulin secretion.* Biochem J, 2015. **466**(2): p. 203-18.
5. Rodriguez-Diaz, R., et al., *Paracrine Interactions within the Pancreatic Islet Determine the Glycemic Set Point.* Cell Metab, 2018. **27**(3): p. 549-558.e4.
6. Ashcroft, F.M. and P. Rorsman, *Diabetes mellitus and the beta cell: the last ten years.* Cell, 2012. **148**(6): p. 1160-71.
7. Dolensek, J., M.S. Rupnik, and A. Stozer, *Structural similarities and differences between the human and the mouse pancreas.* Islets, 2015. **7**(1): p. e1024405.
8. Eberhard, D. and E. Lammert, *The pancreatic beta-cell in the islet and organ community.* Curr Opin Genet Dev, 2009. **19**(5): p. 469-75.
9. Cabrera, O., et al., *The unique cytoarchitecture of human pancreatic islets has implications for islet cell function.* Proc Natl Acad Sci U S A, 2006. **103**(7): p. 2334-9.
10. Cohrs, C.M., et al., *Vessel Network Architecture of Adult Human Islets Promotes Distinct Cell-Cell Interactions In Situ and Is Altered After Transplantation.* Endocrinology, 2017. **158**(5): p. 1373-1385.
11. Bonner-Weir, S., B.A. Sullivan, and G.C. Weir, *Human Islet Morphology Revisited: Human and Rodent Islets Are Not So Different After All.* J Histochem Cytochem, 2015. **63**(8): p. 604-12.
12. Bosco, D., et al., *Unique arrangement of alpha- and beta-cells in human islets of Langerhans.* Diabetes, 2010. **59**(5): p. 1202-10.
13. Lammert, E. and P. Thorn, *The Role of the Islet Niche on Beta Cell Structure and Function.* J Mol Biol, 2019.
14. Halban, P.A., et al., *The possible importance of contact between pancreatic islet cells for the control of insulin release.* Endocrinology, 1982. **111**(1): p. 86-94.
15. Vergari, E., et al., *Insulin inhibits glucagon release by SGLT2-induced stimulation of somatostatin secretion.* Nat Commun, 2019. **10**(1): p. 139.
16. Otter, S. and E. Lammert, *Exciting Times for Pancreatic Islets: Glutamate Signaling in Endocrine Cells.* Trends Endocrinol Metab, 2016. **27**(3): p. 177-188.
17. Maechler, P., *Glutamate pathways of the beta-cell and the control of insulin secretion.* Diabetes Res Clin Pract, 2017. **131**: p. 149-153.
18. Wojtusciszyn, A., et al., *Insulin secretion from human beta cells is heterogeneous and dependent on cell-to-cell contacts.* Diabetologia, 2008. **51**(10): p. 1843-52.
19. Bosco, D., L. Orci, and P. Meda, *Homologous but not heterologous contact increases the insulin secretion of individual pancreatic B-cells.* Exp Cell Res, 1989. **184**(1): p. 72-80.
20. Speier, S., et al., *Cx36-mediated coupling reduces beta-cell heterogeneity, confines the stimulating glucose concentration range, and affects insulin release kinetics.* Diabetes, 2007. **56**(4): p. 1078-86.

21. Gan, W.J., et al., *Cell polarity defines three distinct domains in pancreatic beta-cells.* J Cell Sci, 2017. **130**(1): p. 143-151.
22. Parnaud, G., et al., *Cadherin engagement improves insulin secretion of single human beta-cells.* Diabetes, 2015. **64**(3): p. 887-96.
23. Konstantinova, I., et al., *EphA-Ephrin-A-mediated beta cell communication regulates insulin secretion from pancreatic islets.* Cell, 2007. **129**(2): p. 359-70.
24. Bonner-Weir, S., *Morphological evidence for pancreatic polarity of beta-cell within islets of Langerhans.* Diabetes, 1988. **37**(5): p. 616-21.
25. Almaca, J., et al., *The Pericyte of the Pancreatic Islet Regulates Capillary Diameter and Local Blood Flow.* Cell Metab, 2018. **27**(3): p. 630-644.e4.
26. Nyman, L.R., et al., *Glucose-dependent blood flow dynamics in murine pancreatic islets in vivo.* Am J Physiol Endocrinol Metab, 2010. **298**(4): p. E807-14.
27. Chandra, R. and R.A. Liddle, *Neurohormonal regulation of pancreatic secretion.* Curr Opin Gastroenterol, 2012. **28**(5): p. 483-7.
28. Thorens, B., *Neural regulation of pancreatic islet cell mass and function.* Diabetes Obes Metab, 2014. **16 Suppl 1**: p. 87-95.
29. Roder, P.V., et al., *Pancreatic regulation of glucose homeostasis.* Exp Mol Med, 2016. **48**: p. e219.
30. Gautam, D., et al., *A critical role for beta cell M3 muscarinic acetylcholine receptors in regulating insulin release and blood glucose homeostasis in vivo.* Cell Metab, 2006. **3**(6): p. 449-61.
31. Marroqui, L., et al., *Role of leptin in the pancreatic beta-cell: effects and signaling pathways.* J Mol Endocrinol, 2012. **49**(1): p. R9-17.
32. Seufert, J., *Leptin effects on pancreatic beta-cell gene expression and function.* Diabetes, 2004. **53 Suppl 1**: p. S152-8.
33. Rorsman, P. and M. Braun, *Regulation of insulin secretion in human pancreatic islets.* Annu Rev Physiol, 2013. **75**: p. 155-79.
34. Gilon, P., et al., *Control mechanisms of the oscillations of insulin secretion in vitro and in vivo.* Diabetes, 2002. **51 Suppl 1**: p. S144-51.
35. Gilon, P., et al., *Calcium signaling in pancreatic beta-cells in health and in Type 2 diabetes.* Cell Calcium, 2014. **56**(5): p. 340-61.
36. Satin, L.S., et al., *Pulsatile insulin secretion, impaired glucose tolerance and type 2 diabetes.* Mol Aspects Med, 2015. **42**: p. 61-77.
37. Berggren, P.O. and O. Larsson, *Ca2+ and pancreatic B-cell function.* Biochem Soc Trans, 1994. **22**(1): p. 12-8.
38. Nesher, R. and E. Cerasi, *Modeling phasic insulin release: immediate and time-dependent effects of glucose.* Diabetes, 2002. **51 Suppl 1**: p. S53-9.
39. Drucker, D.J., *Mechanisms of Action and Therapeutic Application of Glucagon-like Peptide-1.* Cell Metab, 2018. **27**(4): p. 740-756.
40. Nauck, M.A. and J.J. Meier, *Incretin hormones: Their role in health and disease.* Diabetes Obes Metab, 2018. **20 Suppl 1**: p. 5-21.
41. Drucker, D.J., J.F. Habener, and J.J. Holst, *Discovery, characterization, and clinical development of the glucagon-like peptides.* J Clin Invest, 2017. **127**(12): p. 4217-4227.
42. Elrick, H., et al., *PLASMA INSULIN RESPONSE TO ORAL AND INTRAVENOUS GLUCOSE ADMINISTRATION.* J Clin Endocrinol Metab, 1964. **24**: p. 1076-82.
43. Moens, K., et al., *Expression and functional activity of glucagon, glucagon-like peptide I, and glucose-dependent insulinotropic peptide receptors in rat pancreatic islet cells.* Diabetes, 1996. **45**(2): p. 257-61.

44. Stewart, A.F., et al., *Human beta-cell proliferation and intracellular signaling: part 3.* Diabetes, 2015. **64**(6): p. 1872-85.
45. Hauge-Evans, A.C., et al., *Somatostatin secreted by islet delta-cells fulfills multiple roles as a paracrine regulator of islet function.* Diabetes, 2009. **58**(2): p. 403-11.
46. Kailey, B., et al., *SSTR2 is the functionally dominant somatostatin receptor in human pancreatic beta- and alpha-cells.* Am J Physiol Endocrinol Metab, 2012. **303**(9): p. E1107-16.
47. Bertrand, G., et al., *Glutamate stimulates insulin secretion and improves glucose tolerance in rats.* Am J Physiol, 1995. **269**(3 Pt 1): p. E551-6.
48. Maechler, P. and C.B. Wollheim, *Mitochondrial glutamate acts as a messenger in glucose-induced insulin exocytosis.* Nature, 1999. **402**(6762): p. 685-9.
49. Feldmann, N., et al., *Reduction of plasma membrane glutamate transport potentiates insulin but not glucagon secretion in pancreatic islet cells.* Mol Cell Endocrinol, 2011. **338**(1-2): p. 46-57.
50. Gheni, G., et al., *Glutamate acts as a key signal linking glucose metabolism to incretin/cAMP action to amplify insulin secretion.* Cell Rep, 2014. **9**(2): p. 661-73.
51. Vetterli, L., et al., *Delineation of glutamate pathways and secretory responses in pancreatic islets with beta-cell-specific abrogation of the glutamate dehydrogenase.* Mol Biol Cell, 2012. **23**(19): p. 3851-62.
52. Hoy, M., et al., *Increase in cellular glutamate levels stimulates exocytosis in pancreatic beta-cells.* FEBS Lett, 2002. **531**(2): p. 199-203.
53. Eto, K., et al., *Glucose metabolism and glutamate analog acutely alkalinize pH of insulin secretory vesicles of pancreatic beta-cells.* Am J Physiol Endocrinol Metab, 2003. **285**(2): p. E262-71.
54. Gammelsaeter, R., et al., *A role for glutamate transporters in the regulation of insulin secretion.* PLoS One, 2011. **6**(8): p. e22960.
55. Braun, M., et al., *Gamma-aminobutyric acid (GABA) is an autocrine excitatory transmitter in human pancreatic beta-cells.* Diabetes, 2010. **59**(7): p. 1694-701.
56. Vakilian, M., Y. Tahamtani, and K. Ghaedi, *A review on insulin trafficking and exocytosis.* Gene, 2019. **706**: p. 52-61.
57. Saltiel, A.R. and C.R. Kahn, *Insulin signalling and the regulation of glucose and lipid metabolism.* Nature, 2001. **414**(6865): p. 799-806.
58. Petersen, M.C. and G.I. Shulman, *Mechanisms of Insulin Action and Insulin Resistance.* Physiol Rev, 2018. **98**(4): p. 2133-2223.
59. Posner, B.I., *Insulin Signalling: The Inside Story.* Can J Diabetes, 2017. **41**(1): p. 108-113.
60. Czech, M.P., *Insulin action and resistance in obesity and type 2 diabetes.* Nat Med, 2017. **23**(7): p. 804-814.
61. Bruning, J.C., et al., *Role of brain insulin receptor in control of body weight and reproduction.* Science, 2000. **289**(5487): p. 2122-5.
62. Plum, L., M. Schubert, and J.C. Bruning, *The role of insulin receptor signaling in the brain.* Trends Endocrinol Metab, 2005. **16**(2): p. 59-65.
63. Goldfine, A.B. and R.N. Kulkarni, *Modulation of beta-cell function: a translational journey from the bench to the bedside.* Diabetes Obes Metab, 2012. **14 Suppl 3**: p. 152-60.
64. Kulkarni, R.N., *Receptors for insulin and insulin-like growth factor-1 and insulin receptor substrate-1 mediate pathways that regulate islet function.* Biochem Soc Trans, 2002. **30**(2): p. 317-22.

65. Kulkarni, R.N., et al., *Tissue-specific knockout of the insulin receptor in pancreatic beta cells creates an insulin secretory defect similar to that in type 2 diabetes.* Cell, 1999. **96**(3): p. 329-39.
66. Rhodes, C.J., et al., *Direct autocrine action of insulin on beta-cells: does it make physiological sense?* Diabetes, 2013. **62**(7): p. 2157-63.
67. International Diabetes Federation, *IDF Diabetes Atlas, 9th edition*. Brussels; 2019.
68. Saeedi, P., et al., *Global and regional diabetes prevalence estimates for 2019 and projections for 2030 and 2045: Results from the International Diabetes Federation Diabetes Atlas, 9(th) edition.* Diabetes Res Clin Pract, 2019. **157**: p. 107843.
69. Welters, A. and E. Lammert, *Part VI Pancreas, Diabetes mellitus*, in *Metabolism of Human Diseases*, E. Lammert and M. Zeeb, Editor. 2014, Springer-Verlag Wien. p. 163-169.
70. Ferrannini, E., *Sodium-Glucose Co-transporters and Their Inhibition: Clinical Physiology.* Cell Metab, 2017. **26**(1): p. 27-38.
71. World Health Organization, *Definition and diagnosis of diabetes mellitus and intermediate hyperglycaemia. Report of a WHO/IDF Consultation*. Geneva; 2006.
72. World Health Organization, *Use of Glycated Haemoglobin (HbA1c) in the Diagnosis of Diabetes Mellitus: Abbreviated Report of a WHO Consultation*. Geneva; 2011.
73. World Health Organization, *Classification of Diabetes Mellitus 2019*. Geneva; 2019.
74. Atkinson, M.A., G.S. Eisenbarth, and A.W. Michels, *Type 1 diabetes.* Lancet, 2014. **383**(9911): p. 69-82.
75. Hattersley, A., et al., *ISPAD Clinical Practice Consensus Guidelines 2006-2007. The diagnosis and management of monogenic diabetes in children.* Pediatr Diabetes, 2006. **7**(6): p. 352-60.
76. Vaxillaire, M., A. Bonnefond, and P. Froguel, *The lessons of early-onset monogenic diabetes for the understanding of diabetes pathogenesis.* Best Pract Res Clin Endocrinol Metab, 2012. **26**(2): p. 171-87.
77. Murphy, R., S. Ellard, and A.T. Hattersley, *Clinical implications of a molecular genetic classification of monogenic beta-cell diabetes.* Nat Clin Pract Endocrinol Metab, 2008. **4**(4): p. 200-13.
78. Anik, A., et al., *Maturity-onset diabetes of the young (MODY): an update.* J Pediatr Endocrinol Metab, 2015. **28**(3-4): p. 251-63.
79. Ewald, N., et al., *Prevalence of diabetes mellitus secondary to pancreatic diseases (type 3c).* Diabetes Metab Res Rev, 2012. **28**(4): p. 338-42.
80. Hart, P.A., et al., *Type 3c (pancreatogenic) diabetes mellitus secondary to chronic pancreatitis and pancreatic cancer.* Lancet Gastroenterol Hepatol, 2016. **1**(3): p. 226-237.
81. Resmini, E., et al., *Secondary diabetes associated with principal endocrinopathies: the impact of new treatment modalities.* Acta Diabetol, 2009. **46**(2): p. 85-95.
82. Pandit, M.K., et al., *Drug-induced disorders of glucose tolerance.* Ann Intern Med, 1993. **118**(7): p. 529-39.
83. Takasu, N., et al., *Forty-year observation of 280 Japanese patients with congenital rubella syndrome.* Diabetes Care, 2005. **28**(9): p. 2331-2.
84. Forrest, J.M., M.A. Menser, and J.A. Burgess, *High frequency of diabetes mellitus in young adults with congenital rubella.* Lancet, 1971. **2**(7720): p. 332-4.

85. Immanuel, J. and D. Simmons, *Screening and Treatment for Early-Onset Gestational Diabetes Mellitus: a Systematic Review and Meta-analysis.* Curr Diab Rep, 2017. **17**(11): p. 115.
86. Guariguata, L., et al., *Global estimates of the prevalence of hyperglycaemia in pregnancy.* Diabetes Res Clin Pract, 2014. **103**(2): p. 176-85.
87. Hod, M., et al., *The International Federation of Gynecology and Obstetrics (FIGO) Initiative on gestational diabetes mellitus: A pragmatic guide for diagnosis, management, and care.* Int J Gynaecol Obstet, 2015. **131 Suppl 3**: p. S173-211.
88. Warshauer, J.T., J.A. Bluestone, and M.S. Anderson, *New Frontiers in the Treatment of Type 1 Diabetes.* Cell Metab, 2020. **31**(1): p. 46-61.
89. Bluestone, J.A., K. Herold, and G. Eisenbarth, *Genetics, pathogenesis and clinical interventions in type 1 diabetes.* Nature, 2010. **464**(7293): p. 1293-300.
90. Fonolleda, M., et al., *Remission Phase in Paediatric Type 1 Diabetes: New Understanding and Emerging Biomarkers.* Horm Res Paediatr, 2017. **88**(5): p. 307-315.
91. Klinke, D.J., 2nd, *Extent of beta cell destruction is important but insufficient to predict the onset of type 1 diabetes mellitus.* PLoS One, 2008. **3**(1): p. e1374.
92. Nguyen, C., et al., *Definition of high-risk type 1 diabetes HLA-DR and HLA-DQ types using only three single nucleotide polymorphisms.* Diabetes, 2013. **62**(6): p. 2135-40.
93. Erlich, H., et al., *HLA DR-DQ haplotypes and genotypes and type 1 diabetes risk: analysis of the type 1 diabetes genetics consortium families.* Diabetes, 2008. **57**(4): p. 1084-92.
94. Noble, J.A., et al., *HLA class I and genetic susceptibility to type 1 diabetes: results from the Type 1 Diabetes Genetics Consortium.* Diabetes, 2010. **59**(11): p. 2972-9.
95. Couper, J.J., et al., *ISPAD Clinical Practice Consensus Guidelines 2018: Stages of type 1 diabetes in children and adolescents.* Pediatr Diabetes, 2018. **19 Suppl 27**: p. 20-27.
96. Yeung, W.C., W.D. Rawlinson, and M.E. Craig, *Enterovirus infection and type 1 diabetes mellitus: systematic review and meta-analysis of observational molecular studies.* Bmj, 2011. **342**: p. d35.
97. Allen, D.W., et al., *Maternal virus infections in pregnancy and type 1 diabetes in their offspring: Systematic review and meta-analysis of observational studies.* Rev Med Virol, 2018. **28**(3): p. e1974.
98. Ziegler, A.G., et al., *Early infant feeding and risk of developing type 1 diabetes-associated autoantibodies.* Jama, 2003. **290**(13): p. 1721-8.
99. Peng, H. and W. Hagopian, *Environmental factors in the development of Type 1 diabetes.* Rev Endocr Metab Disord, 2006. **7**(3): p. 149-62.
100. Chatterjee, S., K. Khunti, and M.J. Davies, *Type 2 diabetes.* Lancet, 2017. **389**(10085): p. 2239-2251.
101. World Health Organization, *Global Report on Diabetes*. Geneva; 2016.
102. Zaccardi, F., et al., *Pathophysiology of type 1 and type 2 diabetes mellitus: a 90-year perspective.* Postgrad Med J, 2016. **92**(1084): p. 63-9.
103. Samuel, V.T. and G.I. Shulman, *The pathogenesis of insulin resistance: integrating signaling pathways and substrate flux.* J Clin Invest, 2016. **126**(1): p. 12-22.
104. Yaribeygi, H., et al., *Insulin resistance: Review of the underlying molecular mechanisms.* J Cell Physiol, 2019. **234**(6): p. 8152-8161.
105. Perry, R.J., et al., *The role of hepatic lipids in hepatic insulin resistance and type 2 diabetes.* Nature, 2014. **510**(7503): p. 84-91.

106. Sesti, G., *Pathophysiology of insulin resistance.* Best Pract Res Clin Endocrinol Metab, 2006. **20**(4): p. 665-79.
107. Kahn, S.E., M.E. Cooper, and S. Del Prato, *Pathophysiology and treatment of type 2 diabetes: perspectives on the past, present, and future.* Lancet, 2014. **383**(9922): p. 1068-83.
108. Christensen, A.A. and M. Gannon, *The Beta Cell in Type 2 Diabetes.* Curr Diab Rep, 2019. **19**(9): p. 81.
109. Vetere, A., et al., *Targeting the pancreatic beta-cell to treat diabetes.* Nat Rev Drug Discov, 2014. **13**(4): p. 278-89.
110. Halban, P.A., et al., *beta-cell failure in type 2 diabetes: postulated mechanisms and prospects for prevention and treatment.* J Clin Endocrinol Metab, 2014. **99**(6): p. 1983-92.
111. Weir, G.C., C. Cavelti-Weder, and S. Bonner-Weir, *Stem cell approaches for diabetes: towards beta cell replacement.* Genome Med, 2011. **3**(9): p. 61.
112. Butler, A.E., et al., *Beta-cell deficit and increased beta-cell apoptosis in humans with type 2 diabetes.* Diabetes, 2003. **52**(1): p. 102-10.
113. Jurgens, C.A., et al., *beta-cell loss and beta-cell apoptosis in human type 2 diabetes are related to islet amyloid deposition.* Am J Pathol, 2011. **178**(6): p. 2632-40.
114. Talchai, C., et al., *Pancreatic beta cell dedifferentiation as a mechanism of diabetic beta cell failure.* Cell, 2012. **150**(6): p. 1223-34.
115. Cinti, F., et al., *Evidence of beta-Cell Dedifferentiation in Human Type 2 Diabetes.* J Clin Endocrinol Metab, 2016. **101**(3): p. 1044-54.
116. Nordmann, T.M., et al., *The Role of Inflammation in beta-cell Dedifferentiation.* Sci Rep, 2017. **7**(1): p. 6285.
117. Butler, A.E., et al., *beta-Cell Deficit in Obese Type 2 Diabetes, a Minor Role of beta-Cell Dedifferentiation and Degranulation.* J Clin Endocrinol Metab, 2016. **101**(2): p. 523-32.
118. Poitout, V. and R.P. Robertson, *Glucolipotoxicity: fuel excess and beta-cell dysfunction.* Endocr Rev, 2008. **29**(3): p. 351-66.
119. Robertson, R.P., *Chronic oxidative stress as a central mechanism for glucose toxicity in pancreatic islet beta cells in diabetes.* J Biol Chem, 2004. **279**(41): p. 42351-4.
120. Gerber, P.A. and G.A. Rutter, *The Role of Oxidative Stress and Hypoxia in Pancreatic Beta-Cell Dysfunction in Diabetes Mellitus.* Antioxid Redox Signal, 2017. **26**(10): p. 501-518.
121. Leloup, C., et al., *Mitochondrial reactive oxygen species are obligatory signals for glucose-induced insulin secretion.* Diabetes, 2009. **58**(3): p. 673-81.
122. Keane, K.N., et al., *Molecular Events Linking Oxidative Stress and Inflammation to Insulin Resistance and beta-Cell Dysfunction.* Oxid Med Cell Longev, 2015. **2015**: p. 181643.
123. Turrens, J.F., *Mitochondrial formation of reactive oxygen species.* J Physiol, 2003. **552**(Pt 2): p. 335-44.
124. Newsholme, P., et al., *Diabetes associated cell stress and dysfunction: role of mitochondrial and non-mitochondrial ROS production and activity.* J Physiol, 2007. **583**(Pt 1): p. 9-24.
125. Morgan, D., et al., *Glucose, palmitate and pro-inflammatory cytokines modulate production and activity of a phagocyte-like NADPH oxidase in rat pancreatic islets and a clonal beta cell line.* Diabetologia, 2007. **50**(2): p. 359-69.

126. Lenzen, S., J. Drinkgern, and M. Tiedge, *Low antioxidant enzyme gene expression in pancreatic islets compared with various other mouse tissues.* Free Radic Biol Med, 1996. **20**(3): p. 463-6.
127. Newsholme, P., et al., *Reactive oxygen and nitrogen species generation, antioxidant defenses, and beta-cell function: a critical role for amino acids.* J Endocrinol, 2012. **214**(1): p. 11-20.
128. Kaneto, H., et al., *Involvement of c-Jun N-terminal kinase in oxidative stress-mediated suppression of insulin gene expression.* J Biol Chem, 2002. **277**(33): p. 30010-8.
129. Harmon, J.S., R. Stein, and R.P. Robertson, *Oxidative stress-mediated, post-translational loss of MafA protein as a contributing mechanism to loss of insulin gene expression in glucotoxic beta cells.* J Biol Chem, 2005. **280**(12): p. 11107-13.
130. Bray, G.A., et al., *Management of obesity.* Lancet, 2016. **387**(10031): p. 1947-56.
131. Guilherme, A., et al., *Adipocyte dysfunctions linking obesity to insulin resistance and type 2 diabetes.* Nat Rev Mol Cell Biol, 2008. **9**(5): p. 367-77.
132. Kwon, H. and J.E. Pessin, *Adipokines mediate inflammation and insulin resistance.* Front Endocrinol (Lausanne), 2013. **4**: p. 71.
133. Engin, A.B., *What Is Lipotoxicity?* Adv Exp Med Biol, 2017. **960**: p. 197-220.
134. Tushuizen, M.E., et al., *Pancreatic fat content and beta-cell function in men with and without type 2 diabetes.* Diabetes Care, 2007. **30**(11): p. 2916-21.
135. Dula, S.B., et al., *Evidence that low-grade systemic inflammation can induce islet dysfunction as measured by impaired calcium handling.* Cell Calcium, 2010. **48**(2-3): p. 133-42.
136. Boni-Schnetzler, M., et al., *Free fatty acids induce a proinflammatory response in islets via the abundantly expressed interleukin-1 receptor I.* Endocrinology, 2009. **150**(12): p. 5218-29.
137. Coppari, R. and C. Bjorbaek, *Leptin revisited: its mechanism of action and potential for treating diabetes.* Nat Rev Drug Discov, 2012. **11**(9): p. 692-708.
138. Bluher, M. and C.S. Mantzoros, *From leptin to other adipokines in health and disease: facts and expectations at the beginning of the 21st century.* Metabolism, 2015. **64**(1): p. 131-45.
139. Mantzoros, C.S., et al., *Leptin in human physiology and pathophysiology.* Am J Physiol Endocrinol Metab, 2011. **301**(4): p. E567-84.
140. Scott, R.A., et al., *An Expanded Genome-Wide Association Study of Type 2 Diabetes in Europeans.* Diabetes, 2017. **66**(11): p. 2888-2902.
141. Xue, A., et al., *Genome-wide association analyses identify 143 risk variants and putative regulatory mechanisms for type 2 diabetes.* Nat Commun, 2018. **9**(1): p. 2941.
142. Grant, S.F., et al., *Variant of transcription factor 7-like 2 (TCF7L2) gene confers risk of type 2 diabetes.* Nat Genet, 2006. **38**(3): p. 320-3.
143. Zhou, Y., et al., *Survival of pancreatic beta cells is partly controlled by a TCF7L2-p53-p53INP1-dependent pathway.* Hum Mol Genet, 2012. **21**(1): p. 196-207.
144. Welters, A., et al., *NMDAR antagonists for the treatment of diabetes mellitus-Current status and future directions.* Diabetes Obes Metab, 2017. **19 Suppl 1**: p. 95-106.
145. Gerstein, H.C., *Diabetes: Dysglycaemia as a cause of cardiovascular outcomes.* Nat Rev Endocrinol, 2015. **11**(9): p. 508-10.

146. Leon, B.M. and T.M. Maddox, *Diabetes and cardiovascular disease: Epidemiology, biological mechanisms, treatment recommendations and future research.* World J Diabetes, 2015. **6**(13): p. 1246-58.
147. Gaede, P., et al., *Multifactorial intervention and cardiovascular disease in patients with type 2 diabetes.* N Engl J Med, 2003. **348**(5): p. 383-93.
148. Sarwar, N., et al., *Diabetes mellitus, fasting blood glucose concentration, and risk of vascular disease: a collaborative meta-analysis of 102 prospective studies.* Lancet, 2010. **375**(9733): p. 2215-22.
149. Rao Kondapally Seshasai, S., et al., *Diabetes mellitus, fasting glucose, and risk of cause-specific death.* N Engl J Med, 2011. **364**(9): p. 829-841.
150. Harding, J.L., et al., *Cancer risk among people with type 1 and type 2 diabetes: disentangling true associations, detection bias, and reverse causation.* Diabetes Care, 2015. **38**(2): p. 264-70.
151. Welters, A., et al., *Need for Better Diabetes Treatment: The Therapeutic Potential of NMDA Receptor Antagonists.* Klin Padiatr, 2017. **229**(1): p. 14-20.
152. Pozzilli, P., et al., *Continuous subcutaneous insulin infusion in diabetes: patient populations, safety, efficacy, and pharmacoeconomics.* Diabetes Metab Res Rev, 2016. **32**(1): p. 21-39.
153. Kovatchev, B., *A Century of Diabetes Technology: Signals, Models, and Artificial Pancreas Control.* Trends Endocrinol Metab, 2019. **30**(7): p. 432-444.
154. Orozco, L.J., et al., *Exercise or exercise and diet for preventing type 2 diabetes mellitus.* Cochrane Database Syst Rev, 2008(3): p. Cd003054.
155. Merlotti, C., A. Morabito, and A.E. Pontiroli, *Prevention of type 2 diabetes; a systematic review and meta-analysis of different intervention strategies.* Diabetes Obes Metab, 2014. **16**(8): p. 719-27.
156. Cardona-Morrell, M., et al., *Reduction of diabetes risk in routine clinical practice: are physical activity and nutrition interventions feasible and are the outcomes from reference trials replicable? A systematic review and meta-analysis.* BMC Public Health, 2010. **10**: p. 653.
157. Dunkley, A.J., et al., *Diabetes prevention in the real world: effectiveness of pragmatic lifestyle interventions for the prevention of type 2 diabetes and of the impact of adherence to guideline recommendations: a systematic review and meta-analysis.* Diabetes Care, 2014. **37**(4): p. 922-33.
158. Davies, M.J., et al., *Management of Hyperglycemia in Type 2 Diabetes, 2018. A Consensus Report by the American Diabetes Association (ADA) and the European Association for the Study of Diabetes (EASD).* Diabetes Care, 2018. **41**(12): p. 2669-2701.
159. DeFronzo, R.A., et al., *Once-daily delayed-release metformin lowers plasma glucose and enhances fasting and postprandial GLP-1 and PYY: results from two randomised trials.* Diabetologia, 2016. **59**(8): p. 1645-54.
160. Tahrani, A.A., et al., *Management of type 2 diabetes: new and future developments in treatment.* Lancet, 2011. **378**(9786): p. 182-97.
161. Hirst, J.A., et al., *Estimating the effect of sulfonylurea on HbA1c in diabetes: a systematic review and meta-analysis.* Diabetologia, 2013. **56**(5): p. 973-84.
162. Nauck, M.A. and J.J. Meier, *The incretin effect in healthy individuals and those with type 2 diabetes: physiology, pathophysiology, and response to therapeutic interventions.* Lancet Diabetes Endocrinol, 2016. **4**(6): p. 525-36.
163. Thrasher, J., *Pharmacologic Management of Type 2 Diabetes Mellitus: Available Therapies.* Am J Med, 2017. **130**(6s): p. S4-s17.

164. Wilding, J.P., *The role of the kidneys in glucose homeostasis in type 2 diabetes: clinical implications and therapeutic significance through sodium glucose co-transporter 2 inhibitors.* Metabolism, 2014. **63**(10): p. 1228-37.
165. Nauck, M.A., et al., *Dapagliflozin versus glipizide as add-on therapy in patients with type 2 diabetes who have inadequate glycemic control with metformin: a randomized, 52-week, double-blind, active-controlled noninferiority trial.* Diabetes Care, 2011. **34**(9): p. 2015-22.
166. Erpeldinger, S., et al., *Efficacy and safety of insulin in type 2 diabetes: meta-analysis of randomised controlled trials.* BMC Endocr Disord, 2016. **16**(1): p. 39.
167. Inzucchi, S.E., et al., *Metformin in patients with type 2 diabetes and kidney disease: a systematic review.* Jama, 2014. **312**(24): p. 2668-75.
168. Ahren, B., *Avoiding hypoglycemia: a key to success for glucose-lowering therapy in type 2 diabetes.* Vasc Health Risk Manag, 2013. **9**: p. 155-63.
169. Monami, M., et al., *A meta-analysis of the hypoglycaemic risk in randomized controlled trials with sulphonylureas in patients with type 2 diabetes.* Diabetes Obes Metab, 2014. **16**(9): p. 833-40.
170. Abdelmoneim, A.S., et al., *Cardiovascular safety of sulphonylureas: over 40 years of continuous controversy without an answer.* Diabetes Obes Metab, 2015. **17**(6): p. 523-532.
171. Butler, P.C., et al., *A critical analysis of the clinical use of incretin-based therapies: Are the GLP-1 therapies safe?* Diabetes Care, 2013. **36**(7): p. 2118-25.
172. Storgaard, H., et al., *Glucagon-like peptide-1 receptor agonists and risk of acute pancreatitis in patients with type 2 diabetes.* Diabetes Obes Metab, 2017. **19**(6): p. 906-908.
173. Tahrani, A.A., A.H. Barnett, and C.J. Bailey, *SGLT inhibitors in management of diabetes.* Lancet Diabetes Endocrinol, 2013. **1**(2): p. 140-51.
174. Li, D., et al., *Urinary tract and genital infections in patients with type 2 diabetes treated with sodium-glucose co-transporter 2 inhibitors: A meta-analysis of randomized controlled trials.* Diabetes Obes Metab, 2017. **19**(3): p. 348-355.
175. Neal, B., et al., *Canagliflozin and Cardiovascular and Renal Events in Type 2 Diabetes.* N Engl J Med, 2017. **377**(7): p. 644-657.
176. Bunck, M.C., et al., *Effects of exenatide on measures of beta-cell function after 3 years in metformin-treated patients with type 2 diabetes.* Diabetes Care, 2011. **34**(9): p. 2041-7.
177. Retnakaran, R., et al., *Liraglutide and the preservation of pancreatic beta-cell function in early type 2 diabetes: the LIBRA trial.* Diabetes Care, 2014. **37**(12): p. 3270-8.
178. Del Prato, S., et al., *Long-term glycaemic response and tolerability of dapagliflozin versus a sulphonylurea as add-on therapy to metformin in patients with type 2 diabetes: 4-year data.* Diabetes Obes Metab, 2015. **17**(6): p. 581-590.
179. Bailey, C.J., A.A. Tahrani, and A.H. Barnett, *Future glucose-lowering drugs for type 2 diabetes.* Lancet Diabetes Endocrinol, 2016. **4**(4): p. 350-9.
180. Abdulreda, M.H., et al., *Liraglutide Compromises Pancreatic beta Cell Function in a Humanized Mouse Model.* Cell Metab, 2016. **23**(3): p. 541-6.
181. Lee, Y.S. and H.S. Jun, *Anti-diabetic actions of glucagon-like peptide-1 on pancreatic beta-cells.* Metabolism, 2014. **63**(1): p. 9-19.
182. Bonadonna, R.C., et al., *Novel antidiabetic drugs and cardiovascular risk: Primum non nocere.* Nutr Metab Cardiovasc Dis, 2016. **26**(9): p. 759-66.

183. Dicpinigaitis, P.V., *Clinical perspective - cough: an unmet need.* Curr Opin Pharmacol, 2015. **22**: p. 24-8.
184. Li, G., et al., *Protective effect of dextromethorphan against endotoxic shock in mice.* Biochem Pharmacol, 2005. **69**(2): p. 233-40.
185. Taylor, C.P., et al., *Pharmacology of dextromethorphan: Relevance to dextromethorphan/quinidine (Nuedexta(R)) clinical use.* Pharmacol Ther, 2016. **164**: p. 170-82.
186. Nelson, K.A., et al., *High-dose oral dextromethorphan versus placebo in painful diabetic neuropathy and postherpetic neuralgia.* Neurology, 1997. **48**(5): p. 1212-8.
187. Shaibani, A.I., et al., *Efficacy and safety of dextromethorphan/quinidine at two dosage levels for diabetic neuropathic pain: a double-blind, placebo-controlled, multicenter study.* Pain Med, 2012. **13**(2): p. 243-54.
188. Yang, L.P. and E.D. Deeks, *Dextromethorphan/quinidine: a review of its use in adults with pseudobulbar affect.* Drugs, 2015. **75**(1): p. 83-90.
189. Garnock-Jones, K.P., *Dextromethorphan/quinidine: in pseudobulbar affect.* CNS Drugs, 2011. **25**(5): p. 435-45.
190. Hamosh, A., et al., *Long-term use of high-dose benzoate and dextromethorphan for the treatment of nonketotic hyperglycinemia.* J Pediatr, 1998. **132**(4): p. 709-13.
191. Bjoraker, K.J., et al., *Neurodevelopmental Outcome and Treatment Efficacy of Benzoate and Dextromethorphan in Siblings with Attenuated Nonketotic Hyperglycinemia.* J Pediatr, 2016. **170**: p. 234-9.
192. Nguyen, L., et al., *Dextromethorphan: An update on its utility for neurological and neuropsychiatric disorders.* Pharmacol Ther, 2016. **159**: p. 1-22.
193. Wollheim, C.B. and P. Maechler, *Beta cell glutamate receptor antagonists: novel oral antidiabetic drugs?* Nat Med, 2015. **21**(4): p. 310-1.
194. Shin, E.J., et al., *The dextromethorphan analog dimemorfan attenuates kainate-induced seizures via sigma1 receptor activation: comparison with the effects of dextromethorphan.* Br J Pharmacol, 2005. **144**(7): p. 908-18.
195. Yin, W.H., et al., *Combination With Low-dose Dextromethorphan Improves the Effect of Amlodipine Monotherapy in Clinical Hypertension: A First-in-human, Concept-proven, Prospective, Dose-escalation, Multicenter Study.* Medicine (Baltimore), 2016. **95**(12): p. e3234.
196. Liu, S.L., et al., *Dextromethorphan reduces oxidative stress and inhibits atherosclerosis and neointima formation in mice.* Cardiovasc Res, 2009. **82**(1): p. 161-9.
197. Marquard, J., et al., *Characterization of pancreatic NMDA receptors as possible drug targets for diabetes treatment.* Nat Med, 2015. **21**(4): p. 363-72.
198. Marquard, J., et al., *Effects of dextromethorphan as add-on to sitagliptin on blood glucose and serum insulin concentrations in individuals with type 2 diabetes mellitus: a randomized, placebo-controlled, double-blinded, multiple crossover, single-dose clinical trial.* Diabetes Obes Metab, 2016. **18**(1): p. 100-3.
199. Scholz, O., A. Welters, and E. Lammert, *Role of NMDA Receptors in Pancreatic Islets*, in *The NMDA Receptors*, K. Hashimoto, Editor. 2017, Humana Press, Cham. p. 121-134.
200. Coleman, D.L. and K.P. Hummel, *Studies with the mutation, diabetes, in the mouse.* Diabetologia, 1967. **3**(2): p. 238-48.
201. Huang, X.T., et al., *An excessive increase in glutamate contributes to glucose-toxicity in beta-cells via activation of pancreatic NMDA receptors in rodent diabetes.* Sci Rep, 2017. **7**: p. 44120.

202. Wu, T.C., et al., *Low-dose dextromethorphan, a NADPH oxidase inhibitor, reduces blood pressure and enhances vascular protection in experimental hypertension.* PLoS One, 2012. **7**(9): p. e46067.
203. Dumas, S.J., et al., *NMDA-Type Glutamate Receptor Activation Promotes Vascular Remodeling and Pulmonary Arterial Hypertension.* Circulation, 2018. **137**(22): p. 2371-2389.
204. Liu, P.Y., et al., *Treatment with dextromethorphan improves endothelial function, inflammation and oxidative stress in male heavy smokers.* J Thromb Haemost, 2008. **6**(10): p. 1685-92.
205. Roshanravan, H., E.Y. Kim, and S.E. Dryer, *NMDA Receptors as Potential Therapeutic Targets in Diabetic Nephropathy: Increased Renal NMDA Receptor Subunit Expression in Akita Mice and Reduced Nephropathy Following Sustained Treatment With Memantine or MK-801.* Diabetes, 2016. **65**(10): p. 3139-50.
206. Callaghan, B.C., et al., *Diabetic neuropathy: clinical manifestations and current treatments.* Lancet Neurol, 2012. **11**(6): p. 521-34.
207. Yoon, Y.H. and M.F. Marmor, *Dextromethorphan protects retina against ischemic injury in vivo.* Arch Ophthalmol, 1989. **107**(3): p. 409-11.
208. North, W.G., et al., *Small-cell lung cancer growth inhibition: synergism between NMDA receptor blockade and chemotherapy.* Clin Pharmacol, 2019. **11**: p. 15-23.
209. Li, L., et al., *GKAP Acts as a Genetic Modulator of NMDAR Signaling to Govern Invasive Tumor Growth.* Cancer Cell, 2018. **33**(4): p. 736-751.e5.
210. Zeng, Q., et al., *Synaptic proximity enables NMDAR signalling to promote brain metastasis.* Nature, 2019. **573**(7775): p. 526-531.
211. Stanciu, C.N., T.M. Penders, and E.M. Rouse, *Recreational use of dextromethorphan, "Robotripping"-A brief review.* Am J Addict, 2016. **25**(5): p. 374-7.
212. Linn, K.A., M.T. Long, and P.S. Pagel, *"Robo-tripping": dextromethorphan abuse and its anesthetic implications.* Anesth Pain Med, 2014. **4**(5): p. e20990.
213. Yesil, P., et al., *A new collagenase blend increases the number of islets isolated from mouse pancreas.* Islets, 2009. **1**(3): p. 185-90.
214. Schindelin, J., et al., *Fiji: an open-source platform for biological-image analysis.* Nat Methods, 2012. **9**(7): p. 676-82.
215. Gonzalez-Rodriguez, S., et al., *Polyglycerol-opioid conjugate produces analgesia devoid of side effects.* Elife, 2017. **6**.
216. Spahn, V., et al., *A nontoxic pain killer designed by modeling of pathological receptor conformations.* Science, 2017. **355**(6328): p. 966-969.
217. Corder, G., et al., *Loss of mu opioid receptor signaling in nociceptors, but not microglia, abrogates morphine tolerance without disrupting analgesia.* Nat Med, 2017. **23**(2): p. 164-173.
218. Pope, L.E., et al., *Pharmacokinetics of dextromethorphan after single or multiple dosing in combination with quinidine in extensive and poor metabolizers.* J Clin Pharmacol, 2004. **44**(10): p. 1132-42.
219. Cummings, J.L., et al., *Effect of Dextromethorphan-Quinidine on Agitation in Patients With Alzheimer Disease Dementia: A Randomized Clinical Trial.* Jama, 2015. **314**(12): p. 1242-54.
220. Hauser, R.A., et al., *Extended-release carbidopa-levodopa (IPX066) compared with immediate-release carbidopa-levodopa in patients with Parkinson's disease and motor fluctuations: a phase 3 randomised, double-blind trial.* Lancet Neurol, 2013. **12**(4): p. 346-56.

221. Pahwa, R., et al., *Randomized trial of IPX066, carbidopa/levodopa extended release, in early Parkinson's disease.* Parkinsonism Relat Disord, 2014. **20**(2): p. 142-8.
222. Hsu, A., et al., *Comparison of the pharmacokinetics of an oral extended-release capsule formulation of carbidopa-levodopa (IPX066) with immediate-release carbidopa-levodopa (Sinemet((R))), sustained-release carbidopa-levodopa (Sinemet((R)) CR), and carbidopa-levodopa-entacapone (Stalevo((R))).* J Clin Pharmacol, 2015. **55**(9): p. 995-1003.
223. Mittur, A., S. Gupta, and N.B. Modi, *Pharmacokinetics of Rytary((R)), An Extended-Release Capsule Formulation of Carbidopa-Levodopa.* Clin Pharmacokinet, 2017. **56**(9): p. 999-1014.
224. Ziegler, A.G., et al., *Seroconversion to multiple islet autoantibodies and risk of progression to diabetes in children.* Jama, 2013. **309**(23): p. 2473-9.
225. Simmons, K.M. and A.W. Michels, *Type 1 diabetes: A predictable disease.* World J Diabetes, 2015. **6**(3): p. 380-90.
226. Raab, J., et al., *Capillary blood islet autoantibody screening for identifying pre-type 1 diabetes in the general population: design and initial results of the Fr1da study.* BMJ Open, 2016. **6**(5): p. e011144.
227. Simmons, K.M., et al., *Screening children for type 1 diabetes-associated antibodies at community health fairs.* Pediatr Diabetes, 2019. **20**(7): p. 909-914.
228. Burkart, V., et al., *Mice lacking the poly(ADP-ribose) polymerase gene are resistant to pancreatic beta-cell destruction and diabetes development induced by streptozocin.* Nat Med, 1999. **5**(3): p. 314-9.
229. Schnedl, W.J., et al., *STZ transport and cytotoxicity. Specific enhancement in GLUT2-expressing cells.* Diabetes, 1994. **43**(11): p. 1326-33.
230. Li, L., et al., *Identification of type 2 diabetes subgroups through topological analysis of patient similarity.* Sci Transl Med, 2015. **7**(311): p. 311ra174.
231. Ahlqvist, E., et al., *Novel subgroups of adult-onset diabetes and their association with outcomes: a data-driven cluster analysis of six variables.* Lancet Diabetes Endocrinol, 2018. **6**(5): p. 361-369.
232. Zaharia, O.P., et al., *Risk of diabetes-associated diseases in subgroups of patients with recent-onset diabetes: a 5-year follow-up study.* Lancet Diabetes Endocrinol, 2019. **7**(9): p. 684-694.
233. Clemmensen, C., et al., *Emerging hormonal-based combination pharmacotherapies for the treatment of metabolic diseases.* Nat Rev Endocrinol, 2019. **15**(2): p. 90-104.
234. Goldenberg, R.M., et al., *Sodium-glucose co-transporter inhibitors, their role in type 1 diabetes treatment and a risk mitigation strategy for preventing diabetic ketoacidosis: The STOP DKA Protocol.* Diabetes Obes Metab, 2019. **21**(10): p. 2192-2202.
235. Dennis, J.M., et al., *Disease progression and treatment response in data-driven subgroups of type 2 diabetes compared with models based on simple clinical features: an analysis using clinical trial data.* Lancet Diabetes Endocrinol, 2019. **7**(6): p. 442-451.
236. Volkow, N.D. and A.T. McLellan, *Opioid Abuse in Chronic Pain--Misconceptions and Mitigation Strategies.* N Engl J Med, 2016. **374**(13): p. 1253-63.
237. Kolodny, A., et al., *The prescription opioid and heroin crisis: a public health approach to an epidemic of addiction.* Annu Rev Public Health, 2015. **36**: p. 559-74.

238. Burma, N.E., et al., *Blocking microglial pannexin-1 channels alleviates morphine withdrawal in rodents.* Nat Med, 2017. **23**(3): p. 355-360.
239. Feng, J., et al., *A new painkiller nanomedicine to bypass the blood-brain barrier and the use of morphine.* Sci Adv, 2019. **5**(2): p. eaau5148.
240. Puig, S. and H.B. Gutstein, *Opioids: keeping the good, eliminating the bad.* Nat Med, 2017. **23**(3): p. 272-273.
241. Godlewski, G., et al., *Targeting Peripheral CB1 Receptors Reduces Ethanol Intake via a Gut-Brain Axis.* Cell Metab, 2019. **29**(6): p. 1320-1333.e8.
242. Tam, J., et al., *Peripheral cannabinoid-1 receptor inverse agonism reduces obesity by reversing leptin resistance.* Cell Metab, 2012. **16**(2): p. 167-79.
243. Jourdan, T., G. Godlewski, and G. Kunos, *Endocannabinoid regulation of beta-cell functions: implications for glycaemic control and diabetes.* Diabetes Obes Metab, 2016. **18**(6): p. 549-57.
244. Fagerholm, V., M. Haaparanta, and M. Scheinin, *alpha2-adrenoceptor regulation of blood glucose homeostasis.* Basic Clin Pharmacol Toxicol, 2011. **108**(6): p. 365-70.
245. Philipp, M. and L. Hein, *Adrenergic receptor knockout mice: distinct functions of 9 receptor subtypes.* Pharmacol Ther, 2004. **101**(1): p. 65-74.
246. Rorsman, P. and F.M. Ashcroft, *Pancreatic beta-Cell Electrical Activity and Insulin Secretion: Of Mice and Men.* Physiol Rev, 2018. **98**(1): p. 117-214.
247. Wess, J., *More is not always better: alpha2A-adrenoceptor expression in type 2 diabetes.* Cell Metab, 2010. **11**(1): p. 3-5.
248. Peterhoff, M., et al., *Inhibition of insulin secretion via distinct signaling pathways in alpha2-adrenoceptor knockout mice.* Eur J Endocrinol, 2003. **149**(4): p. 343-50.
249. Hu, X., et al., *Proteomic exploration of pancreatic islets in mice null for the alpha2A adrenergic receptor.* J Mol Endocrinol, 2005. **35**(1): p. 73-88.
250. Metz, S.A., J.B. Halter, and R.P. Robertson, *Induction of defective insulin secretion and impaired glucose tolerance by clonidine. Selective stimulation of metabolic alpha-adrenergic pathways.* Diabetes, 1978. **27**(5): p. 554-62.
251. Angel, I., R. Niddam, and S.Z. Langer, *Involvement of alpha-2 adrenergic receptor subtypes in hyperglycemia.* J Pharmacol Exp Ther, 1990. **254**(3): p. 877-82.
252. Devedjian, J.C., et al., *Transgenic mice overexpressing alpha2A-adrenoceptors in pancreatic beta-cells show altered regulation of glucose homeostasis.* Diabetologia, 2000. **43**(7): p. 899-906.
253. Rosengren, A.H., et al., *Overexpression of alpha2A-adrenergic receptors contributes to type 2 diabetes.* Science, 2010. **327**(5962): p. 217-20.
254. Liggett, S.B., *alpha2A-adrenergic receptors in the genetics, pathogenesis, and treatment of type 2 diabetes.* Sci Transl Med, 2009. **1**(12): p. 12ps15.
255. Hoy, M., et al., *Imidazoline NNC77-0074 stimulates insulin secretion and inhibits glucagon release by control of Ca(2+)-dependent exocytosis in pancreatic alpha- and beta-cells.* Eur J Pharmacol, 2003. **466**(1-2): p. 213-21.
256. Savontaus, E., et al., *Reduced blood glucose levels, increased insulin levels and improved glucose tolerance in alpha2A-adrenoceptor knockout mice.* Eur J Pharmacol, 2008. **578**(2-3): p. 359-64.
257. Fagerholm, V., et al., *Altered glucose homeostasis in alpha2A-adrenoceptor knockout mice.* Eur J Pharmacol, 2004. **505**(1-3): p. 243-52.
258. Tang, Y., et al., *Genotype-based treatment of type 2 diabetes with an alpha2A-adrenergic receptor antagonist.* Sci Transl Med, 2014. **6**(257): p. 257ra139.

259. Fagerholm, V., M. Scheinin, and M. Haaparanta, *alpha2A-adrenoceptor antagonism increases insulin secretion and synergistically augments the insulinotropic effect of glibenclamide in mice.* Br J Pharmacol, 2008. **154**(6): p. 1287-96.
260. Hsu, W.H., D.D. Schaffer, and M.H. Pineda, *Yohimbine increases plasma insulin concentrations of dogs.* Proc Soc Exp Biol Med, 1987. **184**(3): p. 345-9.
261. Abdel-Zaher, A.O., I.T. Ahmed, and A.D. El-Koussi, *The potential antidiabetic activity of some alpha-2 adrenoceptor antagonists.* Pharmacol Res, 2001. **44**(5): p. 397-409.
262. Furman, B.L., *Streptozotocin-Induced Diabetic Models in Mice and Rats.* Curr Protoc Pharmacol, 2015. **70**: p. 5.47.1-5.47.20.
263. Kolb, H., *Mouse models of insulin dependent diabetes: low-dose streptozocin-induced diabetes and nonobese diabetic (NOD) mice.* Diabetes Metab Rev, 1987. **3**(3): p. 751-78.
264. Goyal, S.N., et al., *Challenges and issues with streptozotocin-induced diabetes - A clinically relevant animal model to understand the diabetes pathogenesis and evaluate therapeutics.* Chem Biol Interact, 2016. **244**: p. 49-63.
265. Like, A.A. and A.A. Rossini, *Streptozotocin-induced pancreatic insulitis: new model of diabetes mellitus.* Science, 1976. **193**(4251): p. 415-7.
266. Szkudelski, T., *The mechanism of alloxan and streptozotocin action in B cells of the rat pancreas.* Physiol Res, 2001. **50**(6): p. 537-46.
267. Hosokawa, M., W. Dolci, and B. Thorens, *Differential sensitivity of GLUT1- and GLUT2-expressing beta cells to streptozotocin.* Biochem Biophys Res Commun, 2001. **289**(5): p. 1114-7.
268. Raza, H., et al., *Elevated mitochondrial cytochrome P450 2E1 and glutathione S-transferase A4-4 in streptozotocin-induced diabetic rats: tissue-specific variations and roles in oxidative stress.* Diabetes, 2004. **53**(1): p. 185-94.
269. Raza, H. and A. John, *Streptozotocin-induced cytotoxicity, oxidative stress and mitochondrial dysfunction in human hepatoma HepG2 cells.* Int J Mol Sci, 2012. **13**(5): p. 5751-67.
270. Ohkuwa, T., Y. Sato, and M. Naoi, *Hydroxyl radical formation in diabetic rats induced by streptozotocin.* Life Sci, 1995. **56**(21): p. 1789-98.
271. Zhang, Y., et al., *Lentinan protects pancreatic beta cells from STZ-induced damage.* J Cell Mol Med, 2016. **20**(10): p. 1803-12.
272. Zhang, W., et al., *Neuroprotective effect of dextromethorphan in the MPTP Parkinson's disease model: role of NADPH oxidase.* Faseb j, 2004. **18**(3): p. 589-91.
273. Qin, L., et al., *Microglial NADPH oxidase is a novel target for femtomolar neuroprotection against oxidative stress.* Faseb j, 2005. **19**(6): p. 550-7.
274. Schuler, D., et al., *Measurement of endothelium-dependent vasodilation in mice-brief report.* Arterioscler Thromb Vasc Biol, 2014. **34**(12): p. 2651-7.
275. Al-Qaisi, M., et al., *Measurement of endothelial function and its clinical utility for cardiovascular risk.* Vasc Health Risk Manag, 2008. **4**(3): p. 647-52.
276. Kolovou, G., et al., *Apolipoprotein E knockout models.* Curr Pharm Des, 2008. **14**(4): p. 338-51.
277. Atochin, D.N. and P.L. Huang, *Endothelial nitric oxide synthase transgenic models of endothelial dysfunction.* Pflugers Arch, 2010. **460**(6): p. 965-74.
278. Bowes, J., et al., *Reducing safety-related drug attrition: the use of in vitro pharmacological profiling.* Nat Rev Drug Discov, 2012. **11**(12): p. 909-22.

279. Stevens, J.L., *Future of toxicology--mechanisms of toxicity and drug safety: where do we go from here?* Chem Res Toxicol, 2006. **19**(11): p. 1393-401.
280. Sanguinetti, M.C., et al., *A mechanistic link between an inherited and an acquired cardiac arrhythmia: HERG encodes the IKr potassium channel.* Cell, 1995. **81**(2): p. 299-307.
281. Redfern, W.S., et al., *Relationships between preclinical cardiac electrophysiology, clinical QT interval prolongation and torsade de pointes for a broad range of drugs: evidence for a provisional safety margin in drug development.* Cardiovasc Res, 2003. **58**(1): p. 32-45.
282. Curran, M.E., et al., *A molecular basis for cardiac arrhythmia: HERG mutations cause long QT syndrome.* Cell, 1995. **80**(5): p. 795-803.
283. Lammert, E., et al., *Dextrorphan-derivatives with suppressed central nervous activity.* International Publication Number: WO 2017/093519 A1, 2017.

List of abbreviations

A

α_{2A}-AR	α_{2A}-adrenergic receptor
ADP	Adenosine diphosphate
ANOVA	Analysis of variance
ApoE	Apolipoprotein E
ATP	Adenosine triphosphate
AUC	Area under the curve

B

BBB	Blood-brain barrier
BCA	Bicinchoninic acid
BMI	Body mass index
BW	Body weight

C

Ca^{2+}	Calcium
$CaCl_2$	Calcium chloride
cAMP	Cyclic adenosine monophosphate
CB_1R	Cannabinoid-1 receptor
CID	Collision-induced dissociation
CNS	Central nervous system
CO_2	Carbon dioxide
CSF	Cerebrospinal fluid
CSII	Continuous subcutaneous insulin infusions
CV	Cardiovascular
CYP	Cytochrome P450

D

DAPI	4’,6-diamidino-2-phenylindole
DPP-4	Dipeptidyl peptidase-4
DXM	Dextromethorphan
DXO	Dextrorphan

E

ECG	Electrocardiogram

EDTA	Ethylenediaminetetraacetic acid
ELISA	Enzyme-linked immunosorbent assay
eNOS	Endothelial nitric oxide synthase
Epac2	Exchange protein directly activated by cAMP 2
ER	Endoplasmic reticulum

F

FBS	Fetal bovine serum
FFA	Free fatty acid
FMD	Flow-mediated dilation

G

GABA	Gamma-aminobutyric acid
GIP	Glucose-dependent insulinotropic polypeptide
GLP-1	Glucagon-like peptide-1
GLUT	Glucose transporter
GPCR	G protein-coupled receptor
Grin1	encodes glutamate ionotropic receptor NMDA type subunit 1
GSIS	Glucose-stimulated insulin secretion
GTT	Glucose tolerance test

H

h	Hour
H_2O_2	Hydrogen peroxide
HbA1c	Hemoglobin A1c
HEPES	4-(2-hydroxyethyl)-1-piperazineethanesulfonic acid
HIP	Hyperglycemia in pregnancy
HLA	Human leukocyte antigen

I

IC_{50}	Half maximal inhibitory concentration
IIDP	Integrated Islet Distribution Program
IFN-γ	Interferone-γ
IL	Interleukin
i.p.	Intraperitoneal
IR	Insulin receptor
IRS	Insulin receptor substrate

K

K^+	Potassium
K_{ATP} channels	ATP-sensitive K^+ channels
kcal	Kilocalorie
KCl	Potassium chloride
KCNH2	encodes potassium voltage-gated channel subfamily H member 2
KRH	Krebs Ringer HEPES

L

LC-MS/MS	Liquid chromatography-tandem mass spectrometry
LSM	Laser scanning microscopy

M

M	Molar
MCP-1	Monocyte chemoattractant protein-1
min	Minute
MODY	Maturity-onset diabetes of the young
MRM	Multiple reaction monitoring

N

Na^+	Sodium
NaCl	Sodium chloride
NADP	Nicotinamide adenine dinucleotide phosphate
$NaHCO_3$	Sodium bicarbonate
NMDA	N-Methyl-D-Aspartate
NMR	Nuclear magnetic resonance
NO	Nitric oxide
NOX	NADPH oxidase

O

OGTT	Oral glucose tolerance test

P

PBS	Phosphate-buffered saline
PDX-1	Pancreatic and duodenal homeobox-1
PKA	Protein kinase A

Q

QC	Quality control
qPCR	Quantitative polymerase chain reaction

R

rcf	Relative centrifugal force
RCT	Randomized clinical trial
RIPA	Radioimmunoprecipitation assay
ROI	Region of interest
ROS	Reactive oxygen species
rpm	Revolutions per minute

S

s	Second
SD	Standard Deviation
SEM	Standard error of the mean
SGLT	Sodium-glucose linked transporter
STZ	Streptozotocin
SUR1	Sulfonylurea receptor 1

T

T1DM	Type 1 diabetes mellitus
T2DM	Type 2 diabetes mellitus
TCF7L2	encodes transcription factor 7-like 2
TNF-α	Tumor necrosis factor-α

U

U	Unit
UHPLC	Ultra-high performance liquid chromatography
US	United States

V

V	Volt
VDCC	Voltage-dependent Ca^{2+} channel
v/v	Volume/volume percentage

W

WHO	World Health Organization

Statutory Declaration

I hereby declare that I wrote the dissertation “Investigation of peripherally active and blood glucose-lowering dextromethorphan derivatives without central nervous side effects” independently and without forbidden outside help according to the “Good Scientific Practice of the Heinrich Heine University Düsseldorf”. I did not use other sources and aid than those indicated, and I marked all positions where I refer to the work of others.
Furthermore, I declare that I did not submit this dissertation, either in full or in part, to any other academic institutions, and did not make any previous attempts to do a PhD.

Düsseldorf,

_____

Okka Scholz

Eidesstattliche Erklärung

Ich versichere an Eides Statt, dass die Dissertation „Untersuchung von peripher aktiven und blutglukosesenkenden Dextromethorphan Derivaten ohne zentralnervöse Nebenwirkungen“ von mir selbstständig und ohne unzulässige fremde Hilfe unter Beachtung der „Grundsätze zur Sicherung guter wissenschaftlicher Praxis an der Heinrich-Heine-Universität Düsseldorf“ erstellt worden ist. Ich habe keine anderen als die angegebenen Quellen und Hilfsmittel verwendet und habe alle Stellen, in denen ich Bezug auf die Arbeit Anderer nehme, als solche kenntlich gemacht.
Außerdem versichere ich, dass die vorliegende Dissertation weder in dieser noch in einer ähnlichen Form von mir bei einer anderen Institution eingereicht wurde und dass keine vorherigen Versuche zur Promotion von mir unternommen wurden.

Düsseldorf,

_____

Okka Scholz

Acknowledgements

First of all, I would like to thank my supervisor **Prof. Dr. Eckhard Lammert** for giving me the opportunity to write my PhD thesis in his lab, for his guidance and supervision as well as for giving me good advice.
I would like to thank **Prof. Dr. Christine Rose** for being my co-supervisor and for giving me good advice and useful critiques.

I would like to thank all the present and former members of the Institute of Metabolic Physiology at the Heinrich Heine University as well as the Institute for Vascular and Islet Cell Biology at the German Diabetes Center, particularly
Dr. Silke Otter for the successful cooperation and for giving me good advice, a lot of help, and motivating words!
Dr. Dr. Alena Welters for the good training and for handing a great project over to me.
Dr. Daniel Eberhard and **Dr. Bengt-Frederik Belgardt** for always answering my questions and for many valuable suggestions.
Barbara Bartosinska, **Silke Jakob** and **Andrea Köster** for their technical support and for providing so much assistance at any time.
Jessica Mrugala, **Haiko Karsjens** and **Laura Wörmeyer** for always having an open ear, for the support, and especially for being my friends.
Anna Branopolski, **Laura Hilger**, **Sofia Urner**, **Linda Lorenz**, **Carina Henning**, and **Angela Pelligra** for the great time in the lab!

I would like to thank my family and friends, particularly
my parents **Heike Scholz** and **Martin Nörder** for supporting me throughout my whole life.
Thomas Soworka for always believing in me.
my housemates, my “Mädels”, and all my friends in cologne for always having a great time together, you are the best!